Sources and pathways of methane formed in oxidative environments

Dissertation

Zur Erlangung des Grades

“Doktor der Naturwissenschaften”

im Promotionsfach Chemie

Frederik Althoff

geboren in Mannheim

Mainz, 2012

Nachwuchsgruppe ORCAS
Max-Planck-Institut für Chemie, Mainz

MAX-PLANCK-INSTITUT FÜR CHEMIE

MAX-PLANCK-GESELLSCHAFT

Fachbereich Chemie,
Pharmazie und Geowissenschaften
Johannes Gutenberg-Universität Mainz

JG | U
JOHANNES GUTENBERG UNIVERSITÄT MAINZ

Dekan:

Prodekan:

1. Berichterstatter:

2. Berichterstatter:

Tag der Mündlichen Prüfung: 26.07.2012

Erklärung

Hiermit versichere ich gemäß § 10 Abs. 3d der Promotionsordnung vom 24.07.2007, dass ich die als Dissertation vorgelegte Arbeit selbst angefertigt und alle benutzten Hilfsmittel (Literatur, Apparaturen, Material) in der Arbeit angegeben habe. Die als Dissertation vorgelegte Arbeit wurde in der Zeit von Februar 2009 bis Juli 2012 am Max-Planck-Institut für Chemie in der ORCAS-Gruppe bei Dr. F.K. und dem Institut für Organische und Makromolekulare Chemie an der Johannes Gutenberg- Universität Mainz im Arbeitskreis von Prof. Dr. H.F. angefertigt.

Wenn die Physik die Farbe ist,

dann ist die Chemie das Gemälde

(If physics is the colour then chemistry is the painting)

Für meine Frau

Summary

Methane is the most abundant reduced organic compound in the atmosphere. As the strongest known long-lived greenhouse gas after water vapour and carbon dioxide methane perturbs the radiation balance of Earth's atmosphere. The abiotic formation of methane requires ultraviolet irradiation of organic matter or takes place in locations with high temperature and/or pressure, e.g. during biomass burning or serpentinisation of olivine, under hydrothermal conditions in the oceans deep or below tectonic plates. The biotic methane formation was traditionally thought to be formed only by methanogens under strictly anaerobic conditions, such as in wetland soils, rice paddies and agricultural waste.

In this dissertation several chemical pathways are described which lead to the formation of methane under aerobic and ambient conditions. Organic precursor compounds such as ascorbic acid and methionine were shown to release methane in a chemical system including ferrihydrite and hydrogen peroxide in aquatic solution. Moreover, it was shown by using stable carbon isotope labelling experiments that the thio-methyl group of methionine was the carbon precursor for the methane produced. Methionine, a compound that plays an important role in transmethylation processes in plants was also applied to living plants. Stable carbon isotope labelling experiments clearly verified that methionine acts as a precursor compound for the methane from plants. Further experiments in which the electron transport chain was inhibited suggest that the methane generation is located in the mitochondria of the plants. The abiotic formation of methane was shown for several soil samples. Important environmental parameter such as temperature, UV irradiation and moisture were identified to control methane formation. The organic content of the sample as well as water and hydrogen peroxide might also play a major role in the formation of methane from soils. Based on these results a novel scheme was developed that includes both biotic and chemical sources of methane in the pedosphere.

Zusammenfassung

Methan ist die am stärksten reduzierte und in der Erdatmosphäre am häufigsten vorkommende organische Verbindung. Nach Wasserdampf und Kohlenstoffdioxid ist Methan das stärkste derzeit bekannte langlebige Treibhausgas. Es hat großen Einfluss auf den Strahlungshaushalt der Erde und trägt somit in großem Maße zur Erderwärmung bei. Abiotisch wird Methan durch Bestrahlung von organischem Material mit energiereichem UV-Licht gebildet oder entsteht in Umgebungen mit hohen Temperaturen und/oder Drücken. Solche Bedingungen herrschen bei der Verbrennung organischer Materialien oder finden sich in hydrothermalen Bereichen, wie dem Meeresboden oder unter tektonischen Platten. Die biotische Methanbildung wird im Allgemeinen Archaeen zugeschrieben, die ausschließlich in sauerstofffreien Bereichen, wie den Faulschlämmen von Reisfeldern oder den Verdauungstrakten von Wiederkäuern, leben. In dieser Arbeit wurden verschiedene chemische Reaktionswege untersucht, die zur Bildung von Methan unter aeroben Umgebungsbedingungen führen. Aus einer Reihe organischer Verbindungen, wie Ascorbinsäure und Methionin, konnte in der Reaktion mit Ferrihydrit und Wasserstoff-peroxid, die Entstehung von Methan nachgewiesen werden. Durch den Einsatz von ^{13}C-markiertem Ausgangsmaterial gelang es, die Thio-Methyl-Gruppe des Methionins als Quelle des produzierten Methans zu identifizieren. In weiteren Experimenten wurde lebenden Pflanzen unter anderem auch Methionin, das eine wichtige Rolle bei Transmethylierungen in Pflanzen spielt, appliziert. Durch die Verwendung von ^{13}C-Markierungen konnte die Thio-Methyl-Gruppe des Methionins auch hier als Vorläuferverbindung für das von Pflanzen produzierte Methan identifiziert werden. Untersuchungen, bei denen die Elektronentransportkette der Pflanzenzellen gestört wurde, deuteten auf Mitochondrien, als Ort der Methan-Entstehung in Pflanzen, hin. Auch für unterschiedliche Bodenproben konnte die abiotische Bildung von Methan nachgewiesen werden. Darüber hinaus gelang es, neben der Bedeutung des Organik- und Wasserstoffperoxid-Gehaltes, den Einfluss wichtiger Umweltfaktoren, wie Temperatur, UV-Strahlung und Feuchtigkeit, auf die Bildung des Methans zu bestimmen. Basierend auf diesen Ergebnissen konnte ein Übersichtsschema erstellt werden, welches sowohl die biotischen, als auch die chemischen Methan-Quellen im Bereich der Pedosphäre zeigt.

Abbreviations

ABA	2-amino butanoic acid
acetyl-CoA	acetyl coenzyme A
ADP	adenosine-5'-diphosphate
Al_2O_3	aluminium(III) oxide
ASC	ascorbic acid
ATP	adenosine-5'-triphosphate
BET	betaine
BY2	bright yellow 2
C18 column	column packed with silica with a $C_{18}H_{37}$ surface
CA	chronoamperometry
CC	choline chloride
CH_3 / CH_3^-	methyl group / methyl anion
CH_4	methane
CIII	respiratory complex III
CIV	respiratory complex IV; cytochrome c oxidase
CO	carbon monoxide
CO_2	carbon dioxide
CoA	coenzyme A
C_{org}	organic carbon
Cu_2O	Copper(I) oxide
CuO	Copper(II) oxide
CV	cyclic voltammetry
Cyt c	cytochrome c
d_f	film thickness of the stationary phase
DFM	difluoromethane
DHASC	dehydroascorbic acid
DNA	deoxyribonucleic acid
dw	dry weight
E_a	activation energy
E_h	redox potential

EI	electron impact / electron ionisation
EMG	electrophilic methyl groups
ESI	electron spray ionisation
ETC	electron transport chain
$FADH_2$ / FAD^+	flavin adenine dinucleotide (reduced / oxidised form)
Fe^{2+}	ferrous ion
Fe^{3+}	ferric ion
FH	ferrihydrite
GC	gas chromatograph
GC-C-IRMS	gas chromatography-combustion-isotope ratio mass spectrometry
GC-FID	gas chromatograph with flame ionisation detector
GHG	greenhouse gas
GU	guaiacol / 2-methoxyphenol
H^+	proton
H_2O	water
H_2O_2	hydrogen peroxide
$H_3CO\cdot$	methoxy radical
$H_3CO_2\cdot$	hydroperoxymethane radical
HA	humic acid
HCHO	formaldehyde
HCl	hydrochloric acid
HCO_2^+	formyloxonium
HCy	homocysteine
HCyA	homocystic acid
HCySO	homocysteine sulphoxide
$HO_2\cdot$	hydroperoxy radical
HPLC	high pressure/performance liquid chromatography
HSBA	4-hydrosulfinyl-2-hydroxybutanoic acid
HT	hematite
i.d.	inner diameter
IMS	intermembrane space
K^+	potassium ion

Lab Air	ambient laboratory air
LC-TOFMS	liquid chromatography with time of flight mass spectrometry
LEU	leucine
LLGHG	long-lived greenhouse gas
LN	lignin
LNS	lignin, sterile
m/z	mass charge ratio
MDC	methyl-donating compound
MeCbl	methylcobalamin
MET	methionine
MFC	mass flow controller
MMET	S-methyl-methionine
MS	mass spectrometer / mass spectroscopy
MS (salt)	Murashige & Skoog (salt)
MSO	methionine sulfoxide
MSO_2	methionine sulfone
n.d.	not detectable
n.m.	not measured
N_2	nitrogen
N_2O	nitrous oxide
NaCN / CN^-	sodium cyanide / cyanide
NADH / NAD^+	nicotinamide adenine dinucleotide (reduced / oxidised form)
NaN_3 / N_3^-	sodium azide / azide
NaOH	sodium hydroxide
NO	nitric oxide
NO_2	nitrogen dioxide
O_2	oxygen
O_3	ozone
OH / ·OH / OH^-	hydroxyl (radical / ion)
P_0	pressure gauge
PC	phosphatidylcholine
PH	peat Hille (Sphagnum peat)

PHS	peat Hille, sterile (Sphagnum peat)
P_i	inorganic phosphor
ppbv	parts per billion by volume; nL L^{-1}
ppmv	parts per million by volume; µL L^{-1}
PreCon	pre-concentration unit
PTFE	polytetrafluoroethylene
ROS	reactive oxygen species
SA	synthetic air
SAM	S-adenosylmethionine
SD	standard deviation
SEM	scanning electron microscopy
SG	soil Gonsenheim (coniferous forest soil A_h)
SHA	soil Hainich (deciduous forest soil A_h)
SiO_2	quartz sand
SL	soil Lerchenberg (deciduous forest soil A_h)
SW	soil Hälverststädt, Wiehnen (deciduous forest soil O_h)
TOF	time-of-flight
tRNA	transfer ribonucleic acid
UV	ultraviolet
VPDB	Vienna Pee Dee Belemnite

Table of Contents

Erklärung **3**

Summary **9**

Zusammenfassung **11**

Abbreviations **13**

Table of Contents **17**

Research aims and thesis outline **21**

Chapter 1

About methane **25**

1.1 Methane and its properties 25
1.2 Methane, an important climate gas 25
1.3 Methane formation in the environment 30
1.3.1 Abiotic methane formation 30
1.3.2 Biotic methane formation 31

Chapter 2

About plants **35**

2.1 Plant cell 35
2.2 Mitochondria 35
2.3 Cellular respiration 36
2.4 Electron transfer chain 37
2.5 Gas exchange 38

Chapter 3

Measurement systems **41**

3.1 GC-FID - Gas chromatograph with flame ionisation detector 41
3.2 PreCon-GC-C-IRMS - Gas chromatography - combustion - isotope ratio mass spectrometry with cryogenic pre-concentration unit 42
3.3 LC-TOFMS - Liquid chromatography with time of flight mass spectrometry 45

Chapter 4

Methane formation by oxidation of ascorbic acid using iron minerals and hydrogen peroxide **47**

4.1 Introduction 47
4.2 Material and Methods 50
4.2.1 Reagents 50

4.2.2 Reaction vials 50
4.2.3 Experimental setup 50
4.2.4 Investigations with different iron containing minerals 50
4.2.5 Investigations with SiO_2 50
4.2.6 Other organic compounds as methane precursors 51
4.2.7 Effect of hydrogen peroxide concentration 51
4.2.8 Effect of pH 51
4.2.9 Effect of reaction volume 51
4.2.10 Effect of headspace atmosphere 52
4.2.11 Methane measurements 52
4.3 Results and discussion 52
4.3.1 Effect of iron mineral form on methane formation 53
4.3.2 Investigations with other organic compounds as methane precursors 54
4.3.3 Factors that control formation of methane from ASC 55
4.4 Conclusions 59

Chapter 5

Abiotic methanogenesis from biomolecules under ambient conditions 61

5.1 Introduction 61
5.2 Methods 63
5.2.1 Compounds tested as methane precursor 63
5.2.2 Methane measurements 63
5.2.3 Isotope measurements 64
5.3 Results and discussion 64
5.3.1 Methane formation from MDSs 64
5.3.2 Identification of the precursor carbon using ^{13}C labelling experiments 65
5.3.3 Parameters affecting methane formation from methionine by the reaction with ascorbic acid, hydrogen peroxide and iron species 66
5.3.4 Postulated route of methane formation - identification of reaction products and intermediates 69
5.4 Acknowledgements 72
5.5 Author contributions 72
5.6 Supplemental 72
5.6.1 Natural role of biomolecules tested as methane precursor 72
5.6.2 Parameters that effect methane formation 73
5.6.3 Isotopic measurements 75
5.6.4 Isotope labelling experiments 75
5.6.5 Mass analysis 76

Chapter 6

Methionine as a precursor of methane in living plants 79

6.1 Introduction 79

6.2 Material and Methods 81
6.2.1 Plant and cell cultivation under sterile conditions 81
6.2.2 Investigations with cells and plants 82
6.2.3 Analytical techniques 83
6.2.4 Statistics 84
6.3 Results and discussion 84
6.3.1 Methane emission from tobacco cell suspensions when treated with different toxins 84
6.3.2 Comparison of methane release from tobacco cell suspensions with and without added methyl-donating compounds (MDCs) when treated with sodium azide 86
6.3.3 Identification of the methane carbon atom precursor using ^{13}C-positionally labelled methionine and intact tobacco plants 88
6.4 Acknowledgments 92

Chapter 7

Release of methane from aerobic soil: an indication of a novel chemical natural process? 93

7.1 Introduction 94
7.2 Materials and methods 96
7.2.1 Origin of samples and preparation 96
7.2.2 Determination of carbon content 96
7.2.3 Experimental setup 96
7.2.4 Methane measurements 97
7.2.5 Calculation of methane emission rate 98
7.2.6 Statistical methods 98
7.3 Results and discussion 99
7.3.1 Organic carbon content of samples 99
7.3.2 Kinetics of methane release from pectin and lignin 99
7.3.3 Release rates of methane from organics, soils and minerals under dry and wet conditions 102
7.3.4 Release rates of methane under dry and wet conditions 106
7.4 Conclusion and outlook 106

Chapter 8

Non-microbial methane formation in oxic soils 109

8.1 Introduction 110
8.1.1 Previous observations of methane formation in aerobic soils 110
8.1.2 Possibility of non-microbial methane formation in soil 111
8.1.3 Temperature dependency 111
8.1.4 Effect of wetting and drying 114
8.1.5 Effect of hydrogen peroxide 115

8.1.6 Effect of ultraviolet radiation 116
8.1.7 Stable carbon isotope composition of methane emitted from soil 117
8.2 Conclusions and Outlook 118
8.3 Materials and Methods 121
8.3.1 Origin of samples and preparation 121
8.3.2 Reaction Vials 122
8.3.3 Determination of organic carbon 122
8.3.4 Methane measurements 122
8.3.5 Isotopic data 122
8.3.6 Temperature dependency 123
8.3.7 Drying-rewetting cycles 123
8.3.8 Experiments with H_2O_2 124
8.3.9 UV irradiation experiments 124
8.3.10 Statistical methods 125
8.4 Acknowledgements 125
8.5 Supplemental 125
8.5.1 Possibility of desorption 125
8.5.2 Exclusion of methane oxidation by methane consuming bacteria 126
8.5.3 Arrhenius plots 127

Chapter 9

Main findings, conclusions and outlook 129

9.1 Main findings 129
9.2 Outlook 131

Chapter 10

Developments 133

10.1 Vial-In-Vial 133
10.2 Electrolysis Chamber 134
10.3 UV-Cell 135
10.4 Plant-Cell 136

Danksagung 137

Bibliography 141

List of figures 157

List of tables 159

Publications 161

Journal articles (Peer-reviewed) 161
Oral presentation 161
Conference abstract 162

Research aims and thesis outline

The findings by Keppler et al. (2006) initiated a controversial debate about methane (CH_4) formation in plants but also about CH_4 formation in oxidative environments in general.

The central goal of this thesis was the development of a chemical system that produces CH_4 under highly oxidative conditions. For the setup only substances were used that appear in biogeosystems, such as plants or soils. Initially, no precursors and mechanisms were known. For this reason a major aim was the identification of CH_4 precursors and pathways of CH_4 formation. As an additional aim, a transfer of the findings from the investigations of the chemical system should be made to living plants to identify metabolic compounds as precursors of the formed CH_4.

The work also involved high sensitive and innovative measurement systems with which it is possible to determine both the quantities and stable isotope composition ($^{13}C/^{12}C$ ratio) of CH_4. Using time-of-flight mass analysis enabled the detection and identification of reaction molecules such as amino acids and their derivatives. The systems are described in Chapter 3, whereas the experimental setups are described in the respective chapters. Some of the experiments and measurements required the development of special analytic tools and vials for laboratory work. These tools are described in Chapter 10.

Chapter 4 shows the development of a chemical system in which CH_4 is produced under highly oxidative conditions. Several organic substances were investigated for their potential to emit CH_4. However, only ascorbic acid was found to produce CH_4 in the presence of ferrihydrite and hydrogen peroxide. Focussing on ascorbic acid numerous reaction parameters of this CH_4 formation have been investigated, such as the influence of pH, reaction volume and time, atmospheric oxygen content and component ratio. For some of those parameters CH_4 production was monitored over 50 hours and more.

Chapter 5 describes the reaction of the chemically system, similar to those shown in Chapter 4, but focusing on biomolecules such as methyl donation compounds (MDCs) that play a major role in transmethylation reactions in biological systems. The focus was directed at the amino acid methionine producing the highest amount of CH_4 compared to the other tested substances. Parameters such as the compound ratio, reaction volume and time have been investigated in detail. For the formed CH_4 a linear dependency of the amount of added

methionine was found. Stable isotope labelling and ^{13}C analysis was used to identify the sulphur bond carbon methyl precursor of the formed CH_4. Based on those findings a reaction scheme was developed that illustrates the abiotic methanogenesis using the amino acid methionine under aerobic and ambient conditions. In this pathway it is clearly shown that the thio-methyl group of methionine is finally reduced to CH_4.

Chapter 6 investigates CH_4 formation from living plants that were supplemented with MDCs, which were already employed in Chapter 5. Tobacco *(Nicotiana tabacum)* was used as a model plant. Establishing the cell culture enabled an easy supplementing with MDC solutions and high performance of experiments compared to the use of intact tobacco plants. Besides using MDCs the toxins NaN_3, NaCN and CO have been investigated to initiate CH_4 from cell suspensions. These three toxins are known to bind to the reactive centre of cytochrome c oxidase (complex IV, CIV) and inhibit the protein from its function to utilise oxygen by reducing it. In either case CH_4 was formed to a significant amount with NaN_3 showing the highest CH_4 production. Without further treatment no significant CH_4 formation was found after the addition of MDCs to the cells. Since MET was the only supplemented substance leading to increased CH_4 formation from cell suspension after addition of NaN_3, MET with ^{13}C-labelled sulphur bound methyl group (—S—$^{13}CH_3$) was supplemented to intact plants. Therefore, supplementations were done by both leaf infiltration and root application. Detecting the supplemented ^{13}C label in the released CH_4 unambiguously proved that MDCs serve as precursor of CH_4 generated by plants.

Moreover, aside the investigation of CH_4 release by living plants experiments were carried out with soil containing different kinds of rotten plant material as CH_4 source, e.g. deciduous and coniferous forest soil and peat. The chemical systems which are described in Chapter 4 and 5 might also play a role in CH_4 formation in soil. The following two chapters (7, 8) present publications where I was not the first author, but in both studies I contributed significantly to the research.

Chapter 7 presents the first investigations on CH_4 release of different soils and soil components at different temperatures. Especially the components humic acid and lignin were expected to be the main sources of generated CH_4. In all cases the release of CH_4 was monitored over 24 h. This allows a good comparability of all samples investigated. The released CH_4 seemed to correlate with the organic amount of the samples and the

temperature. Furthermore, dry and wetted samples have been compared on their behaviour to form CH_4. The results indicate that water plays a major role since all wetted samples showed an increased CH_4 formation.

Chapter 8 develops further the findings described in Chapter 7. We suggest that chemical formation of methane during degradation of soil organic matter may represent the additional soil source that is needed to fully understand the complete methane cycle within the pedosphere. A set of experiments was conducted regarding also environmental factors, such as UV radiation, H_2O_2 content, water content drying and rewetting after drought. Experiments were carried out at different temperatures. In context of earlier findings regarding CH_4 emissions from dried plant material particularly the influence of UV radiation at different intensities was investigated. The entirety of these experiments showed the importance of those environmental factors for CH_4 formation. An increase of temperature or H_2O_2 increased also the formation of CH_4. Interestingly, the CH_4 generation from wetted sample were higher compared to dry ones but the ratio of sample material inserted water seemed to play only subordinated role. Just as the irradiation of dried plant material all soil samples an organic components showed high CH_4 production when being irradiated with UV light. The novel results have been summarised using a plausible scheme showing non-microbial methane formation in the aerobic layers of soils in addition to the known microbial sources.

Chapter 9 summarises the main findings of the research done in this dissertation. An outlook is given including suggestions about future research work.

Chapter 10 presents four self-designed laboratory tools including a gas tight lid for electrolysis experiments and three different experimental vials. The so called “Vial-In-Vial” system provides large sampling headspaces by small reaction volumes. The “UV-Cell” and the “Plant-Cell” are gas tight sample vials fitted with a septa sealed side port for gas sampling and a large opening at the top. After placing the sample, e.g. a plant, inside the vial the top of the vial can be closed opaque or with different transparent material such as non-optical glass, quartz glass or numerous light filters. This also allows the application of different light sources such as UV irradiation.

Theses laboratory tool were essential for the work presented in this dissertation. Especially the cells are also used for other research fields due to their abilities and flexibility in closing at the top opening.

Chapter 1

About methane

1.1 Methane and its properties

Methane (CH_4) is the highest reduced and smallest organic molecule. Its chemical formula is CH_4 and it has a tetrahedral structure. The molecular weight of CH_4 is 16.04 g^{-1} mol. Due to its melting point of –182.6 °C and its boiling point of –161.7 °C its aggregate state at standard conditions is gaseous. It is colourless, odourless and burns with a blue flame. The density at 1013 mbar and 0 °C is 0.7175 kg m^{-3}.

1.2 Methane, an important climate gas

Methane is the most abundant reduced organic compound in the atmosphere with a fraction of about 1.775 ppmv (parts per million by volume; µL L^{-1}) in 2005 (Figure 1.1). Ice core investigations indicate that over the last 800 kyr the abundance of CH_4 in the Earth's atmosphere varied between 350 and 800 ppbv (parts per billion by volume; nL L^{-1}); whereas the lows were found during glacial and highs during interglacial periods (Spahni et al., 2005; Solomon et al., 2007; Loulergue et al., 2008).

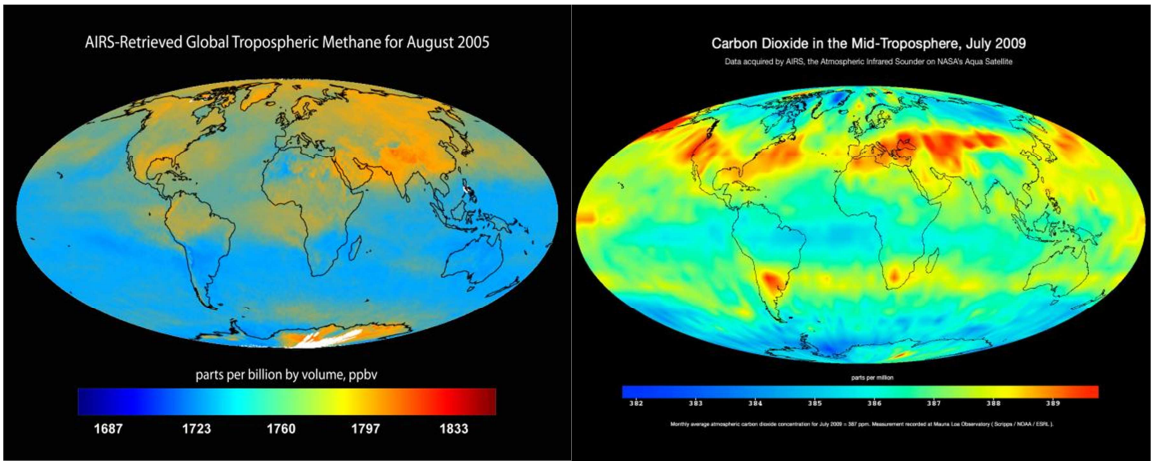

Figure 1.1: Global tropospheric CH_4 (left) and CO_2 (right) in the year 2005 and 2009, respectively. Colour scale on the left side (CH_4) is in ppbv and in ppmv on the right (CO_2) (http://airs.jpl.nasa.gov/image_gallery/gases).

Since the beginning of the industrial period in 1750 the amount of CH_4 has been increased by a factor of about 2.5 (Figure 1.2) and is mainly caused by human activities (Ehhalt et al., 2001). Due to residentially developed countries and the higher occurrence of industry, the

CH_4 average mixing ratio of the Northern Hemisphere is much higher than in the Southern Hemisphere (Rasmussen and Khalil, 1984). The Northern Hemisphere also covers two third of Earth's land surface including most wetlands and rice paddies, known to be most prominent natural CH_4 sources (Fischer et al., 2008; Frankenberg et al., 2008). Observations since the mid-1970s showed that the abundance of CH_4 has increased by about 30 % during that time. The grow rate has decreased substantially from a maximum increasing rate of ca. 14 ppbv yr^{-1} (about 1 %) in the 1980s (Blake and Rowland, 1988; Bousquet et al., 2006) to lows close to zero during 1999 to 2005 (Simpson et al., 2002; Solomon et al., 2007). However, recent research shows again a rising in CH_4 concentrations in 2007 (8.3 ± 0.6 ppbv) and 2008 (4.4 ± 0.6 ppbv).

Changes in the growth rate of CH_4 are related to changes in the imbalance between CH_4 sources and sinks, but are not yet understood (Ehhalt and Prather, 2001).

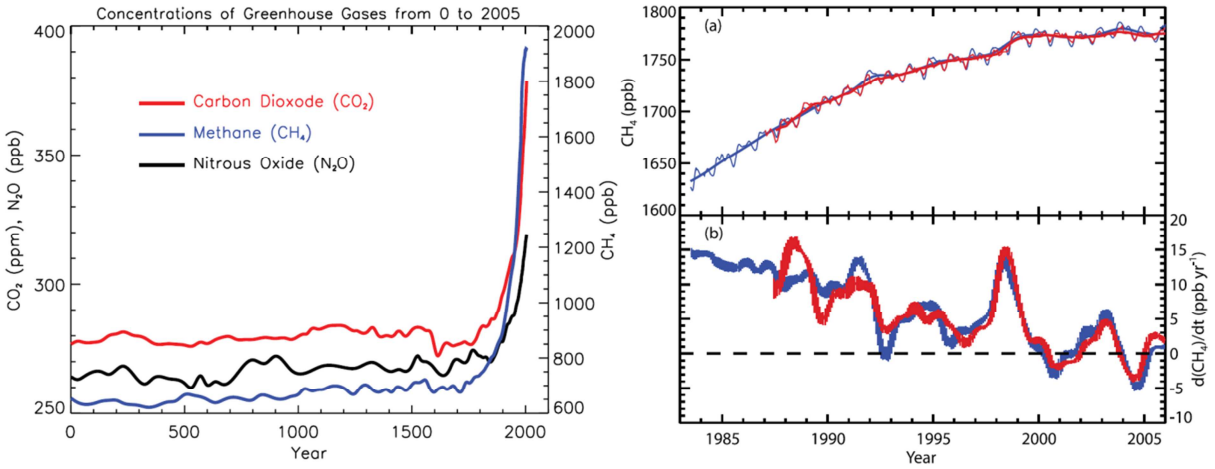

Figure 1.2: Temporal development of atmospheric greenhouse gas concentrations. Left) Change of the concentration of the GHGs CO_2, CH_4 and N_2O (nitrous oxide) in the atmosphere over the last 2000 years. **Right)** (a) Increase of the CH_4 concentration in the atmosphere temporally resolved for the last 25 years (b) and the corresponding increasing/decreasing rates. Different colours symbolises different studies (taken from Forster et al., 2007).

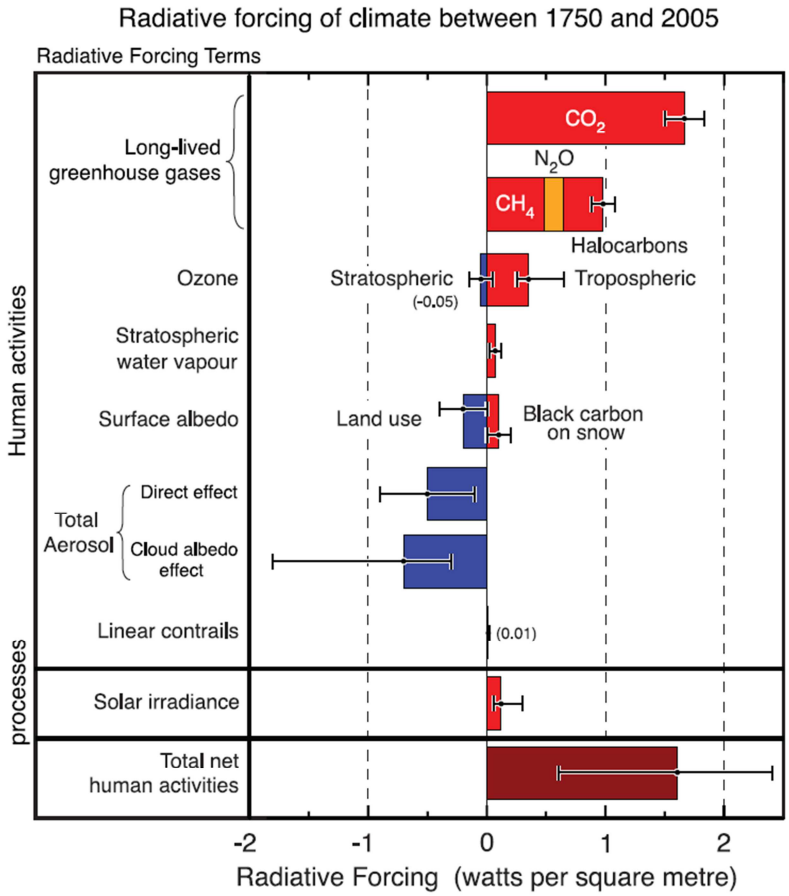

Figure 1.3: Summary of the principal components of the radiative forcing of climate change between 1750 and 2005. The positive effects (red) lead to warming of the climate whereas negative effects (blue) lead to cooling (taken from Forster et al., 2007).

An increase of the CH_4 level in the atmosphere has major implications for the planetary energy balance since CH_4 is the strongest known long-lived greenhouse gas (LLGHG) after water vapour (H_2O) and carbon dioxide (CO_2) (Hansen et al., 1981).

Carbon dioxide and CH_4 perturb atmosphere's radiation balance with a contribution of about 1.6 W m^{-2} and 0.48 W m^{-2} (in 2005), respectively (Forster et al., 2007). Here, CH_4 accounts for 22 % of the radiative forcing of all LLGHGs (2.5 W m^{-2}) (Figure 1.3) (Forster et al., 2007; Kvenvolden, 2005; Lelieveld et al., 1998). Beside the direct radiative forcing contributions of CH_4 also indirect effects are known. The increase of the greenhouse gas (GHG) ozone (O_3) is related to a rising amount of CH_4 in the atmosphere. The decomposition of CH_4 in the troposphere and stratosphere generates H_2O, the strongest known GHG. The contribution to the total CH_4 radiative forcing is estimated to be 2 to 5 % (Forster et al., 2007).

The radiative forcing is based on the re-emission of infrared radiation (Figure 1.4). When sunlight heats up the surface of the Earth, the surface in turn is emitting infrared radiation which is then absorbed by CH_4 in the atmosphere. On a 100 year timescale this absorption is about 25 times higher compared with CO_2 (Lelieveld et al., 1998). By the spherical re-emission of the absorbed infrared radiation from the CH_4 molecules a part of the radiation is reflected to the surface. This results in a rising planetary temperature – the so called greenhouse effect (Lacis et al., 1981).

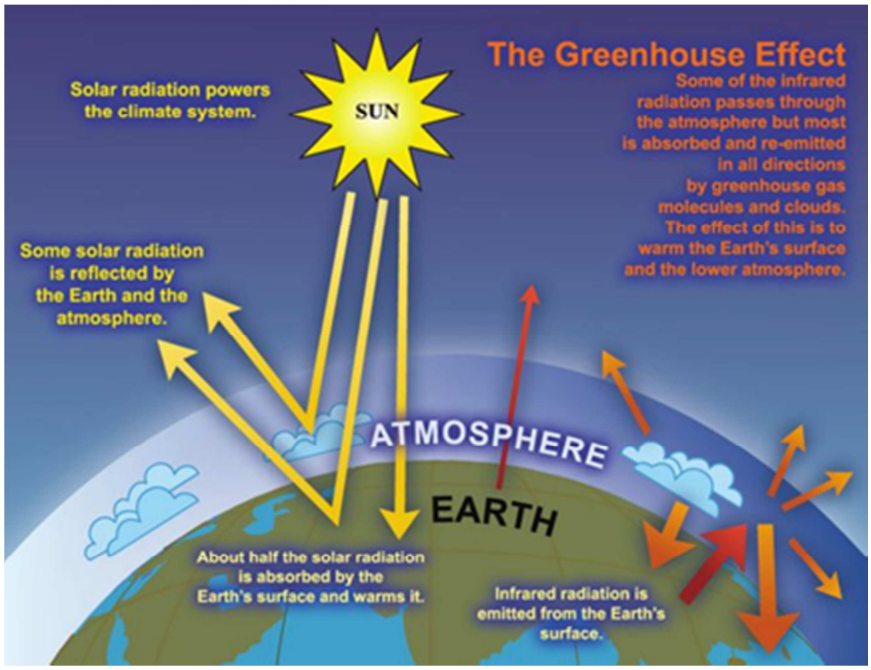

Figure 1.4: An idealised scheme of the natural greenhouse effect. Arrows represent the irradiation from sun (yellow), from Earth's surface (red) and from atmosphere (orange) (taken from Treut et al., 2007).

The lifetime of CH_4 in the atmosphere, which is usually defined as the quotient of the CH_4 burden in the atmosphere and the annual breakdown, is about 12 years (Forster et al., 2007). While 7-11 % of CH_4 are destroyed in the stratosphere, most CH_4 (ca. 80 %) is oxidized by hydroxyl radicals (·OH) in the troposphere (Forster et al., 2007; Lelieveld et al., 1998; Levy, 1971). A minor sink is the reaction with free chlorine (Allan et al., 2005; Platt et al., 2004). Figure 1.5 shows the atmospheric chemistry that leads to a decomposition of CH_4. The total global emission of all CH_4 sources is estimated to be in the range of 600 Tg yr^{-1}. Whereas the anthropogenic contribution with about 410 Tg yr^{-1} (~70 % of the total budget)

clearly dominates the current global budget. That means in contrast that the combination of natural CH_4 sources only account for about one third (Denman et al., 2007).

Formation of hydroxyl radicals

$$O_3 \xrightarrow{h\nu < 310nm} O(^1D) + O_2$$

$$O_3 \xrightarrow{h\nu < 1180nm} O(^3P) + O_2$$

$$O(^1D) + M \longrightarrow O(^3P) + M$$

$$O(^3P) + O_2 + M \longrightarrow O_3 + M$$

$$O(^1D) + H_2O \longrightarrow 2\,\cdot OH \qquad (M = N_2, O_2)$$

Photochemistry of methane

$$CH_4 + \cdot OH \longrightarrow \cdot CH_3 + H_2O$$

$$\cdot CH_3 + O_2 + M \longrightarrow H_3CO_2\cdot$$

In presence of NO_x

$$H_3CO_2\cdot + NO \longrightarrow H_3CO\cdot + NO_2$$

$$H_3CO\cdot + O_2 \longrightarrow HCHO + HO_2\cdot$$

$$HO_2\cdot + NO \longrightarrow \cdot OH + NO_2$$

$$NO_2 \xrightarrow{h\nu} NO + O(^3P)$$

$$O(^3P) + O_2 + M \longrightarrow O_3 + M \qquad (M = N_2, O_2)$$

$$CH_4 + 4O_2 \longrightarrow HCHO + H_2O + 2O_3 \qquad \text{(total reaction)}$$

Figure 1.5: Reactions in the atmosphere that leads to the formation hydroxyl radicals (·OH) and to the decomposition of methane (CH_4). For clarity NO and NO_2 are not written as radicals (Seinfeld and Pandis, 2006; Vigano, 2010).

In anoxic soil layers formed and released CH_4 is often nearly completely consumed by methanotrophic bacteria living in the upper oxygen rich layers of the soil (Conrad, 2009; Dunfield, 2007; Trotsenko and Murrell, 2008). In an energy producing pathway CH_4 is step-by-step oxidized to CO_2 that is emitted from soil or is consumed by plant roots or leaves. This pathway leads from CH_4 to CO_2 over the intermediate products methanol, formaldehyde and formate (Figure 1.6).

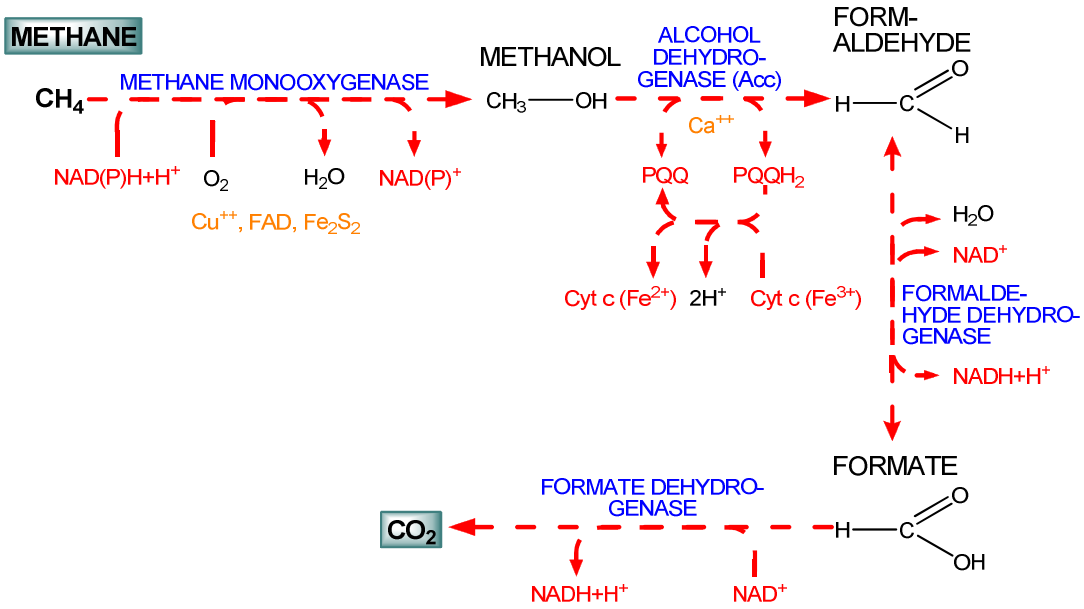

Figure 1.6: Methane consumption by methanotrophs. Anoxic respiration of obligate methylotrophs (taken from Michal (1999), modified).

1.3 Methane formation in the environment

Sources of atmospheric CH_4 can be divided in anthropogenic and natural as well as in biogenic and non-biogenic (Denman et al., 2007).

1.3.1 Abiotic methane formation

Abiotic formation of CH_4 has been reported to occur under conditions that require high pressure and/or temperature. For instance during biomass burning (Crutzen and Andreae, 1990; Fischer et al., 2008) or serpentinisation of olivine, under hydrothermal conditions in the oceans deep or below tectonic plates (Sherwood Lollar et al., 1993, 2002; Holm and Charlou, 2001; Sleep et al., 2004; Lazar and Manning, 2010; Neubeck et al., 2011). In the chemical industry CH_4 is often produced from carbon monoxide and hydrogen gas under high pressure and temperature (cf. Fischer-Tropsch synthesis) (Chernobaev et al., 1997).

Other sources of abiotic CH_4 emissions are the release during the decay of wide fields of methane hydrate at the bottom of the oceans. This source is estimated to contribute about 2 % to the global budget. The general release of CH_4 from oceans is estimated with 3 % (Denman et al., 2007). Recent investigations found CH_4 by the decay of organic matter, e.g. under temperature or the influence of ultraviolet (UV) irradiation from terrestrial plant foliage (Vigano et al., 2009; Bloom et al., 2010). Moreover, soils showed CH_4 formation after

several treatments, such as UV irradiation or heating (Chapter 7, 8) (Jugold and Keppler, 2009; Hurkuck et al., 2012; Jugold et al., 2012).

1.3.2 Biotic methane formation

In general, biotic CH_4 formation is related to methanogenic microorganisms (archaea) as product of the reduction of CO_2 or methyl groups, e. g. from methanol or acetate (Ellefson, 1982; DiMarco et al., 1990; Michal, 1999; Hinderberger et al., 2008). The reaction pathways of CO_2 reduction to CH_4 by archaea is shown in Figure 1.7. Most of the global CH_4 budget is ascribed to these microorganisms living in the anoxic parts of natural wetlands (26 %), rice fields (11 %) and landfills (9 %) or other waste treatment systems. They further occur in the intestines of ruminants and termites (22 %) (Chen and Prinn, 2005; Cicerone and Oremland, 1988; Conrad et al., 1989; Denman et al., 2007). Reeburgh roughly estimated for biogenic sources that about 1 % of the primary productivity results in CH_4 production (Reeburgh, 2003). Only the half amount is then emitted to atmosphere while the remainder is oxidized by closely situated methanotrophs (Hanson and Hanson, 1996; Reeburgh, 2003). To oxidize the CH_4 these methanotrophs need aerobic habitants such as oxic soil layers, micro sites or the surfaces of plant roots (Conrad, 2007). Often syntrophic consortia between methanogens and methanotrophs can be found (Takai et al., 2001; Conrad, 2007).

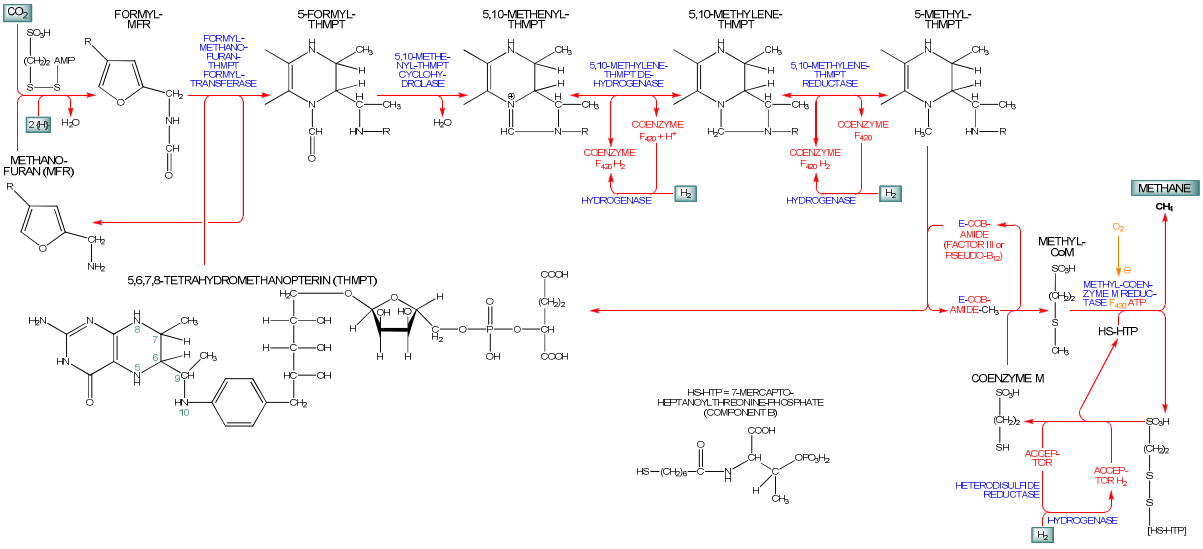

Figure 1.7: Pathways of microbial CH_4 production by reduction of CO_2. Anoxic respiration of *Methanobacterium thermoautotrophicum* (taken from Michal (1999), modified).

It came as a surprise when Keppler et al. (2006) identified plants as a source of CH_4 formation. In the following years this finding has been controversially discussed among the scientific community (Keppler et al., 2006; Dueck et al., 2007; Keppler and Röckmann, 2007; Kirschbaum et al., 2007; Beerling et al., 2008; Keppler et al., 2008; McLeod et al., 2008; Vigano et al., 2008; Wang et al., 2008; Brüggemann et al., 2009; Bruhn et al., 2009; Messenger et al., 2009; Nisbet et al., 2009; Qaderi and Reid, 2009, 2011).

Nevertheless, the findings by Keppler et al. (2006) laid the foundation for the research on non-microbial aerobic CH_4 formation in the biosphere. A historical overview of the aerobic CH_4 formation is given by Vigano (2010) and a detailed differentiation of the investigation results was reviewed by Bruhn et al. (2012). The research field of non-microbial aerobic CH_4 formation differentiated in two main parts. Whereas the first part deals with the aerobic CH_4 formation of detached and often dried plat material, e.g. during heating or UV irradiation, the second one is about CH_4 formation by living plants.

Since the present work involves investigations on CH_4 formation by living plants (Chapter 6), a short overview of this research area is provided in the following paragraph.

In 2005, Frankenberg et al. analysed global CH_4 data retrieved from the SCIAMACHY satellite. They detected unexpectedly elevated CH_4 concentrations in tropical regions above the evergreen forest. This new CH_4 source of 30-40 Tg yr^{-1} (Aug-Nov) could not be explained by the global budget at that time, but with the findings of Keppler et al. (2006) who assessed the strength of CH_4 formation by plants of 62-236 Tg yr^{-1}. But, already in the same year this contribution to the global budget was down scaled by Kirschbaum et al. (2006) to a maximum of 10 % and by Parsons et al. (2006) to around 3-4 % of the budget. At the same time emissions of CH_4 from tropical savannah and forest vegetation (Crutzen, 2006; Sanhueza and Donoso, 2006) were suggested to explain a fraction of the global source strength from plants. Houweling et al. (2006) used atmospheric transport model simulations and compared them with background CH_4 concentrations, values of stable carbon isotope ratios of CH_4 and satellite measurements. These investigations led to an upper limit of 85 Tg yr^{-1} or less than 15 % for the preindustrial global CH_4 budget.

A link of CH_4 emission to stress and injury was found by Qaderi et al. (2009) and Wang et al. (2009, 2011). The CH_4 emission rates found for stressed crops presented by Qaderi et al. (2009) were in the same range as those found by Keppler et al. (2006). However, the use of static chambers flushed with synthetic air and its problems to quantify the CH_4 fluxes remains uncertain and was criticised by Ortega et al. (2008).

In 2009, Brüggemann et al. investigated the CH_4 release using isotope labelling of young poplars grown in a $^{13}CO_2$ atmosphere. Investing the gas phase, they found $^{13}CH_4$ emitted from the poplars. Stable isotope labelling was also used by Wishkerman et al. (2011) who investigated the formation of CH_4 by ^{13}C-labelled tobacco cells (BY2). In their experiments the cells were treated with the cytochrome c oxidase inhibitor NaN_3 acting in the electron transport chain (ETC) of cell's mitochondria. Both clearly confirmed that the CH_4 is produced in plants per se and not by associated micro-organisms.

However, details of CH_4 precursors or reaction paths were still unknown. For plant structure components progresses already have been made. A suggestion for a possible mechanism was given by Sharpatyi (2007) who introduced photo-induced radical reactions in cellulose. Furthermore, methoxy groups of pectin were found to act as CH_4 precursor when pectin was heated or irradiated with UV light (Keppler et al., 2008).

The work presented in this dissertation is another milestone in the research on non-microbial aerobic methane formation. Chapter 4 and 5 propose chemical pathways of CH_4 formation that might take place in many bio systems. Chapter 6 identifies for the first time a precursor component of CH_4 formed in living plants.

Chapter 2

About plants

2.1 Plant cell

The plant cell mainly differs from animal cells by containing a vacuole for cell pressure regulation, storage of compounds as well as lytic compartment, chloroplasts to enable photosynthesis and a cell wall made of cellulose, hemicelluloses and pectin (Figure 2.1). Other organelles are comparable. Here, mentioned are peroxisomes and mitochondria. The abandonment of the peroxisomes is to build and decompose hydrogen peroxide (H_2O_2). Mitochondria are energy producing organelles, for that reason they are often called *the power plant* of the cells (see 2.2).

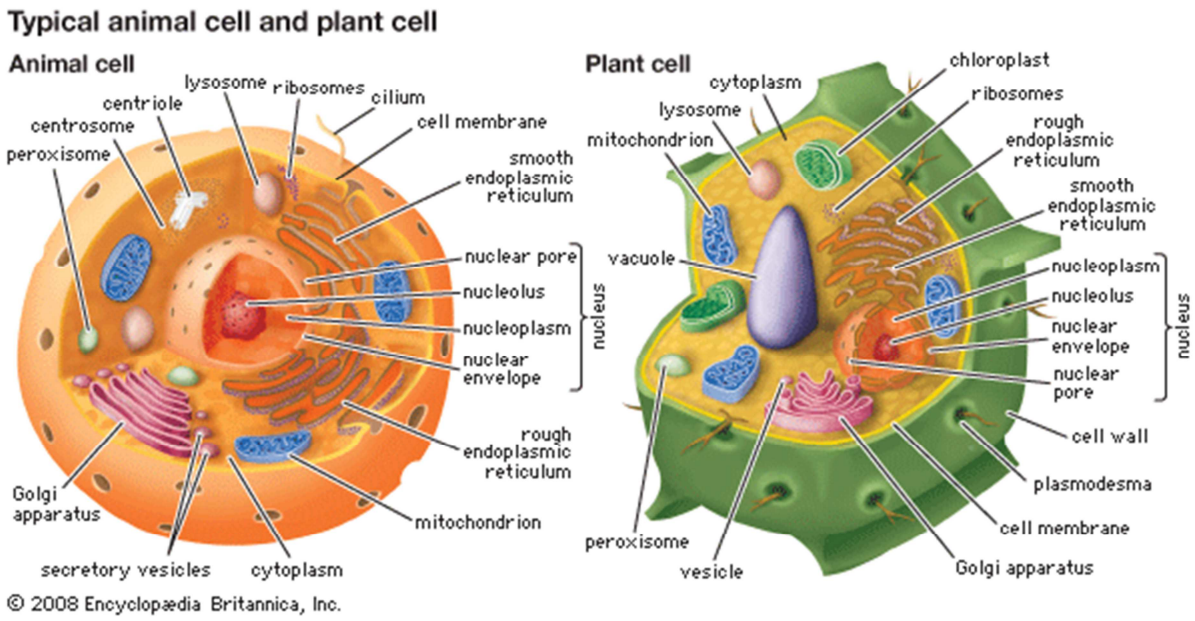

Figure 2.1: Scheme of the composition of an animal cell and a plant cell. Image shows constitution of both an animal cell and a plant cell with their organelles (Image taken from Encyclopaedia Britannica Online, from http://media-1.web.britannica.com/eb-media/02/114902-004-3D619106.gif).

2.2 Mitochondria

Whereas the plant absorbs CO_2 for its growth, mitochondria require oxygen (O_2) for their production of adenosine-5'-triphosphate (ATP) from adenosine-5'-diphosphate (ADP). This consumption of O_2 is part of the photorespiration in which mitochondria, peroxisomes and chloroplasts are mainly involved. A mitochondrion contains an outer and an inner membrane, at which the area between is named the intermembrane space (IMS). The outer

membrane contains a large number of integral proteins (porins) which form channels allowing small molecules and ions to pass the outer membrane. The inner membrane is folded and therefore compartmentalized in numerous cristae, expanding the surface of the inner membrane up to five times and thus increasing the area of ATP synthesis. The matrix of the mitochondrion, the space enclosed by the inner membrane, contains among others the mitochondrial deoxyribonucleic acid (DNA), special mitochondrial ribosomes for protein production from transfer ribonucleic acid (tRNA) and the embedded ATP synthase particles. Furthermore, in the matrix includes the citric acid cycle (Krebs-cycle), a series of energy producing reactions which oxidize acetate to CO_2 and H_2O. Figure 2.2 shows the schematic structure of a mitochondrion.

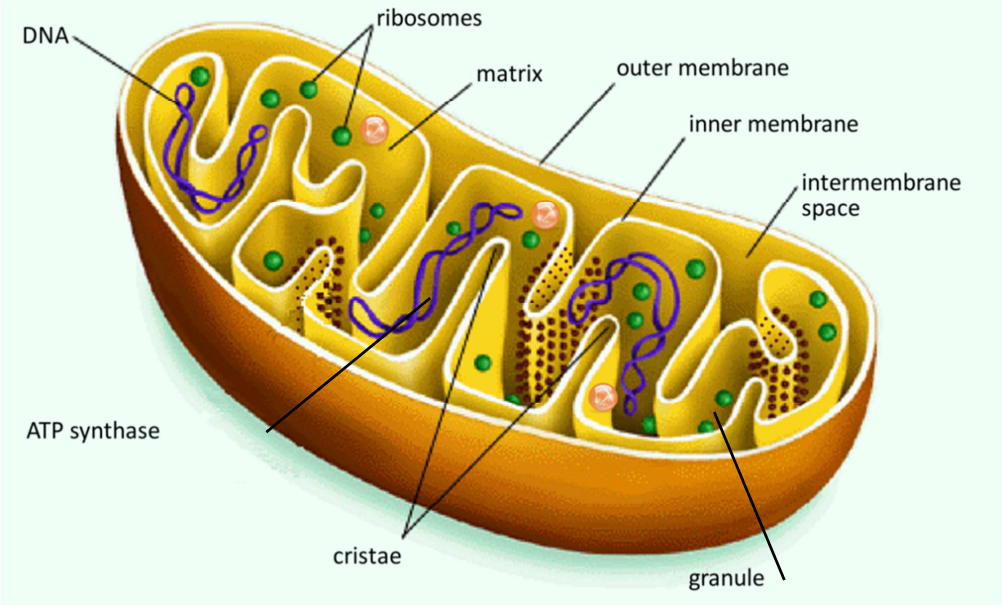

Figure 2.2: Schematic drawing of a mitochondrion cut longitudinally. Shown are the outer membrane, the folded inner membrane with cristae end embedded ATP synthase particles, DNA, granules and ribosomes (Image taken from Encyclopaedia Britannica Online, from http://media-3.web.britannica.com/eb-media/89/22489-004-EE9DC4F5.gif, modified).

2.3 Cellular respiration

The cellular respiration (aerobic respiration) is carried out by mitochondria of eukaryotic cells to gain energy by the synthesis of ATP. The most commonly used starting material is D-glucose but fatty acids and amino acids can be processed as well. These nutrients are oxidized using molecular oxygen (O_2). Thus, D-glucose is completely oxidized to CO_2 and H_2O. Collectively, the cellular respiration can be classified in four parts producing different

amounts of ATP: The glycolysis, the oxidative decarboxylation, the citric acid cycle and the oxidative phosphorylation.

The glycolysis is located at the cytoplasm. During this process D-glucose is converted into two molecules of pyruvate, which are transported through the inner membrane into the matrix of a mitochondrion. Here, pyruvate is decarboxylated and combined with coenzyme A (CoA) to form the thioester acetyl coenzyme A (acetyl-CoA). While passing through the citric acid cycle the CoA is regenerated and attached acetyl is completely oxidised to CO_2 and H_2O. During the oxidation the coenzymes nicotinamide adenine dinucleotide (NAD^+) and flavin adenine dinucleotide (FAD^+) were reduced to NADH and $FADH_2$. However, the highest amount of ATP is gained during oxidative phosphorylation by ATP synthase enzymes which are embedded in mitochondrial cristae. The required energy and proton gradient (chemiosmotic potential) is obtained by the ETC.

2.4 Electron transfer chain

At the inner membrane of mitochondria numerous ATP synthase enzymes are embedded. These enzymes combine inorganic phosphor (P_i) and ADP molecules to ATP. This process requires a proton (H^+) flow from the IMS through the ATP synthase into the mitochondrial matrix. This proton flow is established by a proton gradient (chemiosmotic potential) that is generated by the respiratory complexes I-IV in the inner membrane. The complex I utilize electrons from NADH molecules, produced by the citric acid cycle in the matrix, to pump H^+ from the matrix to the IMS (Figure 2.3).

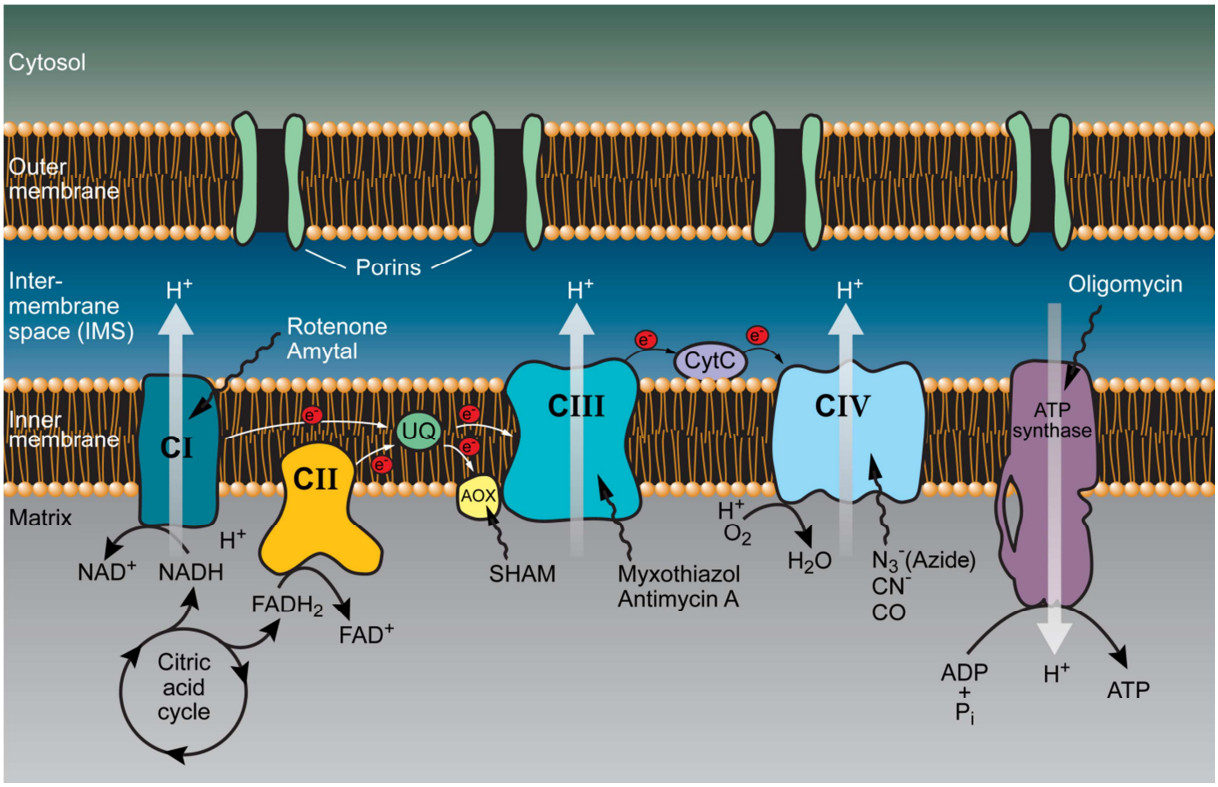

Figure 2.3: Scheme of mitochondrial electron transport chain. Wiggly lines indicate the target of the attributed inhibitors. CI-CIV, respiratory complexes I-IV; UQ, ubiquinone; AOX, alternative oxidase; Cyt c, cytochrome c.

The electrons are then transferred through the inner membrane to complex III (CIII) and subsequently to complex IV (CIV) were they are used in each case to pump H^+ from the matrix to the IMS. From CIII the electrons are shuttled to CIV by reducing cytochrome c (Cyt c) at IMS side of the inner membrane. At CIV the Cyt c gets oxidized and finally electrons are transferred at the matrix side to O_2 that combining with H^+ to H_2O. In addition, this consumption of H^+ increases the chemiosmotic potential of the mitochondrion.

The ETC can be interrupted by several toxins. In Figure 2.3 wiggly lines show where the different toxins inhibit the transfer of the electrons. For instance bind the three toxins azide (N_3^-), cyanide (CN^-) and carbon monoxide (CO) to the reactive centres of the cytochrome c oxidase (CIV).

2.5 Gas exchange

The gas exchange of plants implies the uptake of CO_2 and the emission of water vapour (H_2O) and oxygen (O_2) from and to the surrounding atmosphere, respectively. The exchange itself is driven by diffusion of the molecules. This exchange takes place at pores, so called

stomata, located in leaf and stem epidermis. The pore consists of a pair of guard cells, specialized parenchyma cells, and surrounding subsidiary cells.

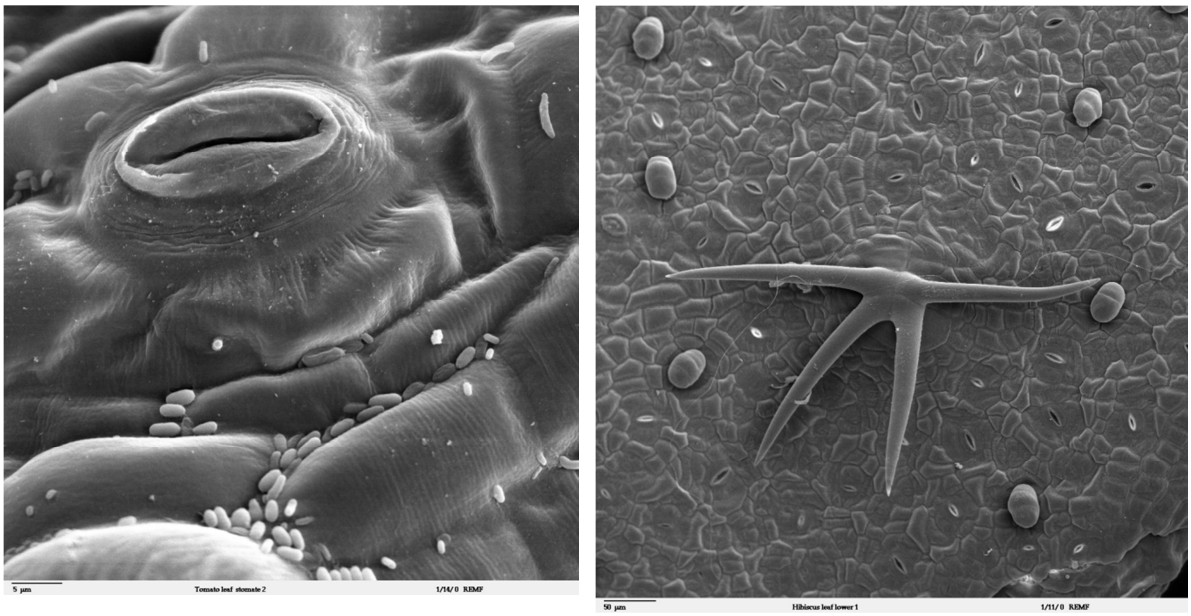

Figure 2.4: Scanning electron resonance (SEM) images of stomata. Left) Single stoma of a tomato leaf (*Lycopersicon esculentum*) with low degree of aperture. Scale bar at the left bottom is 5 µm. **Right)** Hibiscus leaf (*Hibiscus schizopetalus*) with numerous stomata (small slits) and trichomes in the middle. Scale bar at the left bottom is 50 µm (http://remf.dartmouth.edu/images/botanicalLeafSEM/index.html).

The degree of stoma aperture is regulated by the water content of the vacuole and the resulting turgor of the guard cells (Buckley et al., 2011; Lange et al., 1971; Mott and Parkhurst, 1991). Stomata are more opened when turgor is high and guard cells are taut. At this point the surrounding subsidiary cells are limp. Most plants stomata turgor is affected by blue light irradiating the leaves (Farquhar and Sharkey, 1982). The so induced transport of potassium ions (K^+) and malate^{2-} from cytoplasm into the vacuole followed by H_2O diffusion into vacuole due to the rising osmotic pressure (Jarvis and Mansfield, 1981).

In case of H_2O deficiency abscisic acid is released by the plant that results in remove of K^+ and malate^{2-} from guard cells vacuoles. The consequence is an effusion of H_2O from vacuole and decreasing turgor by reverse osmotic pressure. The guard cells are shrinking and the stomata slits are closing. Hence, no further water vapour is lost from leaves (Jarvis and Mansfield, 1981).

Chapter 3

Measurement systems

3.1 GC-FID - Gas chromatograph with flame ionisation detector

Gas chromatography has become one of the most important analytic tools in separation and determination of trace amounts of organic substances, such as CH_4, in gas samples. A Shimadzu GC-14B gas chromatograph was used to determine the amount of formed CH_4.

The principle of compound separation in the gas chromatography system is based on the interaction between the sample compounds and the filling (stationary phase) of the separation column. A carrier gas (mobile phase) is flushing the sample gas mixture through the column. For analysis done in this work synthetic air was used as mobile phase and a 2 m high-grade steel tube (inner diameter of 3.175 mm) packed with Molecular Sieve 5A 60/80 mesh was used as separation column. This molecular sieve adsorbent is a synthetically produced zeolite (aluminosilicate minerals) with a particle size of 60-80 mesh and provides pores of 5 Å. Pores and internal cavities of these zeolites are of extremely uniform dimensions (Sigma-Aldrich). The temperature of the column was set to 125 °C which allows separating the CH_4 from air and carrier gas in an adequate analysis time per sample (2 min).

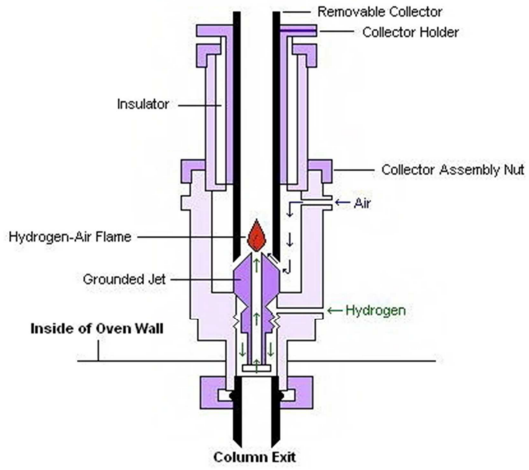

Figure 3.1: Scheme of an flame ionisation detector. Eluted and separated gas sample components reach the detector at the exit of the column at the bottom of the image (http://chemwiki.ucdavis.edu/Analytical_Chemistry/Instrumental_Analysis/Chromatography/Gas_Chromatography?highlight=gas+chomatography).

The gas sample is injected to a six port valve containing a 2 mL sample loop. The sample is transferred from the loop to the column by the carrier gas under a pressure of 300 kPa. After the separation during the passage of the column the CH_4 reaches the detector. In this work a flame ionisation detector (FID) (Figure 3.1) was used to determine the amount of CH_4. Here, the separated and eluted gases coming from the column is mixed with air (45 kPa) and hydrogen (50 kPa) and burned afterwards in a special quartz chamber. Two electrodes supporting 300 V clasp the collector tube of the burner. The FID measures perturbations in the differential voltage due to ions produced in the flame when CH_4 is burned. Thus, a signal in mV is produced as a peak in the chromatogram. The area, received after integration of the peak over the time, is proportional to the amount of CH_4 in the sample. Thus, the measured area can be compared with the area produced by a reference gas containing a known amount of CH_4. The system allows measurements of CH_4 concentrations with a precision of ± 11 ppbv.

3.2 PreCon-GC-C-IRMS - Gas chromatography - combustion - isotope ratio mass spectrometry with cryogenic pre-concentration unit

Determining of the isotopic ratio of ^{13}C and ^{12}C atoms is an important analytical tool to follow reactions and to identify precursors of the products of interest. In this work the $\delta^{13}C$ values of CH_4 were determined using a HP6890 gas chromatograph coupled to a Thermo Finnigan DeltaPlusXL isotope ratio mass spectrometer (GC-C-IRMS, Figure 3.3). The devices are attached to an innovative cryogenic pre-concentration unit (PreCon). This PreCon with several purification and concentration steps was designed within the ORCAS group and built in-house (Figure 3.2). The system allows measurements of $\delta^{13}C$ values of samples containing mixing ratios down to 100 ppbv.

The sample vessel was directly connected to the cryogenic PreCon at inlet 1. Following evacuation of the sample loop (40 mL), a valve was opened to allow transfer of a sample of headspace from the sample vessel to enter the sample loop after passing through an Ascarite II chemical trap for removal of CO_2. Following equilibration, the sample was flushed with helium at 30 mL min^{-1} into two physical traps (Trap 1 and 2, Figure 3.2) which were temperature controlled in the range –196 °C up to 200 °C. The temperature of trap 1 (empty 1/8” stainless steel tube) was set at –150 °C to remove water and potential remaining CO_2. Trap 2 (1/8” stainless steel tube filled with Hayesep D) was cooled to –130 °C, a temperature

sufficient to trap CH_4 quantitatively. After a defined time period (10 min) trap 2 was rapidly heated to 50 °C (~10 s) and CH_4 flushed to a focus trap (50 cm × 0.25 mm i.d. PoraPlot column placed in liquid nitrogen, –196 °C) with helium at a flow rate of 2.5 mL min^{-1}. After 10 min, the focus trap was raised out of liquid nitrogen permitting the transfer of CH_4 to the GC-C-IRMS unit. The GC oven temperature was held isothermal at 30 °C.

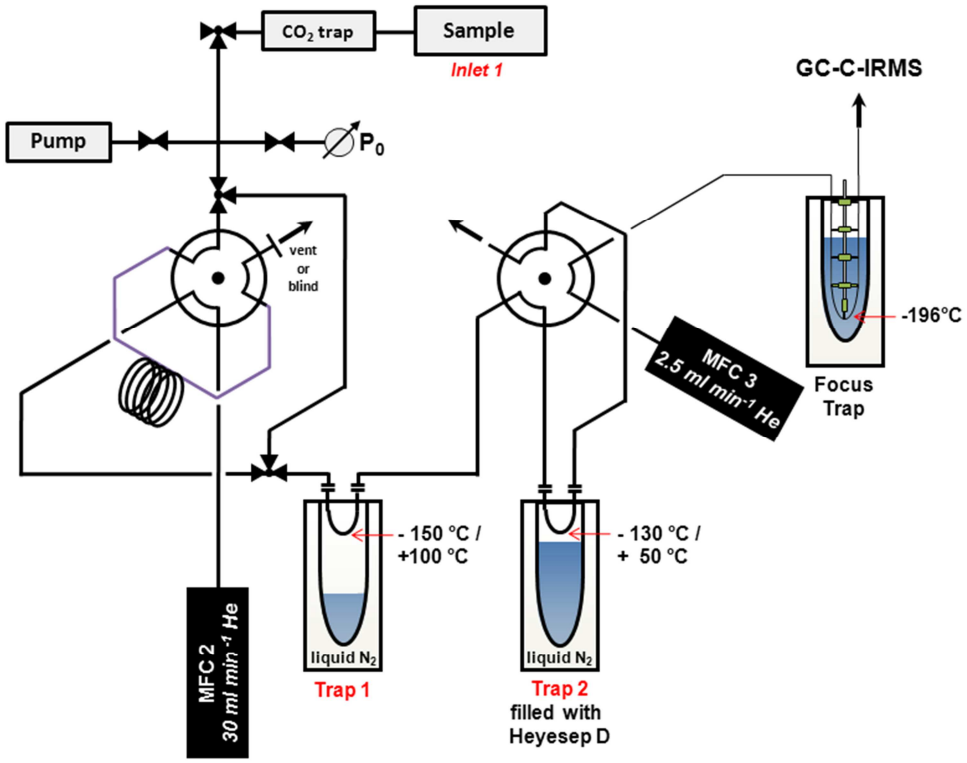

Figure 3.2: Scheme of the cryogenic pre-concentration unit. MFC, mass flow controller; P_0, pressure gauge (taken from Greule et al., 2012, modified).

The PreCon (described above) was directly coupled to the GC-C-IRMS system. After GC separation the analytes are combusted at 960 °C in an oxidative reactor. This reactor consists of a ceramic tube filled with Cu/Pt/Ni wire. Platinum serves as catalyst to oxidise the organic compounds in the sample to CO_2 and H_2O. The required O_2 for this catalysed oxidation is provided from the NiO which is regenerated itself by CuO (see Rct. 1-2). Thus, it is necessary to oxidise the hole reactor after a while when those metal oxides are exhausted.

$$CH_4 + 4NiO \xrightarrow{[Pt],\ \Delta} CO_2 + 2H_2O + 4Ni \qquad \text{(Rct. 1)}$$

$$Ni + 2CuO \longrightarrow NiO + Cu_2O \qquad \text{(Rct. 2)}$$

A followed reduction reactor, an alumina tube containing three Cu wires maintained at 600 °C, reduces any nitrogen oxides to nitrogen. In a next step the generated H_2O is removed by a water permeable Nafion® membrane since formed HCO_2^+ with a molecular mass of 45 that falsify the measurement of $^{13}CO_2$. Through an open split the formed CO_2 reaches the mass spectrometer and gets ionised by an ion source (electron impact; EI). Over another open split also a CO_2 reference gas can be transferred to the source. Dependent on the mass charge ratio (m/z) CO_2 molecules get spread by the influence of a strong magnetic field. At the detector the masses 44, 45 and 46 are registers by Faraday-Cups and a ratio between the different masses is calculated. The three masses of the CO_2 isotopomers can be composed as followed:

m/z 44: $^{12}C^{16}O^{16}O$

m/z 45: $^{13}C^{16}O^{16}O$ and $^{12}C^{17}O^{16}O$

m/z 46: $^{12}C^{16}O^{18}O$

The $^{13}C/^{12}C$ isotopic value is calculated by the quotient of the masses 45 and 44, whereas the amount of the $^{12}C^{17}O^{16}O$ isotopologue is subtracted. This can be done by calculation after recording the mass 46 since the ratio between ^{18}O and ^{17}O is constant in nature.

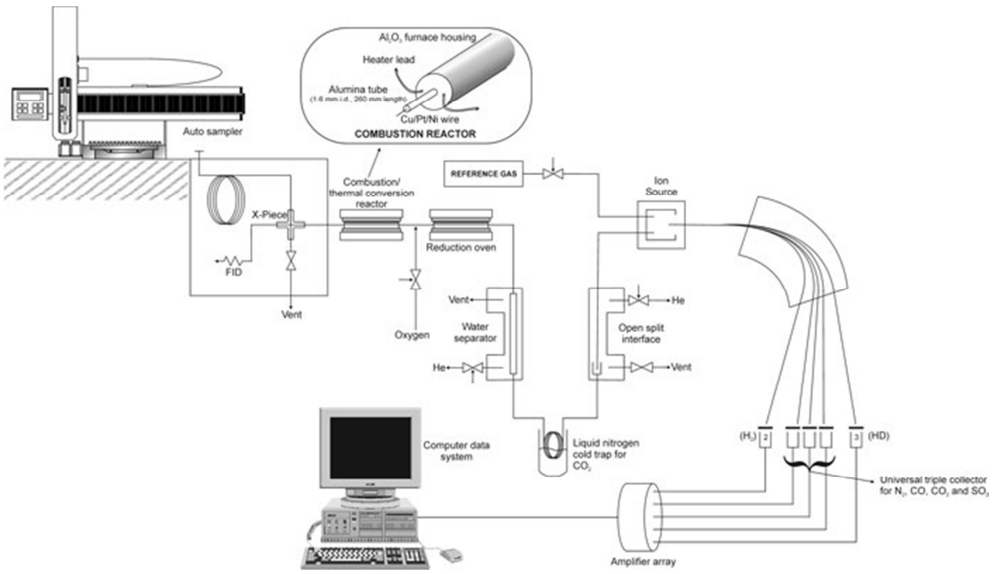

Figure 3.3: A scheme of a typical GC-C-IRMS system. Shown is a system with auto sampler and Faraday-Cups for H_2, HD and a universal triple collector. Beside CO_2 also gases such as N_2 or CO can be detected (http://www.bris.ac.uk/nerclsmsf/techniques/gccirms.html).

3.3 LC-TOFMS - Liquid chromatography with time of flight mass spectrometry

The mass analysis of molecules with small often proved to be difficult. Since the reaction products in this work own masses below 300 da an Agilent 1100 series HPLC coupled to an Agilent 6510 Q-TOF (Agilent Technologies, USA) was just for their identification.

The setup of the high performance liquid chromatograph (HPLC) is shown in Figure 3.4. The injected sample is flushed under high pressure through the separation column by a carrier liquid (mobile phase), consisting of a mix of different solvents. Often solvents are mixed with a gradient to increase separation performance. For product separation in this work a reverse phase column was used. This column consists of a 15 cm long stainless steel tube packed with surface modified silica. This surface is covert with strait alkyl chains with a length of 18 C-atoms (C18 column).

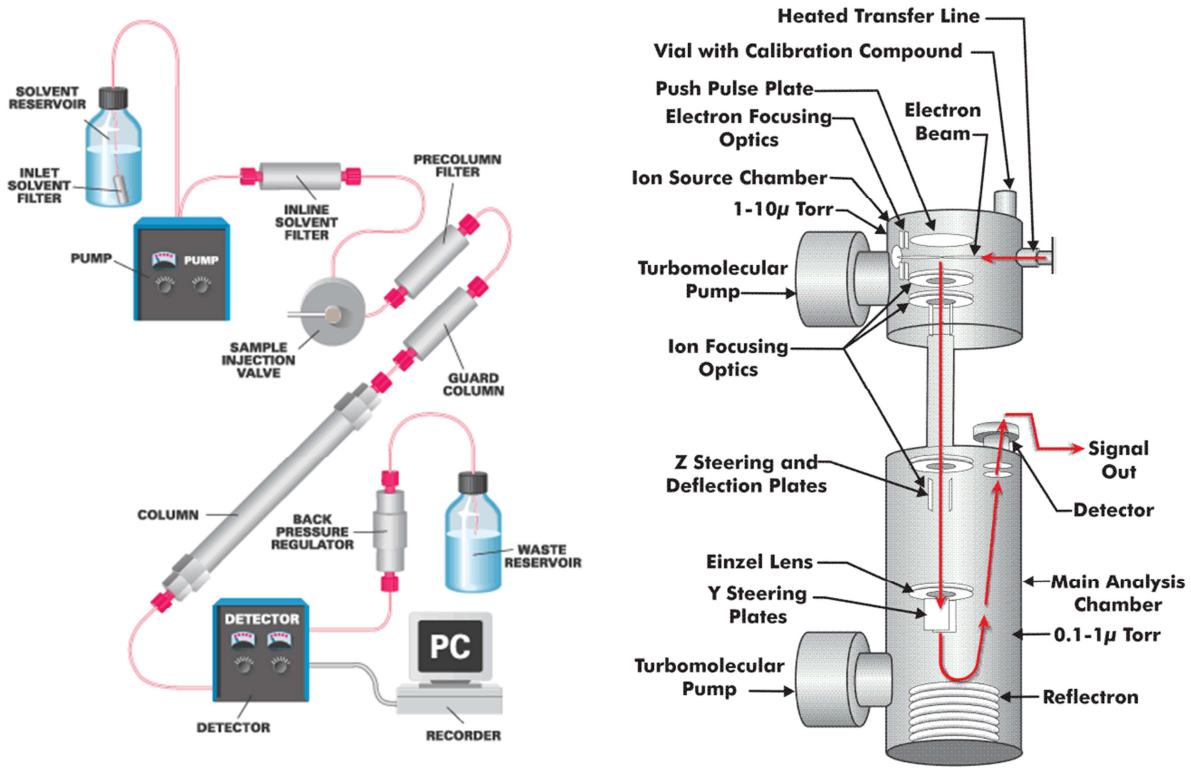

Figure 3.4: Components of the LC-TOFMS. Left) Schematic drawing of an HPLC setup. At the LC-TOFMS system the column output is connected to the heated transfer line of the mass device. **Right)** Schematic drawing of a TOFMS. The image shows the ion source chamber with acceleration pulse plate and the flight tube with reflectron and detector (http://www.idex-hs.com/support/upchurch/hplc_center.aspx; http://www.leco.com/products/sep_sci/pegasus _4d/ Pegasus4D.html, modified).

After the separation by the HPLC the single sample compounds are transferred to the time-of-flight (TOF) mass analysis device (Figure 3.4). The solved components are nebulised together with a reference in an ionisation chamber. While colliding with an electron spray (ESI) from an ion source sample components are ionised. A vacuum is transferring the beam to the analytic part of the device. The small solution droplets are now focussed to a beam by skimmers and electronic lenses. The solvent is split off and the ion beam is focussed to a thin ion band. Quadrupole mass analysers are used to filter the molecule ions of the sample depending on their mass/charge ratio. In a next chamber arriving molecule ions are fragmented by the collision with a reaction gas. With the help of an electronically pulse an amount of fragments is split off from the beam and accelerated to the flight tube. Here, depending on their mass the fragments require different times to reach the top and to fall way back to the surface of the detector unit. Often a contrary charged ion reflector/mirror (reflectron) is mounted at the end of the tube that further increases the separation effect of the fragments. The impacts of the single fragments are converted to photons and afterwards to electronically signals. The performance of this analysis method is very high. The acceleration plate can pulse up 10,000 times per second and one pulse can contain about 100,000 data points. This provides a spectrum with excellent ion statistics.

Chapter 4

Methane formation by oxidation of ascorbic acid using iron minerals and hydrogen peroxide

Published in *Chemosphere,* 2010.

Frederik Althoff[1]*, Alke Jugold*[1] *and Frank Keppler*[1]

Abstract

The possibility of methane formation in an oxidative environment has been intensely debated, especially since the discovery of methane generation by living plants. However, recent studies with animal tissue suggested that under specific conditions aerobic methane formation is also possible. Here, we investigated the generation of methane in an abiotic model system using bioavailable substances. We show formation of methane in a highly oxidative media, using ascorbic acid, ferrihydrite and hydrogen peroxide as reagents. Methane production was shown to be related to reagent ratio, reaction volume and pH. A 2:1 ratio of hydrogen peroxide to ascorbic acid, catalytic amounts of ferrihydrite and acidic conditions (pH 3) enhanced formation of methane. We further show that gaseous oxygen has a strong influence with higher levels found to inhibit methane formation. This study is a first step towards providing an insight for the reaction mechanism of methane formation that would be applicable to aerobic environments.

Keywords: ferrihydrite; goethite; vitamin C; oxidative environment

4.1 Introduction

Methane (CH_4) is the most abundant reduced organic compound in the atmosphere and plays a central role in atmospheric chemistry (Lelieveld et al., 1998). Sources of atmospheric CH_4 in the biosphere have until recently been attributed to originate from strictly anaerobic microbial processes, e.g. in wetland soils and the intestinal tract of ruminants. The only known exception was CH_4 production during incomplete combustion of biomass (Crutzen

[1] Max-Planck-Institute of Chemistry, J.-J.-Becher-Weg 27, 55128 Mainz, Germany.

and Andreae, 1990; Fischer et al., 2008) where formation was considered to occur via the recombination of methyl radicals with hydrogen atoms. It came as a surprise when Keppler et al. (2006) recently demonstrated that plants produce CH_4 also under aerobic conditions. Over the last three years the scientific community has debated the existence of this source (Dueck et al., 2007; Ferretti et al., 2007; Keppler and Röckmann, 2007; Kirschbaum et al., 2007; Vigano et al., 2008; Wang et al., 2008; Nisbet et al., 2009). According to established 'textbook' knowledge formation of a highly reduced molecule such as CH_4 in an oxidative environment under ambient conditions is highly unlikely. Therefore, a number of researchers have attempted to provide alternate explanations for the observed release of CH_4 from plants. For example, CH_4 emissions from vegetation may arise from methanogenesis that takes place in anoxic microenvironments of plant tissue or from dissolution of soil CH_4 and its transport above ground in the transpiration stream (Terazawa et al., 2007; Das and Baruah, 2008).

However, very recent observations in plant and animal biology (including stable isotope studies) have provided unambiguous evidence that several pathways exist by which CH_4 is generated under aerobic conditions (Ghyczy et al., 2008; Keppler et al., 2008; Keppler et al., 2009; Messenger et al., 2009). Based on their original work, Keppler et al. (2006) suggested the possibility of the involvement of the methyl moiety of the esterified carboxyl group (methoxyl group) of pectin in CH_4 formation. Consequently, Keppler et al. (2008) employed stable isotope analysis to demonstrate that methoxyl groups in plant pectin are indeed precursors of CH_4. McLeod et al. (2008) and Bruhn et al. (2009) further demonstrated the role of methoxyl groups in CH_4 formation when production from pectin upon UV irradiation virtually ceased following its de-methylesterification. Although details of the mechanism are still unknown, the studies of Keppler et al. (2008), McLeod et al. (2008) and Bruhn et al. (2009) provided an initial insight into potential plant precursors involved in CH_4 formation. Furthermore, an important role of UV-generated reactive oxygen species (ROS) was postulated by Messenger et al. (2009), who used ROS-generators to reveal that hydroxyl radicals and singlet oxygen are involved in CH_4 formation from methoxyl groups of pectin.

An alternative formation pathway for non-methanogenic CH_4 formation in animal cells was proposed by Ghyczy et al. (2003, 2008) who observed CH_4 formation in rat liver mitochondria. Based on their findings they hypothesized that electrophilic methyl groups

(EMG) of phosphatidylcholine (PC) molecules (a key building block of animal and plant membrane bilayers) are potential electron acceptors that may be converted to CH_4 if there is a deficiency of oxygen (Boros et al., 1999). To support their premise the authors further demonstrated formation of CH_4, carbon monoxide (CO) and carbon dioxide (CO_2) from a reaction mixture of hydrogen peroxide (H_2O_2), ferric ion (Fe^{3+}), ascorbic acid and choline (Ghyczy et al., 2003, 2008); natural components that are now known to be ubiquitous constituents in biological systems. The authors reported that whilst both CO and CO_2 production were independent of the presence of choline, CH_4 formation was only observed when it was included. These results indicate that the generation of CO and CO_2 in these reactions was a result of the oxidative breakdown of ascorbic acid, whereas CH_4 is presumably provided by the methyl groups of choline. However, as these reactions were both rapid and uncontrolled, i.e. the temperature of this exothermic reaction rose rapidly up to 95 °C with CH_4 formation observable after a few seconds, it is very difficult to compare them with biochemical reactions occurring in natural biological systems such as plants.

Intrigued by the findings of Ghyczy et al. (2003, 2008), we were particularly interested in examining the role of ascorbic acid in the formation of CH_4. We assumed that next to CO and CO_2, the CH_4 formation would also be possible when the reaction was performed under more controlled conditions. For this reason we examined the reaction of ascorbic acid, iron and hydrogen peroxide in much more detail. Thus, as well as ferric ions we also used different iron minerals such as ferrihydrite, goethite, hematite and lepidocrocite in our investigations. These iron compounds are ubiquitous in water, soil (Schwertmann et al., 1987) and biosystems like plants, animals and humans (Lewin et al., 2005). In living systems where higher levels of free iron are known to be toxic (Garcia-Alfonso et al., 1996), iron is present in complexes, e.g. heme or ferritin, a protein with a ferrihydrite similar core that plays a key role in controlling levels of iron in plants and animals (Lewin et al., 2005). We monitored reaction parameters, i.e. pH and oxygen content, that would likely influence formation of CH_4. Additionally, several other organic compounds were also tested for their ability to produce CH_4 with ferrihydrite and hydrogen peroxide under described controlled reaction conditions.

4.2 Material and Methods

4.2.1 Reagents

Ascorbic acid (ASC), acetylsalicylic acid, chitin, choline chloride, L-methionine, 2-methoxyphenol (guaiacol), pyrocatechol, pyruvic acid, vanillin, hydrogen peroxide 30 % (H_2O_2), iron(III) nitrate nonahydrate, quartz sand (SiO_2) and sodium hydroxide 0.1 M (NaOH) were obtained from Sigma, Taufkirchen, Germany, in the highest purity available. Ferrihydrite (FH), goethite, hematite and lepidocrocite were synthesized as prescribed by Schwertmann and Cornell (2000). Double distilled water (H_2O) filtered with an ELGA UHQ-II-MK3 was used for these investigations.

4.2.2 Reaction vials

Two types of glass vial were used: 40 mL, obtained from Supelco (27184) and 360 mL, made in-house by modification of a 300 mL Erlenmeyer-flask (Duran Group, 21 216 39) to fit the neck and thread of the 40 mL vial. Both types of vial were sealed using a hole type screw cap (Supelco, 27187) fitted with a PTFE/silicone septum (Supelco, 27188-U).

4.2.3 Experimental setup

All samples were prepared in a fume hood.

4.2.4 Investigations with different iron containing minerals

Different amounts (4 to 80 µmol) of the iron minerals (FH, goethite, hematite and lepidocrocite) were placed in the 360 mL vials. To each vial, 500 µmol ASC dissolved in 4 mL H_2O were added and the vials sealed with the screw cap containing a PTFE lined silicone septum. One mmol H_2O_2 in 1 mL H_2O was injected into each vial through the septum with a syringe. Vials plus contents were incubated at 22 ± 2 °C with shaking at 160 rpm and the headspace analysed for CH_4 content at various time intervals.

4.2.5 Investigations with SiO_2

Different amounts of SiO_2 (15 to 7500 µmol) were placed in 40 mL vials and 50 µmol ASC dissolved in 0.9 mL H_2O added to each. The vials were sealed as before and 100 µmol H_2O_2 in 0.1 mL H_2O injected into each through the septum and the samples incubated as above for 5 h. At the end of the incubation period the vial headspace was analysed for CH_4 content.

4.2.6 Other organic compounds as methane precursors

Choline, vanillin, acetylsalicylic acid, chitin, choline chloride, L-methionine, 2-methoxyphenol (guaiacol), pyrocatechol and pyruvatic acid were all tested for their potential to release methane. Four µmol FH were placed in 40 mL vials and 50 µmol of the organic compound dissolved in 0.9 mL H_2O added to each. The vials were sealed as before and 100 µmol H_2O_2 in 0.1 mL H_2O injected through the septum and the samples incubated as above for 5 h prior to CH_4 headspace analysis.

4.2.7 Effect of hydrogen peroxide concentration

H_2O_2 solutions were prepared in concentrations between 0.1 and 5.0 M. Four µmol FH were placed in 40 mL vials and 50 µmol ASC dissolved in 0.9 mL H_2O were added to each. The vials were sealed and concentrations from 10 to 400 µmol H_2O_2 in 0.1 mL H_2O were injected through the septum and the samples incubated for 5 h prior to CH_4 headspace analysis.

4.2.8 Effect of pH

Experiments were conducted at pH 1, 3, 5, 7, 9 and 12. For all pH values 100 µmol ASC were dissolved in 0.4 mL H_2O and stirred in a small glass beaker with a magnetic stirrer. After adjusting the respective pH value by addition of hydrochloric acid (HCl) (0.1 M) or NaOH (0.1 M) with the aid of a pH meter (Mettler Toledo FE 20), the solutions were filled up to 2 mL with phosphate buffer (Sørensen) of the respective pH. One mL of this adjusted solution was transferred to a 40 mL vial containing 4 µmol FH, before the vial was closed. Then 100 µmol H_2O_2 in 0.1 mL H_2O were injected through the septum and the samples were shaken for 5 h before gas phase was analysed.

4.2.9 Effect of reaction volume

A series of samples were prepared with constant reagent amounts but with varying reaction volumes between 0.2 and 5 mL. For 0.2 and 0.5 mL reaction volume, 4 µmol FH were placed in a 2 mL vial and 50 µmol ASC in either 0.1 or 0.4 mL H_2O added. These 2 mL vials were then positioned at the bottom of the 40 mL vials. For 1 to 5 mL the reagents were directly placed in the 40 mL vials. The vials were sealed and 100 µmol H_2O_2 in 0.1 mL H_2O injected through the septum and for the lower reaction volumes directly into the 2 mL vial. The samples were shaken for 5 h prior to CH_4 headspace analysis.

4.2.10 Effect of headspace atmosphere

Samples were prepared in a similar fashion to that described above (see other organic compounds as methane precursors) except that prior to the start of the experiment the reaction vials and stock solutions were flushed with synthetic air (20.9 % O_2), pure oxygen, or pure nitrogen for 15 min at rates of 250 mL min^{-1}.

4.2.11 Methane measurements

Headspace (5 mL) from the sealed glass vials was sampled using a Hamilton gas syringe (1010SL 10 mL SYR (22/2"/2)L) fitted with a point style no. 5 (RN NDL 6/PK (22/2"/5)L) needle and analysed by a gas chromatograph (column: 2 m, Ø=3.175 mm high-grade steel tube packed with Molecular Sieve 5A 60/80 mesh from Supelco) equipped with a flame ionization detector (GC-FID) (Shimadzu GC-14B). Quantification of CH_4 was performed by direct comparison of peak area with that obtained with two reference standards containing 8.905 and 1.905 ppm. All samples were prepared in triplicate (n=3) unless otherwise stated in the manuscript. Control samples (blanks) were prepared in a similar fashion to that described for the samples but without the addition of FH. The control measurements usually reflected the CH_4 background concentration of laboratory (range 2-2.2 ppm).

4.3 Results and discussion

In a first step we repeated the experiments reported by Ghyczy et al. (2003, 2008) using ascorbic acid (ASC), hydrogen peroxide (H_2O_2) and ferric ion (Fe^{3+}) as reactants. Upon addition of Fe^{3+} to a solution of ASC, the colour of the solution immediately changed from yellow to colourless, because of the reduction of Fe^{3+} to Fe^{2+} (ferrous ion) by ASC. As expected, addition of H_2O_2 changed the colour back to yellow according to the Fenton reaction. No measurable CH_4 was observed in the headspace above the solutions after the 24 h incubation period. These initial experiments were conducted at high concentrations (10 mM) of Fe^{3+} but we also applied dilutions of Fe^{3+} and Fe^{2+} in 10 % steps down to trace concentrations (0.1 µM) and varied the order of reagent addition, e.g. by adding Fe^{3+} to a solution containing ASC and H_2O_2. Furthermore we used Cu^{2+} to induce the Fenton reaction because it's known to generate more effectively OH radicals (Fry et al., 2002). None of the experiments led to significant CH_4 production. These findings are consistent with those reported by Ghyczy et al. (2003) when only ASC, H_2O_2 and dissolved Fe^{2+} or Fe^{3+} were used as reagents. They also indicate that the sequence of reactions producing CH_4 from ASC differs

from the Fenton reaction, that generates OH radicals which can attack organic compounds (Fry, 1998; Fry et al., 2002) and generate CH_4 from dimethyl sulfoxide (Repine et al., 1979).

4.3.1 Effect of iron mineral form on methane formation

Next, instead of using dissolved Fe^{3+}, we investigated several iron oxyhydroxides such as ferrihydrite ($5Fe_2O_3 \cdot 9H_2O$), goethite (α-FeOOH), hematite (α-Fe_2O_3) and lepidocrocite (γ-FeOOH). These minerals are known to have large surface areas, e.g. ferrihydrite with up to 600 $m^2\ g^{-1}$ (Schwertmann and Cornell, 2000), which are advantageous for surface and complexation reactions (Vikesland and Valentine, 2002). Furthermore, these naturally occurring iron minerals can initiate mineral catalysed Fenton-like reactions when hydrogen peroxide is provided and cause degradation of organic compounds (Liou and Lu, 2008). Moreover, it has been shown that the reductive dissolution of iron from FH can oxidise organic aromatic compounds such as catechol and guaiacol with the formation of CO_2 (Pracht et al., 2001) and halomethanes (Keppler et al., 2000).

Ferrihydrite, with about 60 nmol CH_4 formation after 53 h, was found to be the best iron source (Figure 4.1). This was followed by lepidocrocite (30 nmol) whilst with hematite and goethite little or no formation of CH_4 was observed. The redox potential (E_h) measured during the reaction, where FH was used as the mineral phase, was in the range of +300 to +500 mV indicating a highly oxidative environment. CH_4 formation was not observed in any experiment which had been performed without the addition of H_2O_2 or iron minerals. Moreover when different amounts of finely powdered quartz sand (SiO_2) were used as a direct replacement for FH no formation of CH_4 was noted. Based on these results all further experiments in this study were conducted with FH as the iron mineral species.

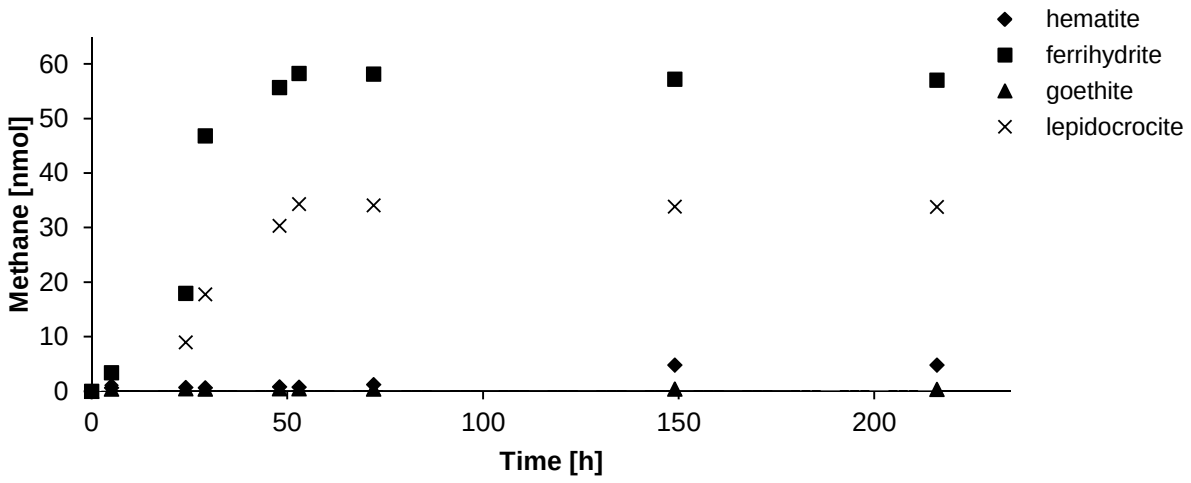

Figure 4.1: Formation of methane using different iron mineral species. The initial amounts of compounds were 4 µmol FH, 20 µmol hematite and 40 µmol of the other iron mineral species (equates to 40 µmol Fe), 500 µmol ASC and 1000 µmol H_2O_2 in 10 mL H_2O (360 mL vial). Data show mean value (n=3). The RSD ranged from 5 to 20 %.

4.3.2 Investigations with other organic compounds as methane precursors

We also studied a number of other organic chemicals (see Figure 4.2) for CH_4 formation when using FH and H_2O_2. As some of the compounds tested, such as choline, 2-methoxyphenol, vanillin and L-methionine, contained a methyl group it was considered that this moiety might react with FH and H_2O_2 and then recombine with hydrogen to form CH_4 by a radical mechanism similar to that recently described by Sharpatyi et al. (2007) and Messenger et al. (2009). However, ASC was the only compound of the nine chosen candidate chemicals found to produce CH_4. An explanation could be that ASC has the property to deliver protons as an acid (pK_a = 4.17) and provide electrons from the deprotonated form in a radical way. However, delineation of the reaction pathway was beyond the scope of this present study.

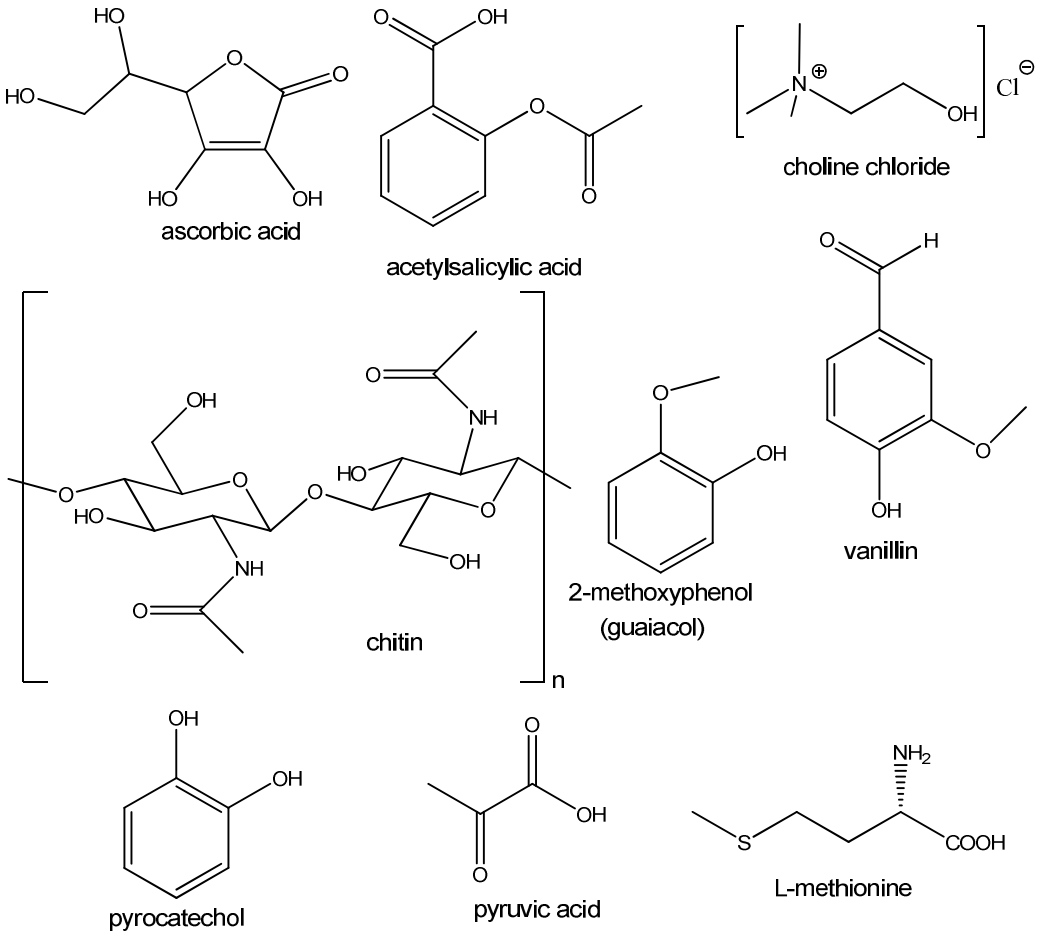

Figure 4.2: Chemical structure of organic compounds tested for methane formation.

4.3.3 Factors that control formation of methane from ASC

A series of parameters, including concentration of FH and H_2O_2, pH, reaction volume and gas atmosphere, anticipated to affect formation of CH_4 from ascorbic acid were investigated.

4.3.3.1 Time course with different amounts of ferrihydrite

Methane formation as a function of time with varying amounts of suspended FH and same concentrations of dissolved ASC and H_2O_2 was studied (Figure 4.3). The experiments were conducted over a 53 h period and samples of headspace were measured for CH_4 content after 5, 24, 29 and 53 h. In addition headspace from samples containing 40 and 80 µmol FH was also measured after 0.5 and 2.5 h. All samples showed significant CH_4 formation over time but with very different apparent kinetics. Interestingly, two main trends were clearly visible: (1) with higher amounts of suspended FH lower maximum formation of CH_4 was found, and (2) with lower amounts of FH it took a longer time to reach maximum formation. For example, samples containing 5 µmol FH produced on average 105 nmol of CH_4 after 29 h whereas with 80 µmol FH production with a maximum of 20 nmol CH_4 was already

completed after a reaction time of only 2.5 h. Thus, further experiments were conducted with lower amounts of FH.

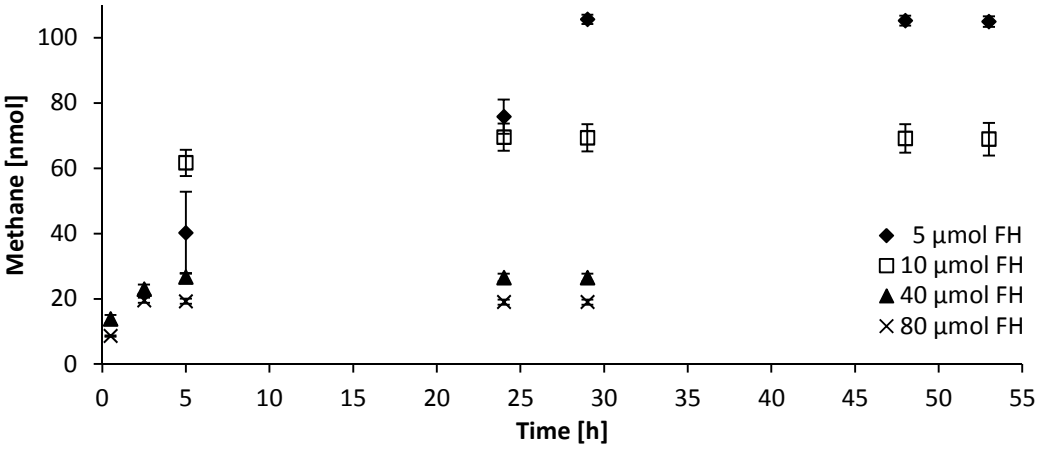

Figure 4.3: Time course formation of methane. Time course using different amounts of FH, varying between 5 and 80 µmol, 500 µmol ASC and 1000 µmol H_2O_2 in 10 mL H_2O (360 mL vial). Data show mean value ± SD (n=3).

4.3.3.2 Effect of ferrihydrite and hydrogen peroxide reactant ratios

A set of experiments was designed to optimize CH_4 production by altering the molar ratio between FH and H_2O_2 whilst maintaining a constant amount of ascorbic acid (Figure 4.4).

Experiments described in 3.3.1 were repeated but his time with amounts of suspended FH varying between 1 and 12 µmol. Headspace samples were measured for CH_4 content after 5 and 24 h. From Figure 4.4a it can be seen that after a 5 h incubation period CH_4 formation increased as the amounts of FH were decreased from 12 to 4 µmol. No further increase in CH_4 was observed in the range of 4 to 1 µmol FH after 5 h incubation time. Monitoring the same samples after the 24 h incubation period did not significantly change the amount of CH_4 formed when the amount of FH added was 4 µmol or more. However, after the longer incubation period a different trend was observed when FH was below 4 µmol where CH_4 formation increased with decreasing FH content. This pattern is in accordance with the results shown in Figure 4.3 and again suggests that whilst smaller amounts of FH will cause higher CH_4 formation this will require longer incubation times. For practical reasons it was not possible to reduce the amount of suspended FH to values below 1 µmol.

In the case where FH and ASC were both kept constant and concentration of H_2O_2 was varied (Figure 4.4b), maximum CH_4 formation was observed with 100 µmol H_2O_2 and a molar ratio of H_2O_2:ASC of 2:1. For these experiments nine replicate samples were measured (n=9) since large standard deviations, particularly when CH_4 formation was highest, were observed. Increasing the reaction time from 24 to 48 h did not further increase the CH_4 production. Combining the results presented in Figure 4.3 indicates that there are probably at least two competing reactions controlling the formation of CH_4.

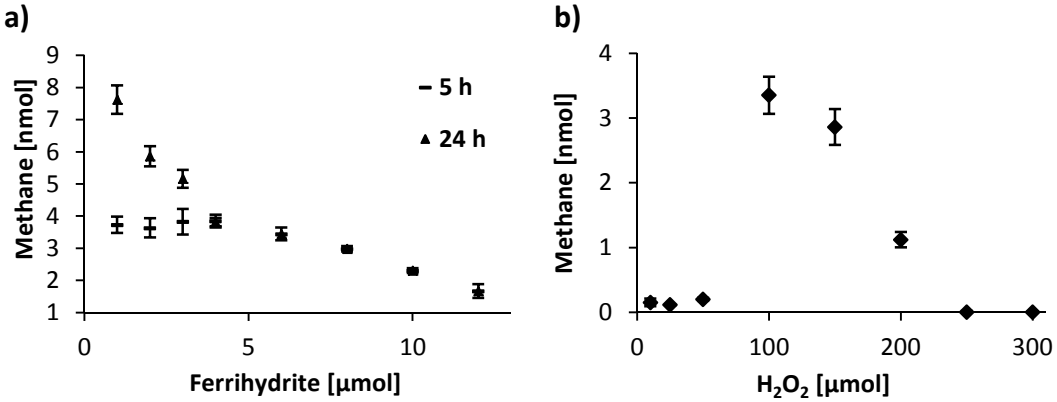

Figure 4.4: Effect on ferrihydrite and hydrogen peroxide on methane production. Methane formation from (a) 50 µmol ASC, 100 µmol H_2O_2 with varying amounts of FH in 1 mL H_2O (40 mL vial), measured after 5 and 24 h and (b) varying amounts of H_2O_2 added to 50 µmol ASC and 4 µmol FH in 1 mL H_2O (40 mL vial), measured after 5 h. (Data show mean value ± SD, n=3 (a); n=9 (b)).

4.3.3.3 Effect of pH and reaction volume

To test the influence of the pH on CH_4 formation an experiment was conducted where production was monitored across the pH range 1-12. Highest CH_4 formation (ca. 3.5 nmol) was observed at pH 3, whilst at higher pH (5 to 12) little or no formation was measured (Figure 4.5a). At pH 1 the amount of CH_4 produced (around 1 nmol) was significantly higher than at pH ≥ 5 but considerably lower than at pH 3. One plausible explanation may be that deprotonation of ASC plays a role in the generation of CH_4 in the reaction with FH and H_2O_2. At pH 3, where highest CH_4 formation was measured, the equilibrium of ASC is towards the deprotonated form (pK_a = 4.25) and this might increase the reactivity of the oxygen-atom(s) of ASC. At pH 1 the equilibrium is shifted towards the protonated form and the –OH groups of the ASC molecules might then not react as easily with other compounds, e.g. OH radicals or Fe^{2+}/ Fe^{3+}. In addition the lower pH range increases the dissolution of FH and also supports the Fenton reaction (in opposite to pH 5, where the solubility of FH is limited and

where little CH_4 was measured). However, there are many other possibilities which might explain our observations such as surface charge and catalytic capacity changing greatly with pH.

In another set of experiments we evaluated the effect of reaction volume on CH_4 formation whilst keeping the amounts of reactants constant. Therefore 50 µmol ASC, 4 µmol FH and 100 µmol H_2O_2 were placed in varying volumes ranging from 0.2 to 5 mL. Because small amounts like 0.2 and 0.5 mL did not fully cover the bottom of the 40 mL vial, these volumes were placed in 2 mL glass vials, which then were inserted into the 40 mL vials. The effect of the reaction volume on CH_4 formation is shown in Figure 4.5b. The measured amounts of CH_4 after the 24 h incubation were in the range from 9.7 to 0.7 nmol for 0.2 to 5 mL respectively, and thus increase exponentially with the decrease of the volume. This demonstrates that higher reactant concentrations will increase CH_4 formation when the ratio between them is kept constant.

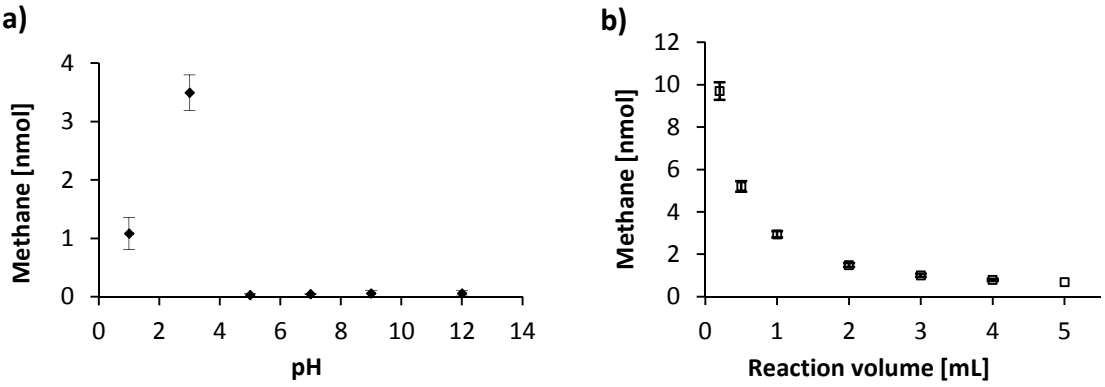

Figure 4.5: Effect of pH and reaction volume on methane formation. (a) pH and (b) reaction volume. Reaction time 24 h. Data show mean value ± SD (n=3).

4.3.3.4 Effect of headspace atmosphere on methane formation

To determine the influence of oxygen on the formation of CH_4, several experiments were conducted under different gas atmospheres. Therefore, the reaction vials and stock solutions were flushed with synthetic air (20.9 % O_2), pure oxygen, or pure nitrogen prior to the start of the experiment. Surprisingly, the highest amounts of CH_4 (9.7 nmol) were observed when samples were incubated under a N_2 atmosphere, followed by those under laboratory and synthetic air (ca. 2 nmol). In contrast, no CH_4 production was found when samples were incubated under a 100 % O_2 atmosphere (Figure 4.6).

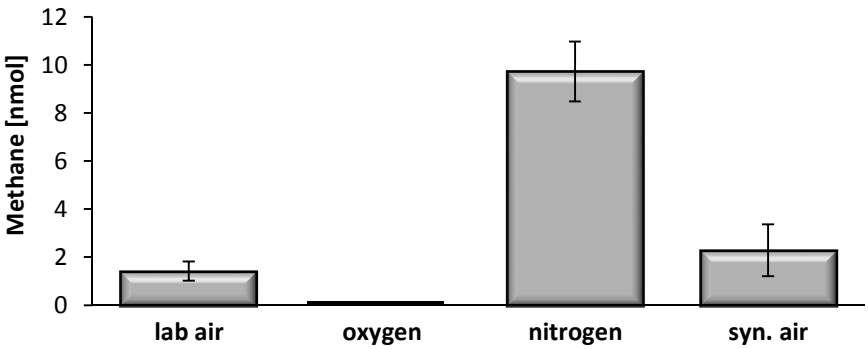

Figure 4.6: Methane formation under different gas atmospheres. The initial amounts of reactants were 50 µmol ASC, 4 µmol FH and 100 µmol H_2O_2 in 1 mL H_2O (40 mL vial). Data show mean value ± SD (n=3).

Our results suggest that O_2 plays an important role in the generation of CH_4 from ascorbic acid, FH and H_2O_2, i.e. with increasing concentration oxygen inhibits the formation of CH_4. These results may also explain why little formation of CH_4 was observed at pH ≥ 4 because it is known that at higher pH values the surface-catalysed decomposition of H_2O_2 on iron surfaces is favoured producing non-reactive oxygen species and O_2 (Kremer, 2003). Interestingly, Ghyczy et al. (2008) reported that non-methanogenic generation of CH_4 in mitochondria and eukaryotic cells may be linked to a cellular response to hypoxia.

4.4 Conclusions

Our results show that abiotic formation of CH_4 in a highly oxidative media is possible, when using the three chemical compounds, ascorbic acid, ferrihydrite and H_2O_2, known to be available in natural biosystems. In contrast to the studies of Ghyczy et al. (2003, 2008), who monitored CH_4 formation from ascorbic acid, choline, H_2O_2 and Fe^{2+}/ Fe^{3+}, we used mineral forms of iron instead of dissolved iron species. The physical and chemical properties of the iron mineral species were found to play a key role in the CH_4 formation under oxidative conditions. Equally important is the chemical structure including the functional groups of the (HO-) of the ascorbic acid, although it is unknown from which carbon atom CH_4 is derived. A ratio of 2:1 between H_2O_2 and ascorbic acid, catalytic amounts of ferrihydrite and an acidic pH all enhanced formation of CH_4 under aerobic conditions. However, we also observed that increasing oxygen concentrations above ambient levels severely inhibit the formation of CH_4 in our reaction system.

Although the reaction pathway of CH_4 formation from ascorbic acid is currently unknown, this study was a first step towards tracking CH_4 formation using a chemical system under highly oxidative conditions. To fully delineate the reaction pathway, much more detailed analytical measurements and use of other more sophisticated techniques will be essential. Our next immediate steps will include detailed measurements of other volatiles such as CO and CO_2, determination of dissolved ferric and ferrous iron and also stable carbon isotope measurements following the employment of various ^{13}C positionally labelled ascorbic acids.

Acknowledgements:

We thank John Hamilton for reviewing the paper, Carl Brenninkmeijer and Dieter Scharffe for analytical support (GC-FID). We also thank Jennifer Rinne, Markus Greule and Kirsten Achenbach for assistance. This work was funded by the ESF and DFG (EURYI Award to F.K.).

Chapter 5

Abiotic methanogenesis from biomolecules under ambient conditions

Submitted to *Nature Chemistry*, 2012.

Frederik Althoff[1], Kathrin Benzing[2], Peter Comba[2], Colin McRoberts[3] and Frank Keppler[1]

Abstract

Methane is a greenhouse gas, and plays an important role in atmospheric chemistry. In nature it is produced by both biotic and abiotic processes. Abiotic formation is known to occur under environmental conditions with either high pressure and/or high temperature. Here we present a novel chemical reaction that forms methane from biomolecules under ambient atmospheric pressure and temperature. When using ascorbic acid, iron minerals and hydrogen peroxide as reagents heteroatom bonded methyl groups of organic compounds were converted into methane. Highest yields were observed for L-methionine, a compound that plays a major role in transmethylation reactions in living systems. Stable isotope labelling experiments unambiguously verify that the thio-methyl group of methionine is the carbon precursor of methane. This novel chemical route of methane generation is suggested to be involved in aerobic methane formation in the biosphere, particularly in living organisms such as plants and animals.

Keywords: methionine; ascorbic acid; ferrihydrite; stable isotopes

5.1 Introduction

The greenhouse gas methane (CH_4) is the most abundant reduced organic trace gas in the atmosphere and plays an important role in tropospheric and stratospheric chemistry. Various sources of CH_4 are known to exist in nature, and recently the number of suggested biological sources has been increased (Keppler et al., 2009).

[1] Max-Planck-Institute for Chemistry, Hahn-Meitner-Weg 1, 55128 Mainz, Germany.
[2] University of Heidelberg, Anorganisch-Chemisches Institut, INF 270, 69120 Heidelberg, Germany.
[3] Department of Agriculture and Rural Development for Northern Ireland, Newforge Lane, Belfast BT9 5PX, UK.

In general, natural formation of CH_4 – so called methanogenesis – can be classified into biotic and abiotic. Biotic methanogenesis usually refers to archaea living under anaerobic conditions in wetlands, rice fields, landfills or the gastrointestinal tracts of ruminants and termites. Abiotic formation of CH_4 has been reported to occur under conditions that require high pressure and/or temperature, for instance during biomass burning or serpentinisation of olivine, under hydrothermal conditions in the oceans deep or below tectonic plates (Sherwood Lollar et al., 1993, 2002; Holm and Charlou, 2001). In the chemical industry CH_4 is often produced from carbon monoxide and hydrogen gas under high pressure and temperature (cf. Fischer-Tropsch synthesis).

Over the past years non-microbial CH_4 formation has also been observed in living biological systems such as plants (Keppler et al., 2006, 2009; Brüggemann et al., 2009; Wishkerman et al., 2011) and animals (Ghyczy et al., 2008). Whereas the biochemistry of methanogenesis in microbes is well described (Thauer, 1998), possible pathways of CH_4 generation from plants and animals are still under investigation. However, a comprehensive understanding of all environmentally important CH_4 sources and sinks as well as the parameters that control emissions is a prerequisite to fully understand the global biogeochemical cycle of CH_4.
In particular CH_4 formation and emissions by both dead and living plants (Keppler et al., 2006) has been intensely discussed in recent years (Dueck et al., 2007; Keppler and Röckmann, 2007; Keppler et al., 2009; Nisbet et al., 2009). It has been shown that CH_4 can be produced abiotically from plant material by exposing it to ultraviolet (UV) irradiation (Keppler et al., 2008; McLeod et al., 2008; Vigano et al., 2008; Bruhn et al., 2009). A reaction of reactive oxygen species (ROS) with methoxyl groups of pectic polysaccharides was suggested as a possible route to CH_4 formation under UV radiation (Messenger et al., 2009). On the other hand two recent studies (Brüggemann et al., 2009; Wishkerman et al., 2011) using ^{13}C-labelled plant species have clearly demonstrated that there is continuous formation of CH_4 in living plants without any microbial contribution. Although the reaction pathway for CH_4 formation in living plants is still unknown, it has been hypothesised that electrophilic methyl groups (EMG) of biomolecules such as phosphatidylcholine or methionine might be carbon precursors of CH_4 in living cells (Ghyczy et al., 2003, 2008; Keppler et al., 2009; Wishkerman et al., 2011).

Furthermore, Althoff et al. showed that ascorbic acid produces CH_4 in the presence of hydrogen peroxide and iron oxide (Althoff et al., 2010). However, no chemical pathway producing CH_4 under these oxic conditions has been identified so far.

In this study we have investigated a chemical reaction system that utilizes organic compounds for the generation of CH_4 under both ambient (1000 mbar and 22 °C) and aerobic (~20 % O_2) conditions. We have used so called 'methyl-donating compounds' (MDC) and ascorbic acid (ASC), iron oxides and hydrogen peroxide (H_2O_2) as reagents. MDCs such as methionine (MET), methylcobalamin (MeCbl), choline (CC) and betaine (BET) are known to play a key role in bio-methylation reactions and methyl group metabolism of plants and animals (Michal, 1999). The importance of these compounds in the metabolism of organisms is described in more detail in the Supplementary information.

5.2 Methods

5.2.1 Compounds tested as methane precursor

Choline chloride (CC), 2-methoxyphenol (guaiacol), betaine (BET), leucine (LEU), S-adenosylmethionine (SAM), L-methionine, methionine sulfoxide (MSO), methionine sulfone (MSO_2), and methylcobalamin (MeCbl) were all tested for their potential to release methane. Four µmol FH were weight in 1.5 mL crimp glasses. These glasses were placed in the 360 mL vials which were sealed using a hole type screw cap (Supelco, 27187) fitted with a PTFE/silicone septum (Supelco, 27188-U) before 0.5 µmol of the organic compound dissolved in 0.4 mL H_2O, 50 µmol ASC dissolved in 0.5 mL H_2O and 100 µmol H_2O_2 in 0.1 mL H_2O, were injected to each 1.5 mL vial through the septum. The samples were in general incubated at 22 ± 2 °C for 24 or 48 h prior to CH_4 headspace analysis.

5.2.2 Methane measurements

Headspace (5 mL) from the sealed glass vials was sampled using a Hamilton gas syringe needle and analysed by a gas chromatograph (column: 2 m, Ø=3.175 mm (i. d.) high-grade steel tube packed with Molecular Sieve 5A 60/80 mesh from Supelco) equipped with a flame ionization detector (GC-FID) (Shimadzu GC-14B). Quantification of CH_4 was performed by direct comparison of peak area with that obtained with two reference standards containing 8.905 and 1.835 ppm. All samples were prepared in triplicate (n=3) unless otherwise stated in the manuscript. Control samples (blanks) were prepared in a similar fashion to that

described for the samples but without the addition of MDC. The control measurements usually reflected the CH_4 background concentration of laboratory (range 2-2.2 ppm).

5.2.3 Isotope measurements

$^{13}C/^{12}C$ -isotope ratios were determined using IRMS system (ThermoFinnigan Deltaplus XL, Thermo Finnigan, Bremen, Germany). A volume of about 40 mL headspace gas from sample was transferred to an evacuated sample loop (40 mL). Interfering compounds were separated by gas chromatography and CH_4 was trapped on Hayesep D. The sample was then transferred to the IRMS via an open split. As reference gas carbon dioxide of high purity (carbon dioxide 4.5, Messer Griesheim, Frankfurt, Germany) with a known $\delta^{13}C$ value of -23.64 ‰ (VPDB) was used. All $\delta^{13}C$ values were normalized relative to Vienna Pee Dee Belemnite (VPDB) using a CH_4 standard. Samples were routinely analysed three times (n=3) and the average standard deviations of the GC/C/IRMS measurements were in the range of 0.1 to 0.3 ‰. See supplemental for further information.

5.3 Results and discussion

5.3.1 Methane formation from MDSs

Several organic compounds in particular MDCs were investigated to serve as possible CH_4 precursors when ASC, iron oxide (ferrihydrite, FH) and H_2O_2 were used as reagents.

Figure 5.1 shows the yield of CH_4 formation from different MDCs. Highest yields of CH_4 production of over 10 % (conversion on a molar basis; ca. 50 nmol) were observed for MET and methionine sulfoxide (MSO). The cobalt-bound methyl group of methylcobalamin (MeCbl) showed a production of about 3 %. Although CC contains three methyl groups that are bonded to the same nitrogen atom, only a relatively small conversion to CH_4 of about 0.6 % (2.8 nmol) was measured. Formation of CH_4 from BET, guaiacol (GU) and leucine (LEU) was below the detection limit of the analytical system. The sulphur compounds S-adenosylmethionine (SAM) and methionine sulfone (MSO_2) also showed only little conversion to CH_4 of below 0.5 %. A possible explanation of these results is steric effects and differences in charge distribution in these substrates. In contrast to CC, BET, SAM or MSO_2, where the hetero atom is sterically shielded, in MET and MSO it is exposed and easily attacked by ferryl group. In particular the difference in CH_4 formation between CC and BET support these assumptions, because both compounds have the same $-N^+(CH_3)_3$ group.

They only differ in their functional group at C1 which is larger with the carboxylic group at BET than with the hydroxyl group of CC.

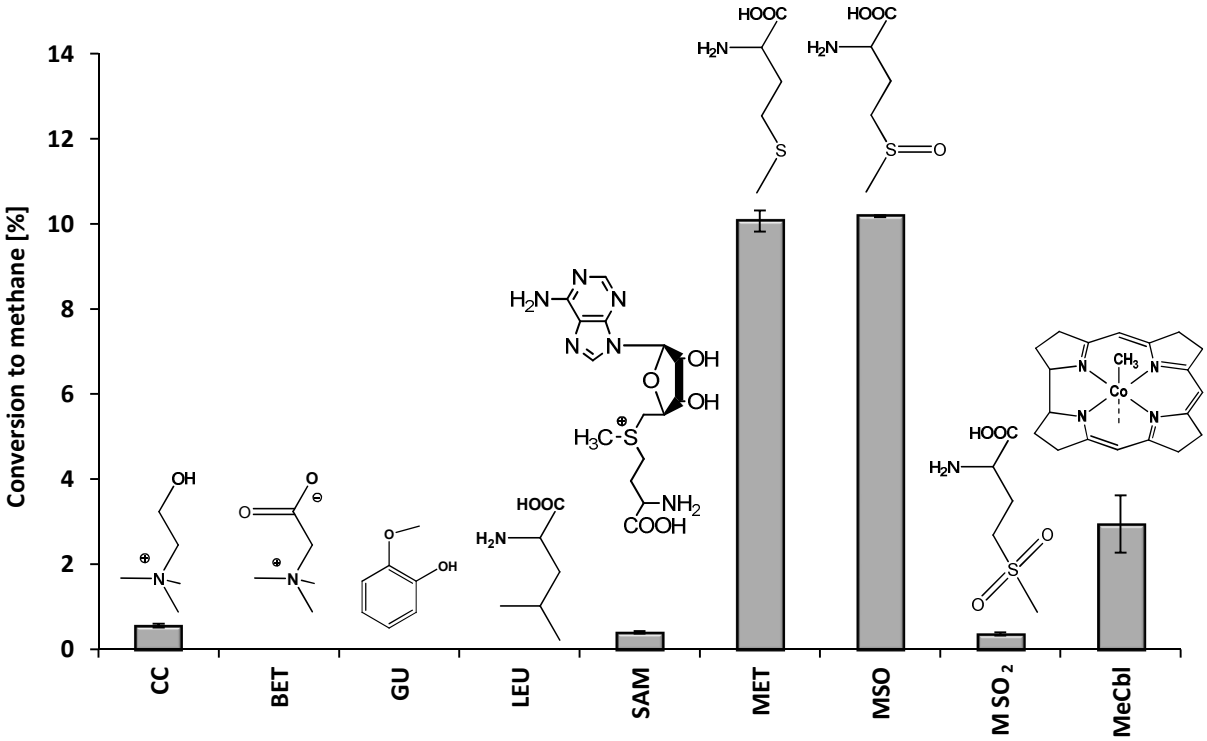

Figure 5.1: Methane formation from different organic compounds in the reaction with ASC, FH, and H_2O_2. Used substances are choline chloride (CC), guaiacol (GU), betaine (BET), leucine (LEU), S-adenosylmethionine (SAM), methionine (MET), methionine sulfoxide (MSO), methionine sulfone (MSO_2), methylcobalamin (MeCbl). Values show molar conversion of organics in percentage. The initial amounts of reactants were 50 µmol ASC, 4 µmol FH, 100 µmol H_2O_2, and 0.5 µmol MDC (1 mL total volume). Data show mean value ± SD (n=3), reaction time of 30 h.

Due to the positive charge of the neighbouring nitrogen and its higher electronegativity the electrons are shifted away from the methyl group's carbon centre. This reduces the reactivity in the latter case. In case of substitution at the methyl group itself substances with two or three methyl groups should deliver higher amounts of CH_4 than groups with only one.

In the following we focused on MET and MSO since they showed the highest CH_4 formation.

5.3.2 Identification of the precursor carbon using ^{13}C labelling experiments

We expected the sulphur bonded CH_3 group of methionine to be the carbon precursor of CH_4. This hypothesis was tested with positionally labelled ^{13}C MET and measuring stable

carbon isotope values ($\delta^{13}C$ values) of CH_4 using gas chromatography combustion isotope ratio mass spectrometry (GC-C-IRMS). When $^{13}CH_3$-MET (~2 % ^{13}C content) was used for the reaction $\delta^{13}C$ values of CH_4 changed drastically to larger values and reflected closely the $\delta^{13}C$ values of the theoretical calculations when considering the isotopically labelled methyl group as the CH_4 precursor. These results unambiguously identify the sulphur-bonded CH_3 group of methionine as the carbon precursor of CH_4.

5.3.3 Parameters affecting methane formation from methionine by the reaction with ascorbic acid, hydrogen peroxide and iron species

Several reaction parameters, including different iron species, concentration of H_2O_2 and ascorbic acid as well as the pH value, anticipated to affect formation of CH_4 from methionine, were investigated.

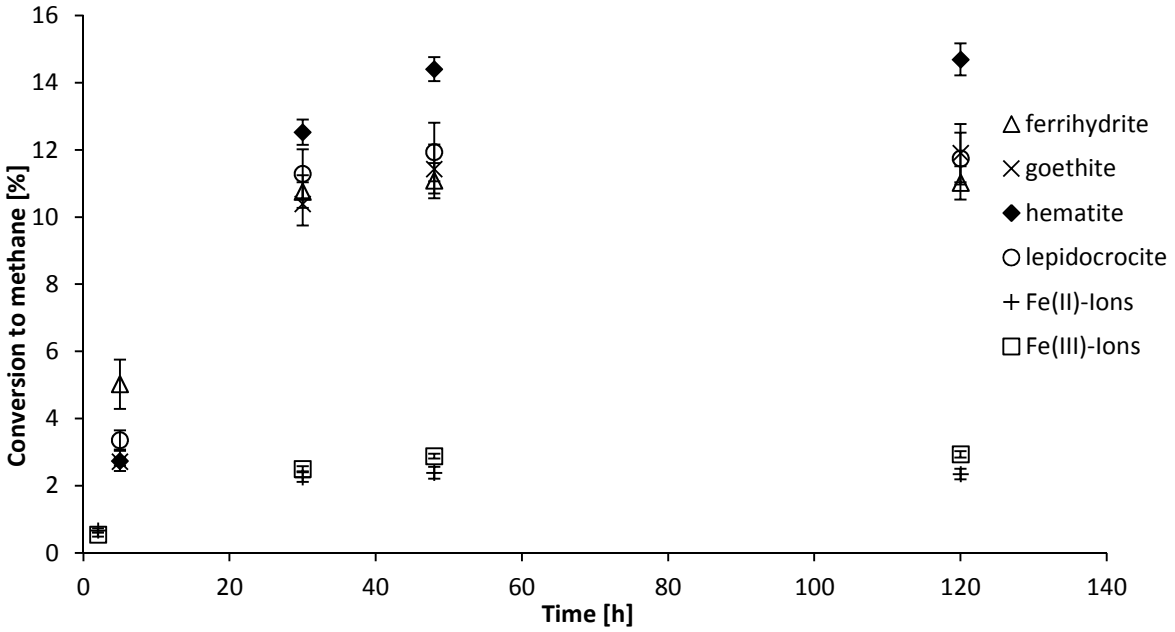

Figure 5.2: The effect of different iron species on CH_4 formation from MET. The initial amounts of reactants were 50 µmol ASC, 40 µmol Fe (in different species), 100 µmol H_2O_2 and 0.5 µmol MET in 1 mL H_2O end volume. Values were measured after 30 h. Data show mean value ± SD (n=3).

Beside iron salts of Fe^{2+} and Fe^{3+} we investigated the iron minerals ferrihydrite (FH), goethite, hematite (HT) and lepidocrocite in the reaction with MET, ASC and H_2O_2 to form CH_4 (Figure 5.2). All iron species showed CH_4 formation. Whereas after 5 h FH showed the highest CH_4 formation of about 5 %, followed by the other minerals with about 2 %, after

30 h the yields with all minerals were in the same range of 10-12 %. The increase finally reached a plateau after ca. 48 h. While iron salts still showed a conversion of 2 % the minerals reached about 12 %, except for HT which had the highest formation of CH_4 with 14 %. Since structures similar to FH, e.g. the ferritin core, can also be found in living bio systems this iron oxohydroxid was used in further experiments.

We varied the amount of FH and samples were taken for analysis between 2 h and 5 d (Figure 5.6). It emerged that after 2 h higher amounts of FH led to higher yields of CH_4. However, after 5 h all samples resulted in about the same yield of CH_4 and after 30 h CH_4 produced increased with decreasing amounts of added FH. After this time period no further CH_4 formation was detected.

In a next step we looked for the other compound ratios by vary the amount of one compound and keeping the others constant. The maximum CH_4 formation was observed with 50 µmol ASC and 100 µmol H_2O_2 (Figure 5.3) what correlates with a molar ratio of ASC:H_2O_2 of 1:2. When adding MET to these amounts of ASC and H_2O_2 a linear correlation between CH_4 formation and the amount of MET could be found (Figure 5.4).

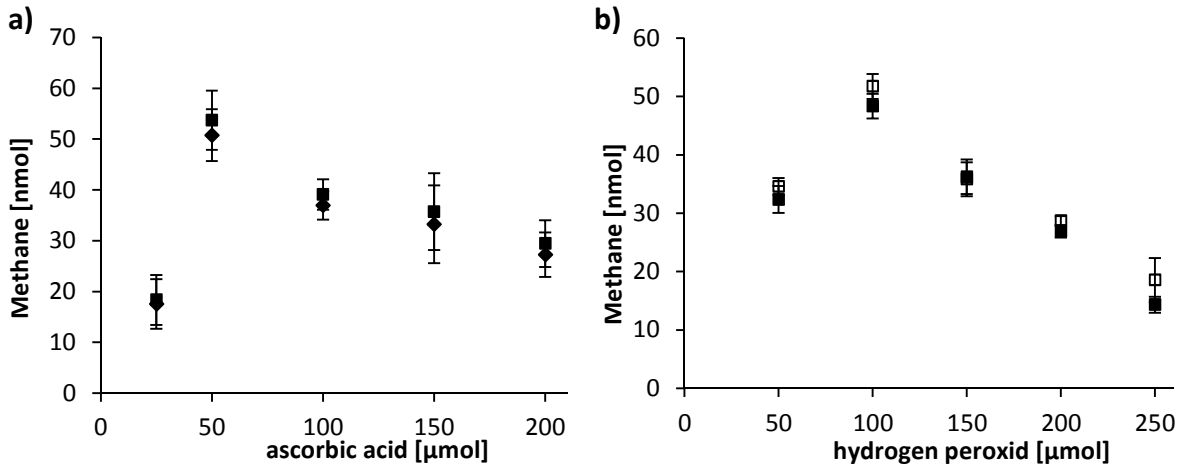

Figure 5.3: Dependency on substance ratio. a) Dependency on ascorbic acid (ASC). Diamonds and squares show CH_4 production after 5 and 30 h, respectively. The initial amounts of reactants were 4 µmol FH, 100 µmol H_2O_2, 0.5 µmol MET and a varying amount of ASC in 1 mL H_2O end volume. **b)** Dependency on hydrogen peroxide (H_2O_2). Black and white squares and show CH_4 production after 30 h and 5 days, respectively. The initial amounts of reactants were 50 µmol ASC, 4 µmol FH, 0.5 µmol MET and a varying amount of H_2O_2 in 1 mL H_2O end volume. Data show mean value ± SD (n=6).

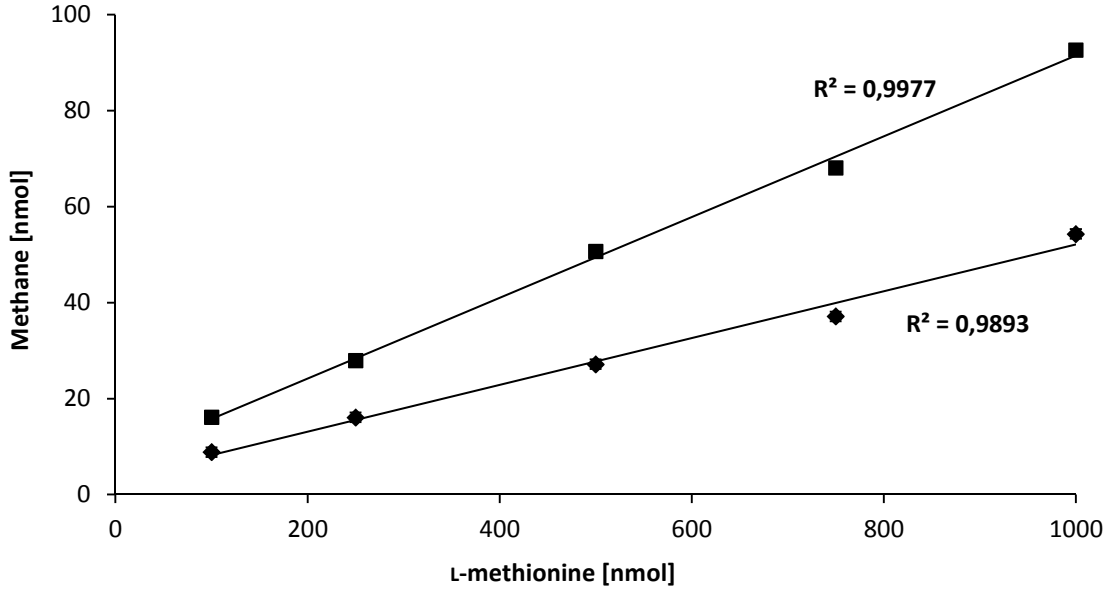

Figure 5.4: Linear dependency of CH_4 formation on amount of methionine. Diamonds and squares show CH_4 production after 5 and 30 h, respectively. The initial amounts of reactants were 50 µmol ASC, 4 µmol FH, 100 µmol H_2O_2, and varying amounts of MET in 1 mL H_2O end volume. Data show mean value ± SD (n=6**)**.

Beside the compound ratio we also run the experiment with different pH and reaction volume. To determine the influence of the pH CH_4 production was monitored across the pH range of 1 to 9. The highest yield of CH_4 was found at pH 3 (Figure 5.7). This might be explained with the need of an acidic pH to solve the FH. Furthermore, to evaluate the effect of the reaction volume on CH_4 formation, we run the experiment using initial amounts of 0.5 µmol Met, 50 µmol ASC, 4 µmol FH and 100 µmol H_2O_2 in different amounts of H_2O reaching from 0.2 to 5 mL. We measured an increasing CH_4 production with decreasing volume (Figure 5.8). At the volume of 0.2 mL over 18.6 % (relative to MET, 93 nmol) CH_4 have been formed. To test the influence of oxygen on the formation of CH_4 several experiments were carried out under different gas atmospheres. Note that all used vials and stock solutions were flushed with N_2, O_2 or synthetic air (SA) respectively prior the start of the experiment. Interestingly, with ~10 % (relative to MET, 50 nmol) the reactions conducted in N_2, SA, and not flashed laboratory air nearly show the same amount of produced CH_4 and about twice as much as the reaction in pure O_2 (Figure 5.9).

5.3.4 Postulated route of methane formation - identification of reaction products and intermediates

Figure **5.5** shows the suggested reaction pathway of CH_4 formation when using MET as the carbon precursor. As described before MET's methyl group has been verified to be the CH_4 precursor group and this is highlighted in dark blue for clarity. After addition of H_2O_2 to the solution MET is immediately and completely oxidized to MSO but no MSO_2 is produced. This explains the very similar values found when MET or MSO are used as substrate.

In solution ASC is deprotonated (pK_a=4.37) leading to pH = 3 of the solution. This is acidic enough to dissolve the FH which then slowly releases Fe^{2+} ions. With ASC and H_2O_2 in the reaction solution both Fe^{2+} and Fe^{3+} are in equilibrium. With exclusively Fe^{2+} or only Fe^{3+} in solution, other reactions which form e.g. O_2 (cf. Fenton reaction) instead of CH_4 seem to dominate, and this may explain the lower yield with simple iron salts.

In the course of the reaction, ASC reduces Fe^{3+} ions and is transformed to the stable dehydroascorbic acid (DHASC) which is not available for further reactions. A possible reason for the maximum yield of 20 % CH_4 (relative to MET) may be that a rising amount of Fe^{3+} since a spiking with other reactants (e.g., ASC, H_2O_2) did not lead to higher yields of CH_4. The analysis showed a large amount of unreacted MSO. In a side reaction the resulting Fe^{2+} ions might react with H_2O_2 in a Fenton-type process, leading to Fe^{3+} ions and ·OH radicals which are known to lead to unspecific radical reactions.

In order to get mechanistic information about the role of the $Fe^{2+/3+}/H_2O_2$ - based reaction, we have carried out similar experiments to those described above, using a thoroughly studied low-molecular-weight biomimetic nonheme iron catalyst (see Figure 5.10 for the structure of these bispidine-base complexes) (Comba et al., 2008). The complex was prepared as described by Comba et al. (1998). These iron(II) precursors are known to form very reactive high-valent Fe=O species with H_2O_2 (Bautz et al., 2007; Comba et al., 2010) and the corresponding ferryl complexes have been shown to also exist in aqueous solution (Bautz et al., 2006). These oxo-complexes have been shown to readily transfer the oxo-group (e.g. in sulfoxidation reactions, i.e. oxidation of MET to MSO) (Jaccob et al., 2011) and to activate CH groups as strong as those of unactivated alkanes (Comba et al., 2009).

Importantly, these reactions and the relevant intermediates have been carefully investigated in detail experimentally and with quantum-chemistry based methods. Indeed, the reactions described above, i.e. with Fe^{2+} provided by minerals lead to analogous products and product ratios when Fe^{2+} is used as well-defined bispidine complex. This indicates that one ferryl ion transfers the oxo group to MET to form MSO. In a second reaction step, a further ferryl species reacts as electrophile with the methyl group of MSO to produce a CH_3 radical. Oxidative demethylation reactions with this type of catalyst have been observed before (Comba et al., 2006) but pathways other than involving Fe^{IV}=O are also conceivable. That is, a detailed mechanistic analysis will need further experimental efforts. Importantly, first qualitative experiments using the spin trap 5,5-dimethylpyrroline-N-oxide (DMPO) and electron paramagnetic resonance spectroscopy (EPR) (Janzen and Zhang, 1995; Yoshimura et al., 1999; Jansson et al., 2010) indicated that methyl radials are formed when the model ferryl complex is reacted with MSO.

The left side of

Figure 5.5 shows the products identified formed during the processes. Both S-C bonds of MSO may be attacked by the ferryl group. The decay products found mainly showed a reduction of the carbon atoms to form CH_4 and 2-amino butanoic acid (ABA) as well as an oxidation of the remaining sulphur moiety to form methanesulfonic acid (MSA) and homocysteic acid (HCyA). Furthermore, we detected two other products which lost their methyl group. These components are homocystic sulfoxide (HCySO) and 4-hydrosulfinyl-2-hydroxybutanoic acid (HSBA), i.e. HCySO with a substituted amino group. As described before the ASC is fully transformed to the stable DHASC after the release of two electrons and two protons.

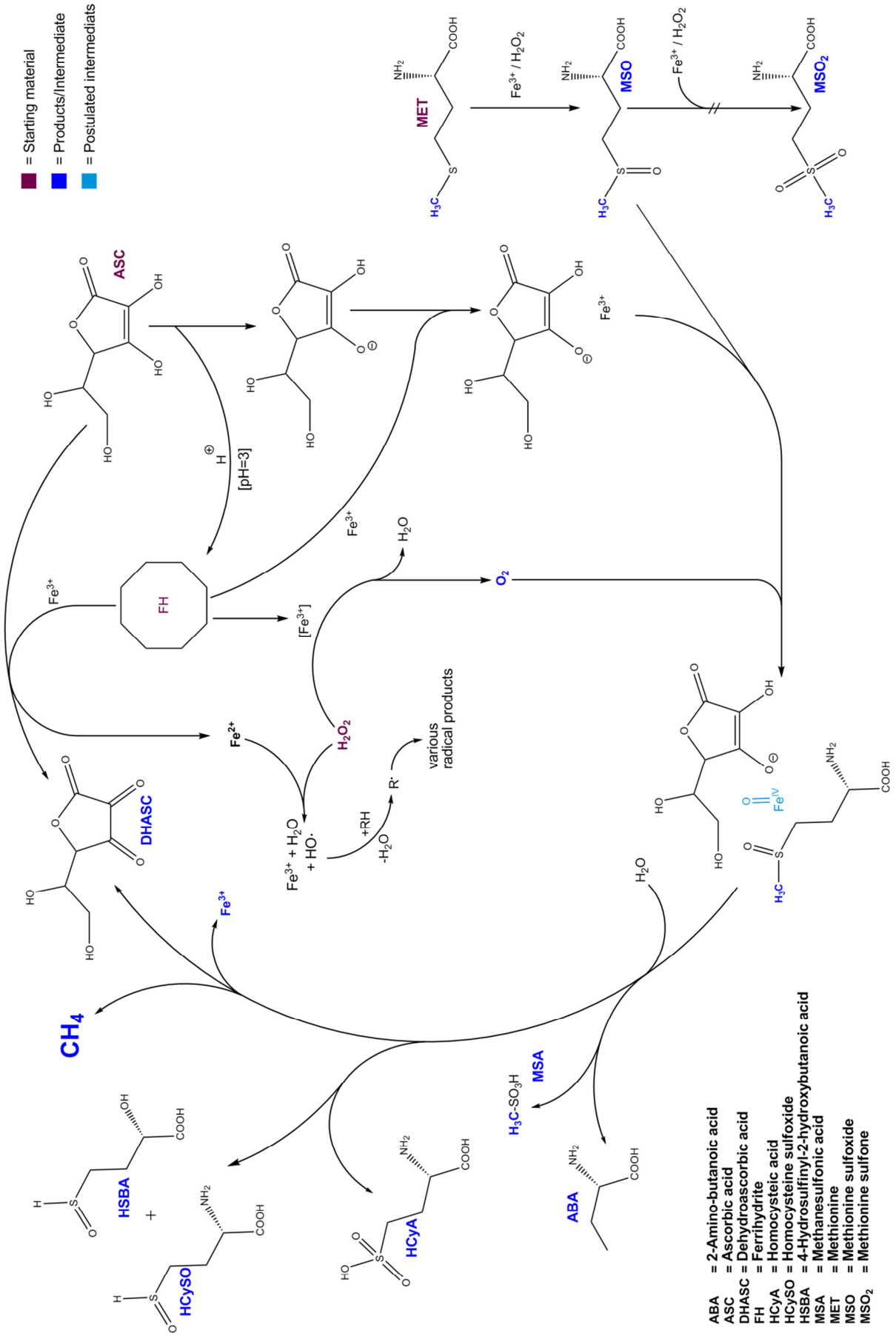

Figure 5.5: Route of CH_4 formation using MET, ASC, FH, and H_2O_2. Note that the Fe^{IV}=O species is postulated (light blue coloured). Methane and its precursor methyl group are highlighted in dark blue. Starting materials are coloured in dark red.

5.4 Acknowledgements

We thank John Hamilton for reviewing the paper, Carl Brenninkmeijer and Dieter Scharffe (GC-FID), Markus Greule (IRMS) and Maren Emmerich (iron determination) and Sabine Studenroth (product identification) for analytical support. We also thank Sonja Jung, Evelyne Kasparek and Ilka Hermes for technical assistance. Thanks to Miklós Ghyczy and Heinz-Friedrich Schöler for helpful discussions. This work was funded by the ESF (EURYI Award to F.K.), (KE 884/2-1 and KE 884/7-1).

5.5 Author contributions

F.A. and F.K. designed the research. F.A. performed the experiments and analysed the data. F.K. analysed the isotopic data. F.A., K.B. and P.K. investigated the iron-complex intermediates and discussed reaction scheme. F.A. and C.M. separated and analysed reaction products. F.A. and F.K. discussed the results and co-wrote the paper.

5.6 Supplemental

5.6.1 Natural role of biomolecules tested as methane precursor

One of the main methylation components required for methyl group metabolism in living organisms is methionine that carries a sulphur bond methyl group (cf. Figure 5.1). Methionine sulfoxide (MSO) is the oxidised form of MET which is able to pass special barriers in an organism and can be reduced at the place where it is needed. Complete oxidation of the sulphur produces methionine sulfone (MSO_2). However, it doesn't play a role in organisms and was just investigated for completeness.

In organisms transfer of methyl groups emanates from S-adenosyl-methionine (SAM) whereof MET, which presents the centre of SAM, is carrying the activated methyl group. After the methyl group is transferred and the rest of methionine is released form SAM as homocysteine (HCy), 5-methyltetrahydrofolate or one of betaine's (BET) methyl group is used for remethylation of the released HCy to MET (Michal, 1999). Betaine itself is the oxidised form of choline (CC), the half of the neurotransmitter acetylcholine. Another important methylation component is methylcobalamine (MeCbl) that is known from the vitamin B_{12} family. The aromatic guaiacol (GU) contains an oxygen bound methyl group. It plays an important role in lignin synthesis of wood. The amino acid leucine (LEU) is important for building up muscle tissue and responsible for its energy budget.

5.6.2 Parameters that effect methane formation

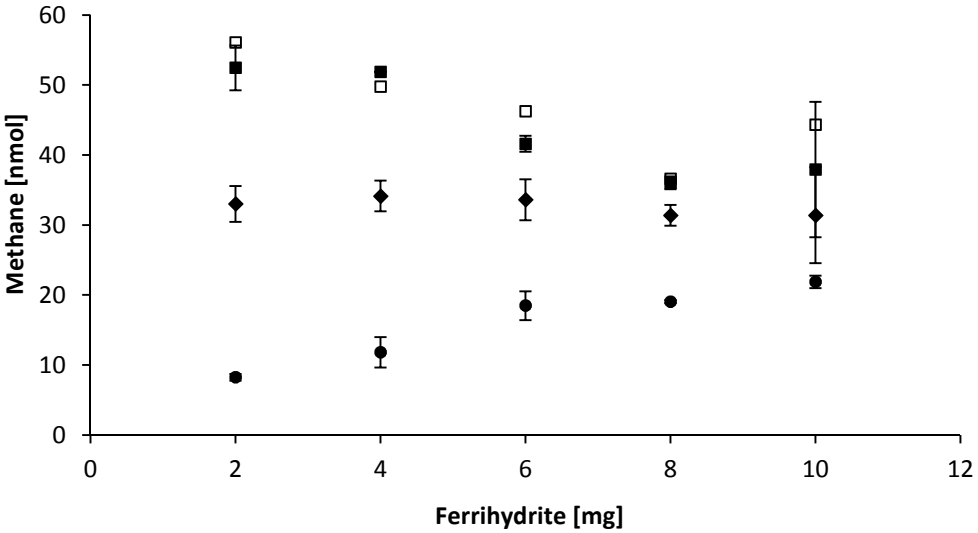

Figure 5.6: Dependency on ferrihydrite (FH). Dots, diamonds, black and white squares show CH_4 production after 2, 5, 30 h and 5 days, respectively. The initial amounts of reactants were 50 µmol ASC, 100 µmol H_2O_2, 500 nmol MET and a varying amount of FH in 1 mL H_2O end volume. Data show mean value ± SD (n=6).

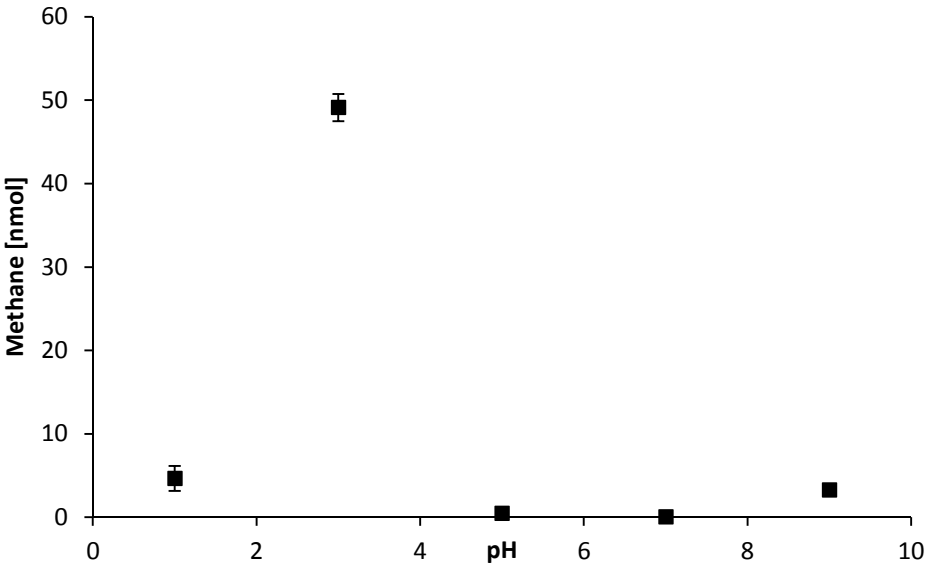

Figure 5.7: Dependency on pH. Squares show CH_4 production after 30 h. The initial amounts of reactants were 50 µmol ASC, 4 µmol FH, 100 µmol H_2O_2 and 0.5 µmol MET in 1 mL H_2O end volume. The pH was adjusted using HCl (0.1 M) or NaOH (0.1 M), phosphate buffer (Sørensen) and a pH meter (Mettler Toledo FE 20). Data show mean value ± SD (n=6).

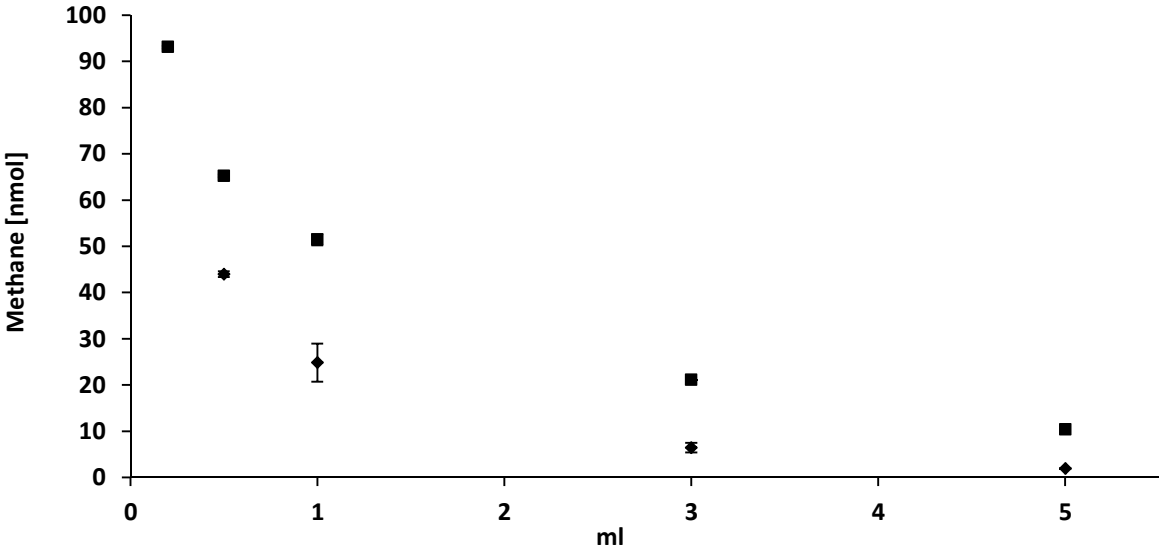

Figure 5.8: Dependency on reaction volume. Diamonds and squares show CH_4 production after 5 and 30 h, respectively. The initial amounts of reactants were 50 µmol ASC, 4 µmol FH, 100 µmol H_2O_2, 0.5 µmol MET and H_2O with varying end volume. Data show mean value ± SD (n=6).

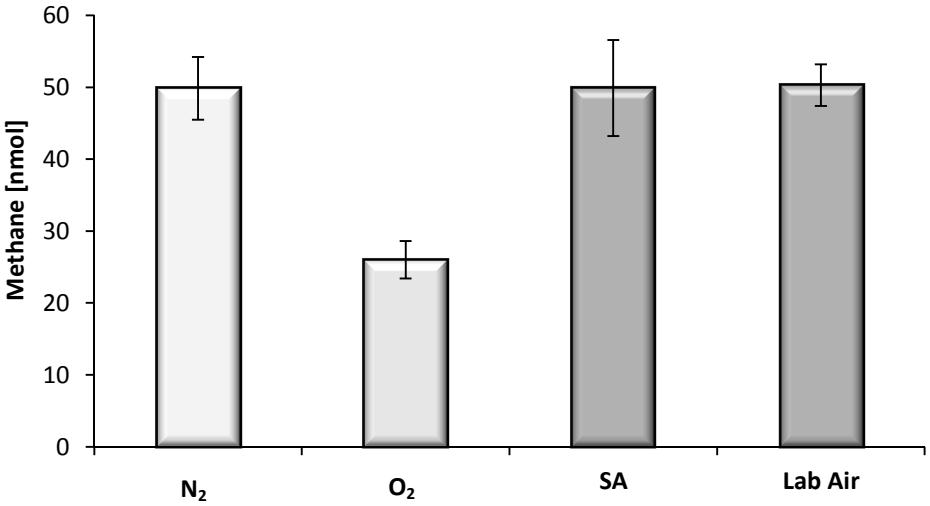

Figure 5.9: Dependency on different atmospheres. The light and dark grey bars represent pure atmospheres (N_2, O_2) and combinations (SA=synthetic air; Lab Air= ambient laboratory air), respectively. Bars show CH_4 production after 30 h. The initial amounts of reactants were 50 µmol ASC, 4 µmol FH, 100 µmol H_2O_2 and 0.5 µmol MET in 1 mL degased H_2O end volume. Data show mean value ± SD (n=6).

Bispidine complex

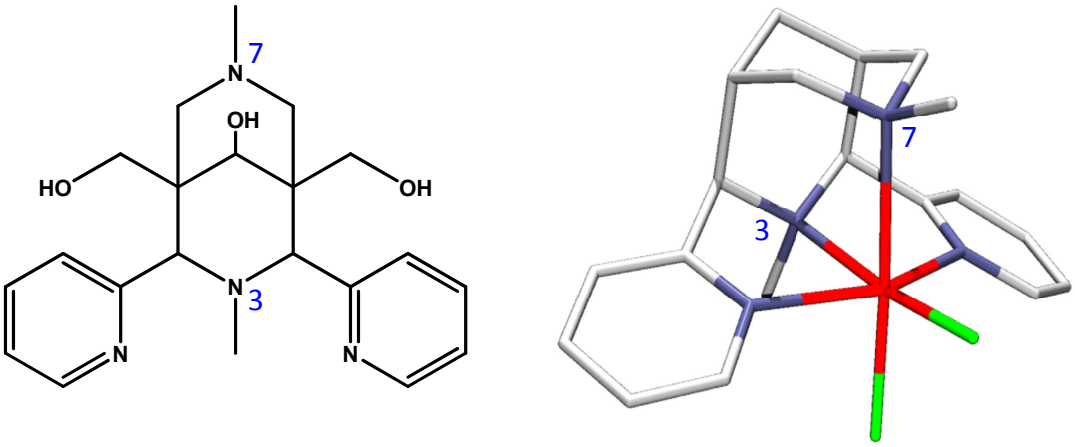

Figure 5.10: Structure of the bispidine ligand (left) and the corresponding ferryl complex (right, hydroxyl and hydroxymethyl groups omitted for clarity). The oxo group is trans to N7, trans to N3 is a solvent molecule, in the solutions used presumably OH_2. The catalyst was prepared in-situ from the Fe^{II} precursor and H_2O_2.

5.6.3 Isotopic measurements

$^{13}C/^{12}C$ -isotope ratios were determined using IRMS system (ThermoFinnigan Deltaplus XL, Thermo Finnigan, Bremen, Germany) and are expressed in the conventional δ notation (Eq. 5.1) in per mill versus VPDB (Vienna Pee Dee Belemnite), defined as:

$$\delta^{13}C_{VPDB} = \frac{\left(\frac{^{13}C}{^{12}C}\right)_{sample}}{\left(\frac{^{13}C}{^{12}C}\right)_{standard}} - 1 \qquad \text{(Eq. 5.1)}$$

$\delta^{13}C$ sample analysis was done using gas chromatography combustion isotope ratio mass spectrometry (GC-C-IRMS) which consists of a cryogenic pre-concentration unit directly coupled to an HP 6890N gas chromatograph (Agilent, Santa Clara, USA), which is connected to an Delta^{PLUS}XL isotope ratio mass spectrometer (ThermoQuest Finnigan, Bremen, Germany) via an oxidation reactor [ceramic tube (Al_2O_3; aluminium(III) oxide), length 320 mm, 0.5 mm i. d., with oxygen activated Cu/Ni/Pt wires inside, reactor temperature 960 °C] and a GC Combustion III Interface (ThermoQuest Finnigan, Bremen, Germany). The gas chromatograph (GC) is fitted with a GS-Carbonplot capillary column (30 m x 0.32 mm i.d., d_f 1.5 µm; Agilent, Santa Clara, USA) and a PoraPlot capillary column (25 m x 0.25 mm i.d., d_f 8 µm; Varian, Lake Forest, USA). Both columns are coupled via a press fit connector.

A tank of high purity carbon dioxide (carbon dioxide 4.5, Messer Griesheim, Frankfurt, Germany) with a known $\delta^{13}C$ value of –23.6 ‰ (VPDB) is used as the working reference gas. All $\delta^{13}C$ values obtained from analysis of methane are corrected using three CH_4 working standards (isometric instruments, Victoria, Canada) calibrated against IAEA and NIST reference substances. The calibrated $\delta^{13}C$ values of the three working standards in ‰ vs. VPDB are –23.9 ± 0.2 ‰, –38.3 ± 0.2 ‰ and –54.5 ± 0.2 ‰.

5.6.4 Isotope labelling experiments

Position-specific ^{13}C labelling experiment were conducted with methionine which had only the carbon atom of the thio-methyl group (-S-methyl-^{13}C) labelled with ^{13}C (Sigma-Aldrich, Taufkirchen, Germany; isotec™ 99 % ^{13}C atoms). The amount of ^{13}C in the thio-methyl group was calculated to be 2 ± 0.05 %, corresponding to a $\delta^{13}C$ (-S-methyl-^{13}C) value of 822 ± 50 ‰. The measured and corrected $\delta^{13}C(CH_4)$ value for the headspace gas of the sample was 763 ± 16 ‰ and thus reflected closely the $\delta^{13}C$(-S-methyl-^{13}C) value of the isotopically labelled thio-methyl group.

5.6.5 Mass analysis

Samples were neutralized with NaOH and centrifuged for 5 min at 14,000 rpm. The supernatant liquid was transferred, centrifuged again at 2000 rpm for 10 min and then an aliquot removed for MS analysis.

Liquid chromatography - time of flight mass spectrometry (LC-TOFMS) analyses were conducted using an Agilent 1100 series HPLC coupled to an Agilent 6510 Q-TOF (Agilent Technologies, USA). Separation was performed using a reverse phase column (Agilent Eclipse Plus C18, 5 µm, 150 × 2.1 mm) together with the corresponding guard column (5 µm, 12.5 × 2.1 mm). The mobile phase consisted of 95 % methanol containing 0.1 % formic acid in channel A, and 5 % methanol containing 0.1 % formic acid in channel B. The system was programmed to perform an analysis cycle consisting of 100 % B for 1 min, followed by gradient elution from 100 % to 5 % B over a 14 min period, hold at 5 % B for 10 min, return to initial conditions over 2 min and then hold these conditions for a further 8 min. The flow rate was 0.20 mL min^{-1} and the injection volume was 5 µL. MS experiments were carried out using ESI in positive ion mode with the capillary voltage set at 4.0 kV. The desolvation gas was nitrogen set at a flow rate of 8 L min^{-1} and maintained at a temperature of 350 °C.

Homocysteine sulphoxide (HCySO) – $C_4H_9NO_3S$

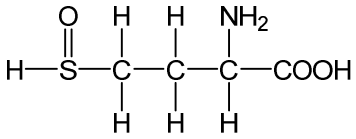

M+H$^+$ Calculated mass 152.03759, found mass 152.03780

M+NH$_4^+$ Calculated mass 169.06414, found mass 169.06445

M+Na$^+$ Calculated mass 174.01953, found mass 174.01992

4-hydrosulfinyl-2-hydroxybutanoic acid (HSBA) – $C_4H_8O_4S$

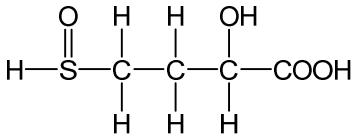

M+H$^+$ Calculated mass 153.02161, found mass 153.02142

M+NH$_4^+$ Calculated mass 170.04808, found mass 170.04808

M+Na$^+$ Calculated mass 175.00360, found mass 175.00360

Evidence of loss of water from this molecule consistent with structure.

Homocystic acid (HCyA) – $C_4H_9NO_5S$

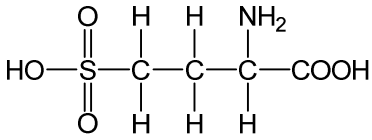

M+H$^+$ Calculated mass 184.02742, found mass 184.02732

2-Amino-butanoic acid (ABA) – $C_4H_9NO_2$

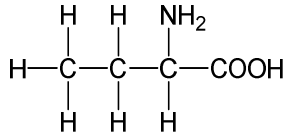

M+H$^+$ Calculated mass 104.07115, found mass 104.07119

Chapter 6

Methionine as a precursor of methane in living plants

Submitted to *Plant, Cell & Environment*, 2012.

Frederik Althoff[1], Steffen Greiner[2], Markus Greule[1] and Frank Keppler[2]

Abstract

The finding that terrestrial plants produce the greenhouse gas methane (CH_4) has led to much discussion and debate, not only about its contribution to the global CH_4 budget, but also as regards the authenticity of the actual observation. Although the phenomenon has recently been accepted for both living and dead plants, the mechanism of formation in living plants still needs to be elucidated and its precursor compounds identified. Here we show that methionine, a compound that plays a major role in transmethylation reactions in plants, acts as a precursor of CH_4 formation in both tobacco cells and intact plants. Employing ^{13}C-labelled methionine clearly identified that the sulphur bound methyl group provided the carbon atom for CH_4 released from intact tobacco plants. Moreover, CH_4 production increased when sodium azide, a compound known to disrupt electron transport flow at the cytochrome c oxidase (complex IV) in plant mitochondria, was added to cell cultures fortified with methionine. Our results suggest that methionine might play an important role in the formation of CH_4 in living plants particularly when they are under abiotic stress conditions.

Keywords: stable isotopes; greenhouse gas; methyl-donating compounds; sodium azide

6.1 Introduction

The observation that plants produce methane (CH_4) under aerobic conditions has caused considerable controversy amongst the scientific community (Keppler et al., 2006, 2008; Dueck et al., 2007; Keppler and Röckmann, 2007; Beerling et al., 2008; McLeod et al., 2008; Vigano et al., 2008; Wang et al., 2008; Brüggemann et al., 2009; Bruhn et al., 2009, 2012; Messenger et al., 2009; Nisbet et al., 2009; Qaderi and Reid, 2009, 2011).

[1] Max-Planck-Institute for Chemistry, Hahn-Meitner-Weg 1, 55128 Mainz, Germany.
[2] Centre for Organismal Studies, Im Neuenheimer Feld 360, 69120 Heidelberg, Germany.

Despite intense scepticism, many recent experimental studies have demonstrated the phenomenon to be true for both dead and living plants (Keppler et al., 2009; Qaderi and Reid, 2011; Wang et al., 2011; Bruhn et al., 2012). Non-microbial CH_4 release has been shown to occur under ultraviolet (UV) irradiation and elevated temperatures from dry and detached fresh plant material (McLeod et al., 2008; Vigano et al., 2008; Bruhn et al., 2009). Pectin has been considered as a source of CH_4 production because of its high degree of methylation (Keppler et al., 2008; Bruhn et al., 2009; Messenger et al., 2009). A reaction of reactive oxygen species (ROS) with pectic polysaccharides was suggested as a possible route to CH_4 formation under UV radiation (Messenger et al., 2009). However, CH_4 can be derived from other structural components as shown with commercially purified lignin and cellulose (Vigano et al., 2009) and even ascorbic acid when placed under highly oxidative conditions (Althoff et al., 2010). For more detailed information, regarding CH_4 formation from dry and fresh detached plants as well from specific plant structural compounds, the reader is referred to a recent review by Bruhn et al. (2012).

In addition, stable isotope techniques have been employed to demonstrate that living plants release CH_4 (Brüggemann et al., 2009; Wishkerman et al., 2011) at rates in the range of 0.16-12 ng g^{-1} dw h^{-1}. Young poplars grown in a $^{13}CO_2$ atmosphere (Brüggemann et al., 2009) and plant cells grown in culture supplemented with ^{13}C-labelled sucrose (Wishkerman et al., 2011) confirmed that CH_4 is produced in plants per se and not by any of their associated micro-organisms. In this context it has been suggested that CH_4 formation was a result of exposure of plants to abiotic stress factors. This would be in accordance with two recent studies by Qaderi and Reid (2009, 2011). Although these results provide support for the contention that living plants release CH_4, the mechanism of formation or identity of its precursors still remain unknown.

Recently Wishkerman et al. (Wishkerman et al., 2011) conducted a study that aimed to provide a further understanding of the mechanism of formation and the identity of precursor compounds. To achieve this they investigated the influence of the toxin sodium azide (NaN_3) on cell cultures of tobacco, sugar beet and grape vine. Sodium azide is a compound known to disrupt electron transport flow at the cytochrome c oxidase (complex IV) in plant mitochondria. The results of the study suggested that site-specific disturbance of the electron transport chain (ETC) at complex IV causes CH_4 formation in

plant cells. A plausible conclusion of this finding is that CH_4 formation in living plants may be an integral part of cellular response towards changes in oxidative status present in all eukaryotes. It has been hypothesized that electrophilic methyl groups of biomolecules such as phosphatidylcholine or methionine could be the carbon precursor for CH_4 in both animal and plant cells (Ghyczy et al., 2003, 2008; Keppler et al., 2009; Wishkerman et al., 2011). However, no pathway involving either of these compounds in CH_4 formation has been identified thus far. It is interesting to note that Althoff and Keppler (2011) investigated a purely chemical reaction system that utilized methyl-donating compounds (MDCs), including methionine, for the generation of CH_4 under ambient conditions. A potential role for the involvement of methionine in CH_4 production in living plants was also highlighted by Bruhn et al. (2012).

In this study we investigated a possible role for the MDCs such as betaine, choline and methionine in the formation of CH_4 in living plants. For this we choose tobacco *(Nicotiana tabacum)* as the model plant since it is easily grown under sterile conditions, both in cell culture and at whole plant level. Stable isotope techniques were employed both to verify *in vivo* CH_4 formation and also to identify the carbon atom precursor of CH_4 when ^{13}C-postionally labelled methionine was utilised.

6.2 Material and Methods

6.2.1 Plant and cell cultivation under sterile conditions

6.2.1.1 Tobacco cells (Nicotiana tabacum cv. BY2)

The medium used for tobacco BY2 batch cell cultures was as follows: 4.3 g L^{-1} MS (Murashige & Skoog) salts, 30 g L^{-1} sucrose , 100 mg L^{-1} myo-inositol, 1 mg L^{-1} thiamine, 0.2 mg L^{-1} 2,4-dichlorophenoxyacetic acid, and 255 mg L^{-1} KH_2PO_4. The pH of the medium was adjusted to 5.7 using KOH. Cell suspensions (50 mL in 250 mL Erlenmeyer flasks) were incubated in the dark at 24 ± 1 °C and shaken at 150 rpm. Cells were sub-cultured weekly by transfer of 5 mL suspension to 45 mL fresh medium. After 6 days growth the cell suspensions were used for experiments.

6.2.1.2 Tobacco plants (Nicotiana tabacum)

The medium used for tobacco plants was as follows: 4.56 g L^{-1} MS salts, 20 g L^{-1} sucrose and 10 g L^{-1} (plant) agar. The pH of the medium was adjusted to 5.8 using KOH and placed into

purpose-made glass vials fitted with a threaded side port sealed with a hole type screw cap and PTFE/silicone septum. An apical cutting of *Nicotiana tabacum* grown under sterile conditions was placed in the medium through the opening at the top, the opening covered with aluminium foil and the vial placed under a light relay that simulated the emission of sunlight (150 μE m^{-2} s^{-1}) with 14 h day/light cycle. Experiments were conducted after rooting when the plants had grown to approx. 8 to 10 cm.

6.2.2 Investigations with cells and plants

6.2.2.1 Cell suspension studies

After the 6 day growth period, cell suspension (4.9 mL; ca. 0.1 g dry mass) was transferred to a sterile vial (40 mL) and MDC solution (100 µL, equivalent to 1 µM in vial for each MDC) added. After a 10 min incubation period, a NaN_3 (12.5 µL, 1 M) or NaCN (12.5 µL, 1 M) solution (equivalent to 2.5 mM in vial) was added and the vial sealed using a hole type screw cap fitted with a PTFE/silicone septum. For experiments using CO, pure CO (1 mL) was injected through the septa into the headspace of the sealed vial using a gas tight syringe. All samples were prepared in five replicates (n=5). Control samples (blanks) were prepared in a similar fashion to that described for the samples but without the addition of MDCs and NaN_3. All samples were incubated for a 24 h period and results are presented as ΔCH_4 (ng g^{-1} dw), the difference between the CH_4 headspace concentrations from sample and blank applied to 1 g of dry substance.

6.2.2.2 Supplementation of whole plants with ^{13}C-methionine

Tobacco plants were grown as described above. Leaf infiltration (Voinnet et al., 2003) was carried out by infiltrating a ^{13}C-methionine (^{13}C-MET) solution into the abaxial air spaces of the leaves (0.3 mL of 10 or 50 mM). For root supplementation, the media was first carefully removed and the plants placed into a sterile glass beaker containing a ^{13}C-MET solution (15 mL, 30 µM) such that only the roots were in contact with the solution. Plants and beakers were placed in the purpose-made glass vials described above. Control samples were prepared in an identical fashion to that for the samples except that an unlabelled methionine (MET) solution was used. After sample preparation the vials were closed using a glass plate and an O-ring fixed with a clamp and then placed under the light relay at 24 ± 1 °C.

6.2.3 Analytical techniques

6.2.3.1 Measurement of headspace CH_4 concentration by GC-FID

Headspace (5 mL) from the sealed glass vials was sampled using a Hamilton gas syringe and needle and analysed by a gas chromatograph fitted with a flame ionization detector (GC-FID) (Shimadzu GC-14B; column: 2 m, Ø=3.175 mm (i.d.) high-grade steel tube packed with Molecular Sieve 5A 60/80 mesh from Supelco). Quantification of CH_4 was performed by direct comparison of the sample peak area with that obtained for two reference standards (8.905 and 1.835 ppm).

6.2.3.2 Dry weight determination

Immediately after CH_4 measurement the vials and contents were stored at –20 °C. Subsequently the lids were removed and the samples were lyophilized for dry weight (dw) determination

6.2.3.3 Continuous flow isotope ratio mass spectrometry for measurement of $\delta^{13}C$ values of CH_4

For isotopic measurements with BY2 cells headspace gas from the vials (350 mL) containing cell suspension (25 mL) was sampled. For experiments with whole tobacco plants the headspace in the incubation vials was tested. In each instance headspace gas (40 mL) from the sample was transferred to an evacuated sample loop (40 mL). Interfering compounds were separated by gas chromatography and CH_4 trapped on Hayesep D. The sample was then transferred to the IRMS (ThermoFinnigan Delta^{plus} XL, Thermo Finnigan, Bremen, Germany) via an open split. As reference gas carbon dioxide of high purity (carbon dioxide 4.5, Messer Griesheim, Frankfurt, Germany) with a known $\delta^{13}C$ value of –23.64 ‰ (VPDB) was used. All $\delta^{13}C$ values were normalized relative to VPDB (Vienna Pee Dee Belemnite) using a CH_4 standard. Samples were routinely analysed three times (n=3) and the average standard deviations of the GC/C/IRMS measurements were in the range of 0.1 to 0.3 ‰.

All $^{13}C/^{12}C$ isotope ratios are expressed in the conventional δ notation in per mil versus VPDB, [‰] using the following equation (Eq. 6.1):

$$\delta^{13}C_{VPDB} = (({}^{13}C/{}^{12}C)_{sample} / ({}^{13}C/{}^{12}C)_{standard}) - 1. \qquad \text{(Eq. 6.1)}$$

6.2.4 Statistics

The statistical comparison between different samples was examined with an open-source software package 'The R Project for Statistical Computing', version 2.11.1 (The R Foundation for Statistical Computing). All statistical tests were performed with a level of significance at α=0.05. Differences between results are given as significant ($p<0.05$) or highly significant ($p<0.001$). In the case of normal distribution and homogeneity of variances, analysis of variances (ANOVA) was used to test differences in emission rates between samples. If the dataset did not show normal distribution and/or homogeneity of variances, a Kruskal-Wallis rank sum-test was employed. Finally a Mann-Whitney-Wilcoxon-test was performed to provide evidence about the significance in differences between single samples.

6.3 Results and discussion

6.3.1 Methane emission from tobacco cell suspensions when treated with different toxins

Figure 6.1 shows CH_4 generation by BY2 cells after treatment with sodium azide (NaN_3), sodium cyanide (NaCN) or carbon monoxide (CO) for 24 h. All three toxins (CN^-, N_3^- and CO) are known to bind to the reactive centre of cytochrome c oxidase (complex IV, CIV) and inhibit the protein from its function to utilise oxygen by reducing it. The electrons required for the reduction of oxygen are provided by the cytochrome c which gets oxidised in return (Møller, 2007). For BY2 cell suspensions when treated with NaN_3 maximum CH_4 production was found at a concentration of 2.5 mM (ca. 100 ng CH_4 g^{-1} dw). A highly significant ($p<0.001$) difference in CH_4 formation was observed for cell suspensions when different concentrations of NaN_3 was added. In comparison, whilst NaCN also exhibited a maximum at 5 mM (ca. 70 ng CH_4 g^{-1} dw), only a significant difference ($p<0.05$) between 2.5 mM and 5 mM and a highly significant difference ($p<0.001$) between 5 and 10 mM was noted. Whilst at concentrations of 1, 5 and 10 mM addition of NaCN would appear to lead to more CH_4 formation than for similar concentrations of NaN_3, at 2.5 mM formation is significantly ($p<0.001$) increased when NaN_3 is used. Therefore, it was decided to use NaN_3 at a concentration of 2.5 mM for all subsequent cell suspension studies. Furthermore, we also measured increased CH_4 formation when CO was added to the headspace indicating that a fraction of the CO had been taken up by the suspended cells. Compared with the findings of Wishkerman et al. (2011), who first investigated the effect of NaN_3 on tobacco cells, the

amounts of CH_4 formed were lower in our experiments. However, a similar trend with maximum CH_4 formation at a concentration of 2.5 mM NaN_3 was noted in both studies. Whereas Wishkerman et al. (2011) only employed NaN_3 for their work, we also tested the additional toxins NaCN and CO. Both compounds also led to the enhanced formation of CH_4 by tobacco cell suspensions. Since each of the three inhibitors increased CH_4 formation, our results add further support to the involvement of the reactive Fe-centre in mitochondria's complex IV of the ETC in the generation of CH_4 in plant and animal cells (Ghyczy et al., 2008; Wishkerman et al., 2011; Boros et al., 2012).

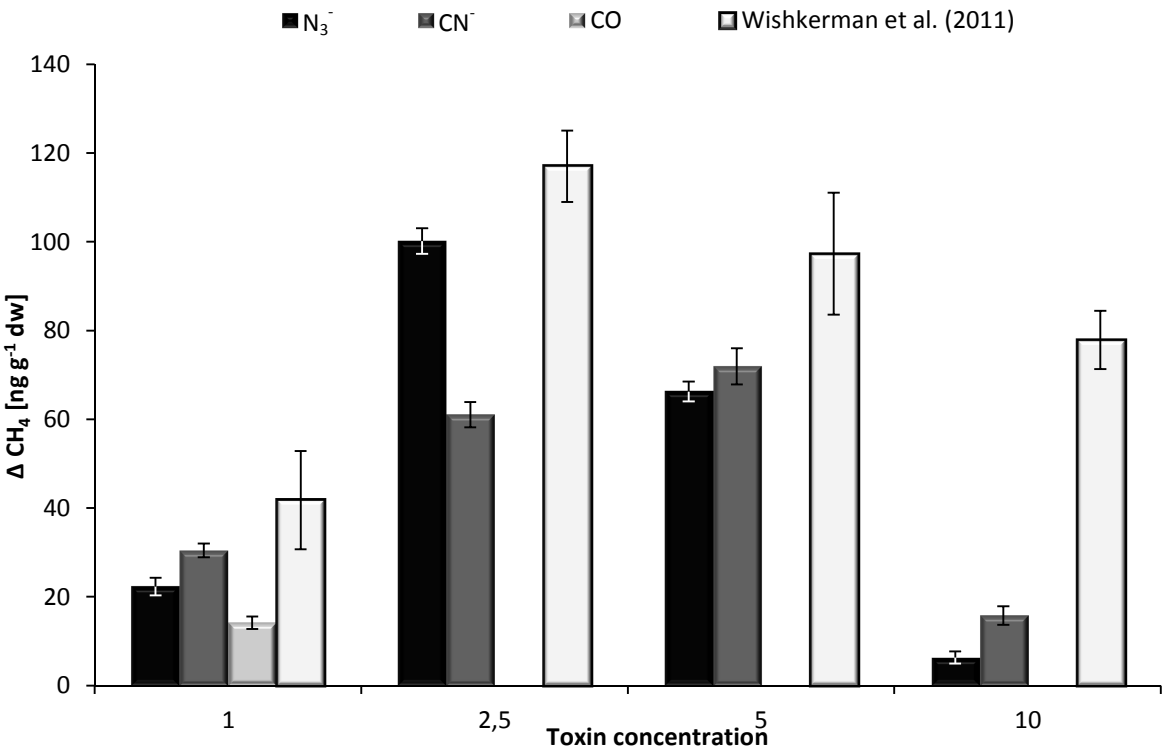

Figure 6.1: Formation of methane from plant cell suspensions when treated with varying concentrations of different cytochrome c oxidase inhibitors (NaN_3, NaCN and CO). Solid black, dark and light grey bars show CH_4 formation 24 h after addition of NaN_3 [mM], NaCN [mM] and CO [mL], respectively. Unfilled bars show results from a similar experiment conducted by Wishkerman et al. (2011). Data show mean value ± SD (n=5).

6.3.2 Comparison of methane release from tobacco cell suspensions with and without added methyl-donating compounds (MDCs) when treated with sodium azide

The formation of CH_4 over a 24 h period was evaluated following treatment of BY2 cell suspensions with the MDCs betaine (BET), choline chloride (CC), leucine (LEU), methionine (MET), S-methyl-methionine (MMET), methionine sulfoxide (MSO) and S-adenosyl-methionine (SAM) and subsequent addition of NaN_3. For comparative purposes a control sample was also prepared where only NaN_3 was added to the cell suspension. Figure 6.2 shows the amount of CH_4 produced from cell suspensions with and without addition of MDCs and treatment with NaN_3. Methionine was the only MDC that induced a highly significant increase ($p<0.001$) in CH_4 production of approximately one-and-a-half times after 24 h. Leucine and MSO showed much smaller (~5 % higher) but not significant ($p>0.05$) CH_4 formation. All of the other applied MDCs did not significantly increase the production of CH_4 when compared with the NaN_3 (2.5 mM) treated but non supplemented BY2 cells (see Figure 6.2). Although we did not find a significant production from MDCs other than Met we cannot entirely rule them out as CH_4 precursors. The reason for this uncertainty is that we could not exclude the possibility that uptake of the MDC by the tobacco cells was the significant limiting factor for their participation in CH_4 formation. Measurement of uptake of the MDCs by the cells was not possible for this study. However based on this experiment we focused on MET as a potential precursor for CH_4 in living plants.

When MET is used in biological systems for methyl transfer reactions, it is usually first activated by catalysis with adenosine-5'-triphosphate (ATP) by the enzyme methionine adenosyltransferase to form S-adenosyl-methionine (SAM). Interestingly, suspensions of BY2 cell supplemented with SAM showed no higher formation of CH_4 even when treated with NaN_3. An explanation for this finding could be that SAM is not readily taken up by the BY2 cells. However, alternatively, CH_4 may be produced by a reaction pathway that does not involve the SAM intermediate. Figure 6.3 shows the relationship between CH_4 formation and the amount of added MET. A significant effect in CH_4 formation ($P<0.05$) was noted when the MET concentration was increased from 0.01 to 0.1 µM and from 10 to 100 µM. However, a highly significant ($p<0.001$) effect was noted for the increase from 0.1 to 1 µM. Maximum CH_4 formation was observed when MET was supplemented in a concentration of 1 µM and decreased again at concentrations above these. The concentration of the free amino acid

MET in plant tissues is usually <100 µM, while that of protein Met is much higher (Inaba et al., 1994; Bruhn et al., 2012). Thus, it could be argued that at the higher concentrations increased levels of MET in the cells could inhibit further uptake of MET from media (Hart and Filner, 1969). However, again, uncertainty remains as to how much MET was actually taken up by the tobacco cells.

These findings do not exclude the possibility that compounds other than MET could also act as sources of CH_4 in plants. Nevertheless we consider the finding that MET is a precursor of CH_4 produced by plants to be another important step towards the elucidation of a biochemical pathway in the biosynthesis of this compound.

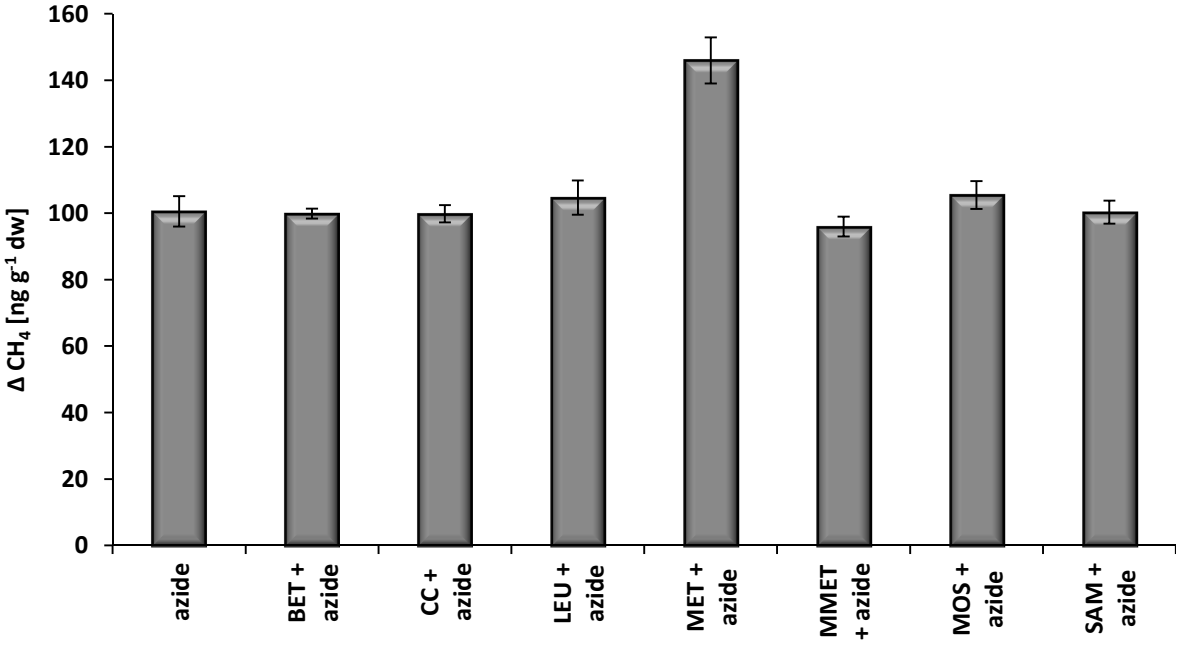

Figure 6.2: Methane formation by BY2 cell suspensions supplemented with different MDCs and treated with NaN_3. Used MDC substances were betaine (BET), choline chloride (CC), leucine (LEU), methionine (MET), S-methyl-methionine (MMET), methionine sulfoxide (MSO) and S-adenosylmethionine (SAM). The concentration of MDCs and NaN_3 in the cell suspension was 1 µM and 2.5 µM, respectively. Note that values are normalized to BY2 cells that were not treated with NaN_3. Data show mean value ± SD (n=5) after a 24 h period.

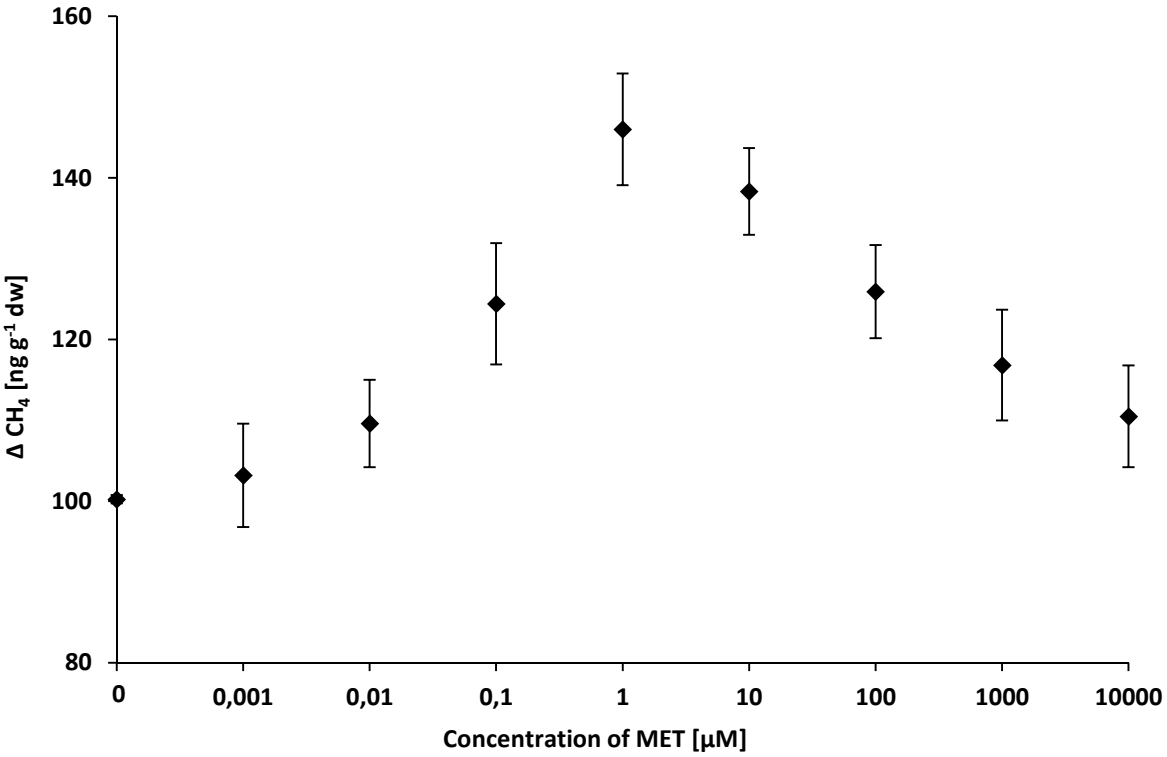

Figure 6.3: Methane formation by BY2 cell suspensions supplemented with different concentrations of methionine. Data show mean value ± SD (n=5) after a 24 h period.

6.3.3 Identification of the methane carbon atom precursor using ^{13}C-positionally labelled methionine and intact tobacco plants

It can be readily envisaged that the thio-methyl group of MET is the likely candidate precursor of CH_4 formation in living plants. This has recently been considered by Bruhn et al. (2012). Interestingly, Althoff and Keppler (2011) demonstrated that the thio-methyl group of MET can be converted to CH_4 under oxic conditions by a purely chemical reaction using only ascorbic acid, iron minerals, hydrogen peroxide and MET. To test this hypothesis we employed MET which had only the carbon atom of the thio-methyl group (–S–$^{13}CH_3$) labelled with ^{13}C (99 % $^{13}CH_3$). Both leaves and roots of tobacco plants were separately supplemented with different concentrations (Figure 6.4) of ^{13}C-labelled methionine (^{13}C-MET). Initially following treatment with or without ^{13}C-MET the headspace gas of all samples showed $\delta^{13}C(CH_4)$ values of around –46 ‰ (ranging from –45.4 to –47.1 ‰) and thus closely reflected the atmospheric background $\delta^{13}C(CH_4)$ values of the laboratory air (–46.1 ± 0.5 ‰). The $\delta^{13}C(CH_4)$ values for the headspace of the tobacco plants containing unlabelled MET did

not change significantly over the entire incubation period. In contrast $\delta^{13}C(CH_4)$ values in the headspace of the tobacco plants where ^{13}C-MET was added at different concentrations to the leaves or roots showed a continuous increase in $\delta^{13}C(CH_4)$ values over the entire incubation period. A change in $\delta^{13}C(CH_4)$ values of around 45.9 and 44.6 ‰ over the 120 h incubation period was measured for tobacco plants where the leaves or roots were treated with 10 µM and 30 µM ^{13}C-MET, respectively. The largest change in $\delta^{13}C(CH_4)$ values of about 240 ‰ was observed for the tobacco plants when the highest concentration (50 mM) of ^{13}C-MET was added to the leaves. Although all treatments with ^{13}C-MET showed more positive $\delta^{13}C(CH_4)$ values after 24 h, the most pronounced increase in values was noted between 24 and 72 h for the 50 mM addition, with an apparent linear relationship between the $\delta^{13}C(CH_4)$ values and incubation time. During this time period the $\delta^{13}C(CH_4)$ values for the tobacco plant treated with 10 µM, 30 µM and 50 mM ^{13}C-MET changed at a rate of 0.45, 0.63 and 4.2 ‰ h^{-1}, respectively. After the 72 h incubation period the rates decreased indicating that less ^{13}C-MET was converted to CH_4. Based on the changes of the $\delta^{13}C(CH_4)$ values, the amount of added ^{13}C-MET and the dry weight of the plants, the calculated emission rates on a plant dry weight basis were found to be 0.055, 0.057 and 0.2 ng CH_4 g^{-1} dw h^{-1} for the tobacco plant treated with 10 µM, 30 µM and 50 mM ^{13}C-MET, respectively. However, these numbers may be somewhat misleading since it is not known if the whole plant was homogenously provided with ^{13}C-MET. Thus we decided a more reasonable approach was to relate the formation of isotopically labelled CH_4 directly to the amount of ^{13}C-MET added to the plant and express it as the molar ratio ($^{13}CH_4$/^{13}C-MET) of produced CH_4. The molar ratio of converted CH_4 at the end of the incubation period (120 h) was 0.01, $1 * 10^{-4}$ and $\sim 1 * 10^{-5}$ for the tobacco plants treated with 10 µM, 30 µM and 50 mM, respectively. These ratios show that highest conversion of CH_4, i.e. one out of 100 ^{13}C-MET molecules, was found for the tobacco plant that was supplemented with 10 µM ^{13}C-MET. Although emission rates on a plant dry weight basis were by an order of magnitude higher for the 50 mM application the CH_4 conversion was much lower (by a factor of 1000). These results clearly verify that the carbon atom of the sulphur bound methyl group of methionine [H_3**C**–S–$(CH_2)_2CH(NH_3)COOH$], is a precursor of methane [**C**H_4] generated by plants. Some tobacco plants with ^{13}C-MET supplementation to both leaves and roots were also treated with NaN_3. Unfortunately, these plants died within a few hours following application of the azide and thus no experimental data could be collected. Such experiments together with

investigations into other plant stress factors in combination with ^{13}C-MET will have to await further studies.

We would like to highlight that for our studies we used plants that were grown under sterile conditions. However, despite these efforts we cannot fully exclude the possibility of the presence of microorganisms including methanogens during our investigations. Nevertheless, the observed kinetics of CH_4 formation using ^{13}C-MET and the $\delta^{13}C(CH_4)$ values of the control samples would not provide any support for the involvement of methanogens in the formation of CH_4.

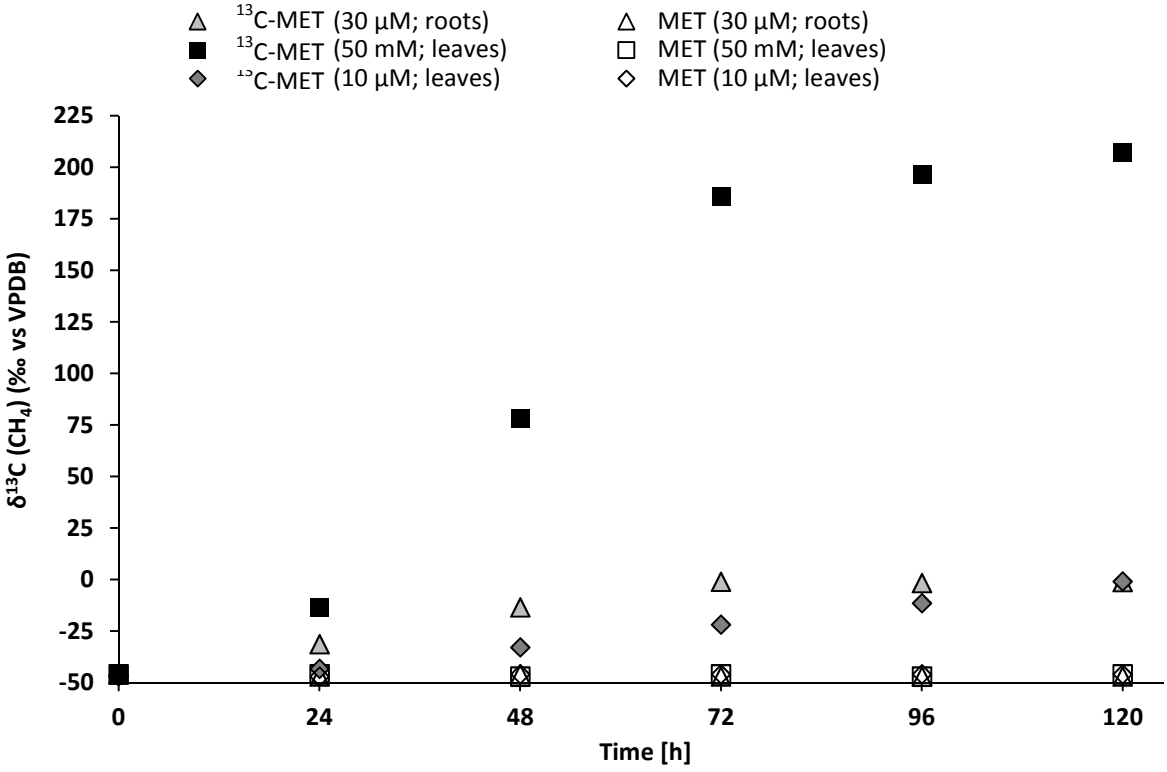

Figure 6.4: Change of $\delta^{13}C$ values of CH_4 produced by intact living plants supplemented with ^{13}C-labelled MET. Solid black squares, solid dark grey diamonds, and solid light grey triangles show $\delta^{13}C(CH_4)$ values measured for intact plants which were treated with 50 mM (leaves), 10 µM (leaves), and 30 µM (roots) ^{13}C-labelled MET respectively, whereas unfilled symbols represent the corresponding treatments with unlabelled MET.

Although a detailed mechanism of the formation of CH_4 in living plants is still missing it has been shown that a site-specific disturbance of the ETC at complex IV causes CH_4 formation in plant cells (Wishkerman et al., 2011). In contrast, the addition of other electron transport chain (ETC) inhibitors (complex II and III) did not result in significant CH_4 formation. This

study is another important step in the elucidation of precursor compounds involved in CH_4 generation in living plants. The studies with ^{13}C-MET clearly shows that the carbon atom of the methyl group of MET is clearly transferred to CH_4. It is most likely that the whole methyl group itself is the precursor group and thus we would like to hypothesise that CH_4 formation occurs in the intermembrane space of the mitochondria likely at the cytochrome c oxidase complex (Figure 6.5). Here the required protons and electrons/ROS for the reduction of the methyl group carbon are available. We suggest that further experiments should aim to confirm the involvement of mitochondria in the formation of CH_4. This could be achieved by treating purified preparations of mitochondria with N_3^-/CN^- or by pre-incubation with different MDCs like MET. Knowing the starting material and the exact location of carbon atom in the material that serves as a CH_4 precursor is an excellent starting point to help further decipher the mechanism involved in its formation. In this context future use of isotope labelling studies similar to those employed in this investigation will greatly assist tracking the route of all other precursors involved in the formation of CH_4.

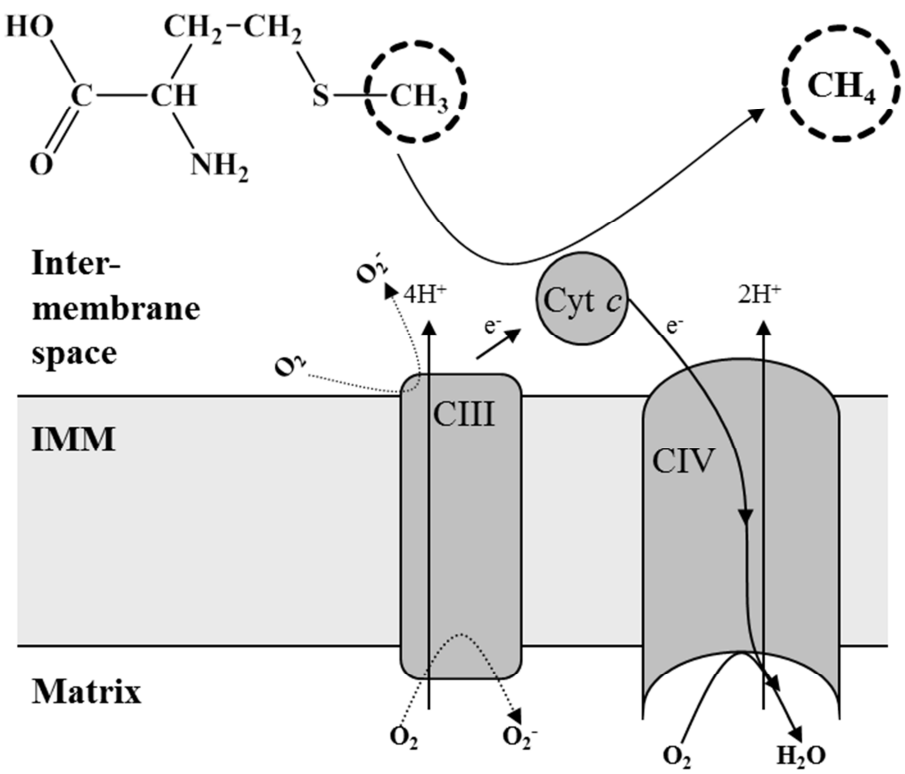

Figure 6.5: Hypothetical scheme of CH_4 formation from methionine during disturbance of complex IV at the ETC in mitochondrial intermembrane space. Chemical structure (top left) shows the amino acid methionine with highlighted methyl group; CIII and CIV, complex III and IV; Cyt *c*, cytochrome c; IMM, inner mitochondrial membrane (Møller, 2007; Wishkerman, 2011, modified).

An understanding of the mechanism involved in the formation of CH_4 in living plants may help the scientific community to decide if this simple molecule also plays a more general physiological role in nature. It appears that in living plants, CH_4 generation may be linked to environmental stress (Qaderi and Reid, 2009, 2011; Wang et al., 2011) and thus it is important to identify environmental factors which control its formation, particularly under abiotic stress. Furthermore, a comprehensive understanding of the processes of CH_4 formation in both dead and living plants and the parameters that control its emissions is a prerequisite to gaining a more reliable estimate of the contribution plants make to the global CH_4 budget.

6.4 Acknowledgments

We thank John Hamilton and Daniela Polag for reviewing the paper. We also thank Sonja Jung, Ilka Hermes and Christoph Hann for assistance. This work was funded by the ESF (EURYI Award to F.K.) and DFG (KE 884/2-1 and KE 884/7-1).

Chapter 7

The work presented in this chapter is the result of the investigations of the diploma student Miriam Hurkuck I supervised during her thesis. We planned the experiments together and discussed the result.

Release of methane from aerobic soil: an indication of a novel chemical natural process?

Published in *Chemosphere,* 2012.

Miriam Hurkuck[1,2,3], Frederik Althoff[1], Hermann F. Jungkunst[2], Alke Jugold[1] and Frank Keppler[1]

Abstract

Methane (CH_4) formation under aerobic conditions has been intensely debated, especially since the discovery of CH_4 generation by both dried plant material and living plants. In this study we test the hypothesis that non-microbial CH_4 formation also occurs in soils. All lyophilised soil samples investigated under aerobic conditions released CH_4 at temperatures ranging from 30 to 70 °C exceeding that allowing normal enzymatic activity to proceed. No emissions were observed for single mineral soil components such as quartz sand, clay mineral and iron oxide. Methane release rates from the soils investigated were found to increase both with increasing temperature and higher organic carbon content. Addition of water to dried soils increased CH_4 release rates up to 8-fold those observed with the dried material. Our results suggest the existence of a chemical process in soils that produces CH_4 under aerobic conditions, a finding which has not been hitherto reported.

Keywords: greenhouse gas; organic matter; clay; iron oxide; lignin; thermal degradation

[1] Max-Planck-Institute for Chemistry, J.-J.-Becher-Weg 27, 55128 Mainz, Germany.
[2] Institute of Geography, Landscape Ecology, University of Göttingen, Goldschmidtstraße 5, 37077 Göttingen, Germany.
[3] Currently at Johann Heinrich von Thünen-Institute, Institute of Agricultural Climate Research, Federal Research Institute for Rural Areas, Forestry and Fisheries, Bundesallee 50, 38116 Braunschweig, Germany.

7.1 Introduction

Methane is the most abundant organic trace gas in the atmosphere and plays an important role both to tropospheric and stratospheric chemistry. Around 70 % of atmospheric CH_4 originates from biogenic sources (Lelieveld et al., 1998; Ehhalt et al., 2001; Denman et al., 2007; Conrad, 2009).

Microbes in soils are known to both emit and consume CH_4. Methanogenic archaea and CH_4 production are typically found at sites where organic matter is decomposed in the absence of oxygen or other oxidants, such as nitrate, sulphate or ferric iron. Due to their strictly anaerobic conditions, natural wetland ecosystems are one of the main sources of biogenic CH_4. Aerobic methanotrophic bacteria are widely distributed in nature, typically at anoxic-oxic interfaces, such as sediments, where they attenuate the flux of CH_4 into the atmosphere (Conrad, 2009).

In 2006 Keppler and co-workers reported direct CH_4 emissions from vegetation foliage under aerobic conditions (Keppler et al., 2006). This controversial work was rapidly followed by a number of similar studies of which several were either unable to reproduce CH_4 emissions by living plants, or disagreed with the global extrapolations provided by Keppler and his co-workers (Dueck et al., 2007; Wang et al., 2008; Nisbet et al., 2009). However, stable isotope labelling studies (Keppler et al., 2008; Vigano et al., 2008, 2009; Brüggemann et al., 2009; Wishkerman et al., 2011) verified that CH_4 is formed from both dead plant tissue and intact living plants. Non-microbial CH_4 release has also been shown to occur under high UV irradiation and elevated temperatures from dry and detached fresh plant material (Vigano et al., 2008). Similar results were also obtained when detached tobacco leaves and plant pectin were placed under UV radiation (280-400 nm) at ambient conditions (McLeod et al., 2008). A reaction between UV-generated reactive oxygen species (ROS) and pectic polysaccharides was suggested as a possible route to CH_4 formation (Messenger et al., 2009). A more detailed overview of our current understanding of CH_4 formation in aerobic environments can be found in a recent concept article by Keppler et al. (2009).

Recently, Althoff et al. (2010) demonstrated abiotic CH_4 formation under ambient conditions using the naturally available chemical compounds ascorbic acid, ferrihydrite and H_2O_2. Although the reaction pathway for CH_4 formation from ascorbic acid is currently unknown, this study was a first step towards tracking CH_4 formation using a chemical system under

highly oxidative conditions. Since CH_4 formation was not detected without the addition of ascorbic acid together with ferrihydrite and H_2O_2, the vinylic hydroxyl groups (HO-) of ascorbic acid as well as the physical and chemical properties of the iron mineral species were thought to play an important role. This chemical model system might also be considered appropriate to soils.

All observations of CH_4 production in soil so far have been attributed to methanogenesis even though some have been for oxic soils. For example, CH_4 release was observed from savannah soils in the dry season (Hao et al., 1988). Ten years later CH_4 production was demonstrated in forest soils even if the total CH_4 balance of the soil was negative (Andersen et al., 1998) and von Fischer and Hedin (2007) reported CH_4 formation in oxic soils using an isotope dilution technique. Anaerobic microsites as a refuge for methanogens has been offered as a possible explanation (Peters and Conrad, 1995) but in experiments conducted by Kammann et al. (2009) soil cores emitted significant amounts of CH_4 even after homogenization, a process that would destroy the anoxic microsites. Von Fischer and Hedin (2007) concluded that it might be premature to assume that methanogens are the sole source for CH_4 production in oxic soils. Although they referred to findings by Rimbault et al. (1988) that some oxic eubacteria produce CH_4 in trace quantities, it indicated that there might also be other processes involved in CH_4 formation in oxic soils. Jugold and Keppler (2009) also posed the question if the formation of CH_4 in soils were possible by a chemical process.

Based on the recent discoveries of aerobic CH_4 formation from dried plant matter, in this study we aimed to test the hypothesis that non-microbial CH_4 formation also occurs in soils. For our investigations several different soil samples were collected, homogenized and lyophilized prior to the start of the study. In addition to the complex soil samples, different compounds considered as single soil components were investigated for their potential to release CH_4. Organic compounds, such as lignin, pectin and cellulose, and mineral compounds, such as vermiculite, lepidocrocite and quartz (sea sand), were chosen for our experiments. All samples were tested for their potential to release CH_4 with increasing temperature (up to 70 °C). Additionally, we tested the influence of water on CH_4 release from both soils and the soil components.

7.2 Materials and methods

7.2.1 Origin of samples and preparation

Terra fusca, i.e. rich in clay soil samples were collected from the topsoil (*Terra fusca* A_h) and the subsoil (*Terra fusca* T) at the 'Nationalpark Hainich', Germany (51° 04' 46'' N, 10° 27' 08 '' E).

Sphagnum peat was sampled from the peat bog 'Großes Torfmoor' near Hille, Germany (52° 19' 24'' N, 8° 42' 35'' E). The material was collected as a bulk sample of the top 10 cm.

α-Cellulose, vermiculite, lignin, sea sand (mainly quartz sand), and apple pectin were obtained from Sigma, Taufkirchen, Germany. Lepidocrocite was synthesized as prescribed by Schwertmann and Cornell (2000). Double distilled water (H_2O) filtered with an ELGA UHQ-II-MK3 was used for these investigations.

All samples were first lyophilised and then homogenized. Roots and twigs were removed before the samples were ground using an ELTA UM105 electronic coffee grinder.

7.2.2 Determination of carbon content

The organic carbon content as % dry weight was determined using a Sulphur and Carbon Analyser (SC-144 DR, LECO). Sample material (0.1-0.5 g) was combusted in a furnace at 1300 °C. Calcium carbonate was employed as the reference standard for calculation of carbon content.

7.2.3 Experimental setup

All experiments were manufactured with 5 g soil material or specific single soil components. Samples were prepared in triplicate and incubated inside in-house manufactured glass vials (modification of a 300 mL Erlenmeyer-flask, Duran Group, with the neck of a 40 mL vial, Supelco). The vials were sealed with screw caps containing septa. PTFE coated silicone septa (Supelco) were used at incubation temperatures below 50 °C whilst above this temperature higher-temperature resistant PTFE silicone septa (Supelco) were employed.

7.2.3.1 Temperature dependency

Samples were incubated for 29 h at 30, 40, 50, and 70 °C using either a GC-oven or a compartment drier. Headspace CH_4 concentrations were measured hourly during the first 8

hours and then after 24, 26, and 29 h. Lignin and *sphagnum* peat were measured at 30 and 50 °C.

7.2.3.2 Wetting experiments

Sterile water was added to lyophilised soil samples (1:1) and headspace CH_4 was measured after incubation as described above. Samples with added water are herein after described as samples under wet conditions.

7.2.3.3 Control

As controls for the experiments with dried samples, empty vials containing only laboratory air were incubated under identical conditions to the samples. Methane concentrations in the controls always reflected the CH_4 background level of laboratory air (2-2.3 ppm). Controls for samples under wet conditions were performed by addition of H_2O (5 mL) to the incubation vial and incubated under identical conditions to the dry samples. Under all incubation conditions CH_4 concentrations were in the same range as that found for the empty vials including only laboratory air.

7.2.4 Methane measurements

Methane measurements were conducted by removal of headspace gas samples (5 mL) with a Hamilton gas syringe. The samples were analysed using a gas chromatograph (column: 2 m, inner diameter Ø = 3.175 mm high-grade steel tube packed with Molecular Sieve 5 A 60/80 mesh from Supelco) equipped with a flame ionization detector (Shimadzu GC-14B).

Two CH_4 gas standards with known concentrations (8.905 ppm and 1.905 ppm in synthetic air) were employed to quantify CH_4 release. The analytical precision of the analytical method was 0.011 ppm (n=20).

7.2.5 Calculation of methane emission rate

Methane emission rate in ng g^{-1} dw (dry weight) h^{-1} was calculated as the following:

$$ER = \frac{(c_v - c_c) \cdot M \cdot V}{G \cdot dw \cdot 24} \quad \text{(Eq. 7.1)}$$

ER	ng g^{-1} dw h^{-1}
c_v	concentration in the vial including sample after 24 hours [ppm]
c_c	concentration in the vial of control after 24 hours [ppm]
M	molar mass of CH_4 [16.04 g mol^{-1}]
V	volume of glass vial [mL]
G	gas constant of CH_4 (analysis at 25 °C) [24.464 L mol^{-1}]
dw	dry weight of sample [g]
24	factor to convert from 24 h (day) to one hour [h]

7.2.6 Statistical methods

All statistical tests were performed with a level of significance at α=0.05. Differences between results with respect to specific environmental conditions are given as significant ($p<0.05$). In case of normal distribution and homogeneity of variances, analysis of variances (ANOVA) was used to test differences in emission rates between the investigated samples. If the dataset did not show normal distribution and/or homogeneity of variances, a Kruskal-Wallis rank sum-test was used. A subsequent Mann-Whitney-Wilcoxon-test gave evidence about significance in differences between single samples.

The statistical comparison of different samples was examined with the open-source software 'The R Project for Statistical Computing', version 2.11.1 (The R Foundation for Statistical Computing).

7.3 Results and discussion

7.3.1 Organic carbon content of samples

As expected the mineral samples, vermiculite, lepidocrocite and quartz sand, did not contain measurable amounts of organic carbon. The organic carbon content of cellulose and pectin were around 43 and 39 %, respectively (Table 7.1). The highest organic carbon content, with nearly 50 %, was found for lignin and *sphagnum* peat. The *Terra fusca* soil samples were much lower in the range of 2 to 6 %.

7.3.2 Kinetics of methane release from pectin and lignin

In a first set of experiments two organic compounds were tested for their potential to produce CH_4 under elevated temperatures. Pectin was chosen because it had previously been shown to produce CH_4 when heated at temperatures ranging from 30 to 70 °C (Keppler et al., 2006, 2008). Although pectin is known to be an important structural compound of the cell wall in plants it is quickly degraded in soils. Thus we also choose lignin, another important plant component, for our experiments since it is a more significant and stable constituent of soil organic matter. Both compounds were heated at 70 °C over a time period of 29 h. Figure 7.1a shows the relationship between CH_4 emissions and incubation time for both pectin and lignin. The linear trend that CH_4 emissions increased with increasing incubation duration was significant for the first 8 h of the experiment and over the whole time period ($p<0.05$). Based on these results it was decided to report all CH_4 release rates in ng g^{-1} dw h^{-1} based on the measurement made after 24 h.

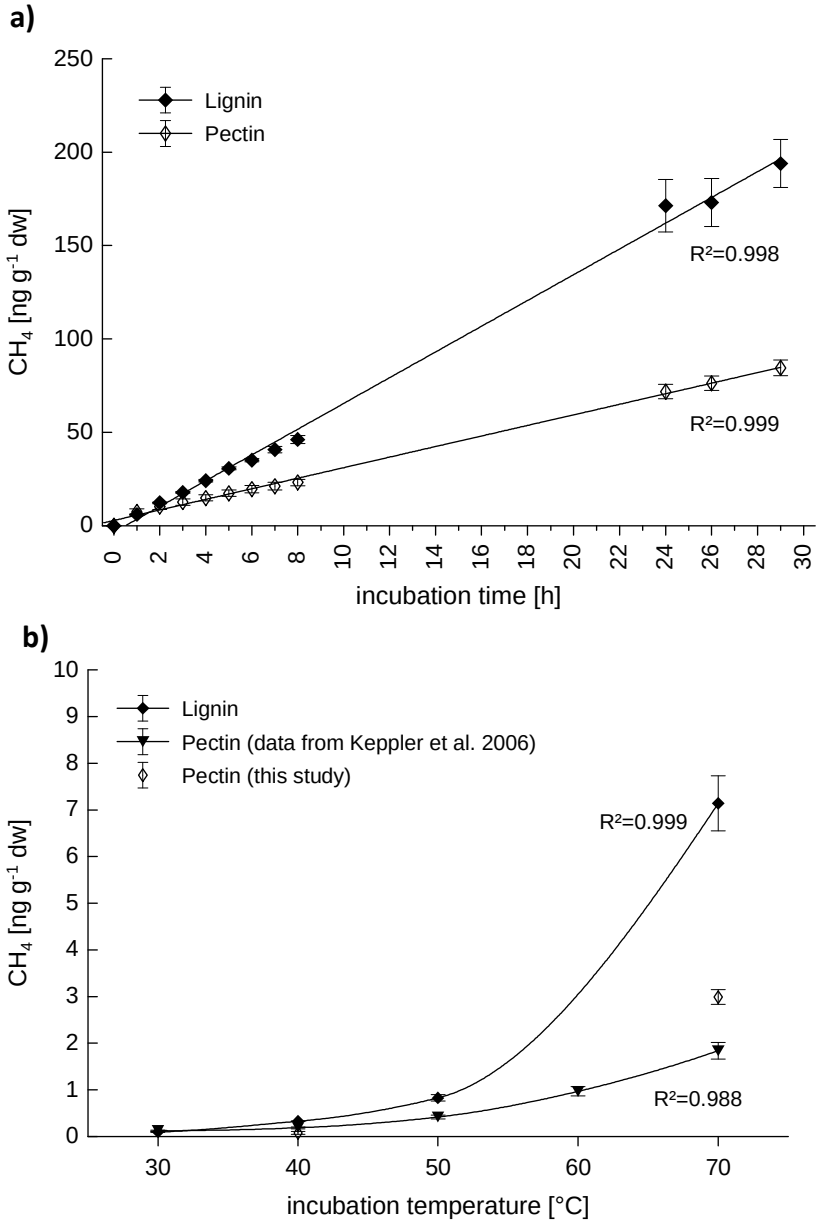

Figure 7.1: Methane release from lignin and pectin. (a) Relationship between CH_4 emissions and incubation time at 70 °C over a 29 h time period. (b) Relationship between CH_4 release rates and incubation temperature across the range 30 to 70 °C. Error bars represent the SD (n=3).

The relationship between CH_4 release and temperature across the range of 30 to 70 °C was similar for both pectin and lignin, with exponential increase of CH_4 release with higher temperatures (Figure 7.1b). At a temperature of 70 °C CH_4 release rates were 71 and 37 ng g^{-1} dw h^{-1} for lignin and pectin, respectively. Interestingly, CH_4 release rates for lignin were approximately twofold higher than those observed for pectin.

Table 7.1: Methane release rates from dry and wet samples.

sample	C_{org} [% dw]	CH_4 emission rates [ng g^{-1} dw h^{-1}]			
		dry 40 °C	**dry 70 °C**	**wet 40 °C**	**wet 70 °C**
Sand (quartz)	< 0.20	n.m.	0.00 ± 0.01	n.m.	0.00 ± 0.03
Vermiculite	< 0.20	0.00 ± 0.04	0.02 ± 0.03	*	*
Lepidocrocite	< 0.20	0.00 ± 0.04	0.01 ± 0.03	*	*
Terra fusca A_h	5.82 ± 0.05	0.08 ± 0.03	0.45 ± 0.02	0.20 ± 0.05	0.97 ± 0.10
Terra fusca T	1.98 ± 0.01	0.03 ± 0.00	0.19 ± 0.02	0.00 ± 0.00	0.18 ± 0.01
Sphagnum peat	49.24 ± 0.25	0.05 ± 0.01	1.87 ± 0.11	0.39 ± 0.04	6.24 ± 0.39
Pectin	38.93 ± 0.34	0.08 ± 0.03	2.99 ± 0.16	0.20 ± 0.02	6.69 ± 0.52
Cellulose	42.45 ± 0.24	0.00 ± 0.03	0.02 ± 0.00	0.04 ± 0.02	0.20 ± 0.02
Lignin	49.55 ± 0.67	0.33 ± 0.01	7.14 ± 0.59	1.89 ± 0.20	7.74 ± 0.77
		dry 30 °C	**dry 50 °C**	**wet 30 °C**	**wet 50 °C**
Sphagnum peat	49.24 ± 0.25	0.05 ± 0.02	n.m.	0.35 ± 0.04	0.66 ± 0.02
Lignin	49.55 ± 0.67	0.10 ± 0.01	0.83 ± 0.07	0.65 ± 0.02	3.10 ± 0.43

± represents the standard deviation (SD; n=3)

dw is dry weight

C_{org} is organic carbon content in % dry weight

n.m. = not measured

*CH_4 concentration remained constant after one hour therefore emission rates could not be calculated over the 24 h incubation period.

7.3.3 Release rates of methane from organics, soils and minerals under dry and wet conditions

In a next step we investigated three different types of soils, organic and mineral compounds for CH_4 release under dry and wet conditions at two different temperatures (40 and 70 °C). Except for lignin and pectin, no experiments at additional temperatures were undertaken due to limitations in sample amounts and laboratory capabilities.

The statistical comparison of organic and mineral samples within the groups revealed missing significance in differences for mineral samples. However, significant differences existed between organic samples.

All three soil samples, namely, peat, *Terra fusca* topsoil (A_h) and subsoil (T) with organic carbon content ranging from 2 to 49 %, showed CH_4 release under the experimental conditions employed (Figures 7.2, 7.3 and Table 7.1). Only the *Terra fusca* sample with the low organic carbon content had CH_4 release rates that were close to the limit of detection (< 0.02 ng g^{-1} dw h^{-1}) when incubated at 40 °C. Addition of water to the *Terra fusca* topsoil (A_h) and *Sphagnum* peat samples in a 1:1 ratio increased CH_4 release rates at both 40 and 70 °C. With the peat sample these increases were approximately 8- and 3-fold, respectively, at these temperatures. Highest CH_4 release was observed for the peat sample under wet conditions with a rate of 6.24 ng g^{-1} dw h^{-1}, approximately 6 and 30 times higher than that for *Terra fusca* A_h and *Terra fusca* T, respectively. Under dry conditions at temperatures of 70 °C and under wet conditions at 40 and 70 °C there was a positive relationship between organic carbon content and CH_4 release of the three soil types investigated.

Soils usually contain a substantial fraction of organic carbon in the form of cellulose, pectin and lignin. The latter compound is likely more important in older and more degraded soils since cellulose and pectin are less stable and thus more readily decomposed by the soil microbes. The three compounds were treated in the same fashion as was done with the soils. Lignin and pectin (Figures 7.2-7.5) both showed a strong response to temperature from 30 to 70 °C with a linear increase over time (24 h). Under wet conditions CH_4 release rates were higher by a factor of 1.08 to 6.50 relative to the dried samples, whereas at higher temperatures (70 °C) the wetting effect was less pronounced for lignin. Cellulose did not show any CH_4 release at 40 °C or 70 °C under dry conditions and only very low CH_4 release rates of 0.24 ng g^{-1} dw h^{-1} at 70 °C following addition of water. This is one to two orders of

magnitude lower when compared with lignin or pectin, indicating that in addition to knowing the organic carbon content of the soil it is equally important to have knowledge of the type of organic material in the soil. Lignin and pectin both contain methoxyl groups whereas cellulose does not. It has been previously shown that methoxyl groups of pectin play an important role in the formation of CH_4 from leaf foliage when exposed to UV irradiation (Keppler et al., 2008; McLeod et al., 2008; Vigano et al., 2008). Thus, the differences in chemical structure particularly the functional groups of the organic matter in soil might also be of importance for release of CH_4 from aerobic soils.

For all mineral samples including vermiculite, lepidocrocite and quartz sand no CH_4 release could be observed under dry conditions. Following addition of water to the mineral samples (ratio 1:1) no measureable amount of CH_4 was emitted from quartz sand. Interestingly when water was added to vermiculite at 40 and 70 °C, CH_4 release rates after one hour was found to be 4 and 8 ng g^{-1} dw, respectively. Methane concentrations in the samples did not change significantly during the next 8 h indicating no further release of this gas. This is in contrast to the kinetics observed with the organic compounds (except cellulose) and soils investigated as they showed a steady increase in CH_4 concentration with time. A plausible explanation could be that CH_4 is released from vermiculite by desorption processes following addition of water. Thus, CH_4 that had been adsorbed from the atmosphere and trapped in the clay structure might be rapidly released again after addition of water. However, Kirschbaum and Walcroft (2008) found only marginal CH_4 release rates from organic compounds due to desorption processes and concluded that desorption is not a quantitatively important factor contributing to observed aerobic CH_4 fluxes from plant leaves. When water was added to lepidocrocite at 40 °C similar kinetics to those found for vermiculite were noted, i.e. CH_4 release during the first hour of incubation (~6 ng g^{-1} dw) with no further release during the following 23 hours. Compared with soils and organic compounds amounts of CH_4 released from minerals is small and might only be considered of relevance for soils under wet conditions with a very low organic carbon content, i.e. soils such as *Terra fusca* T.

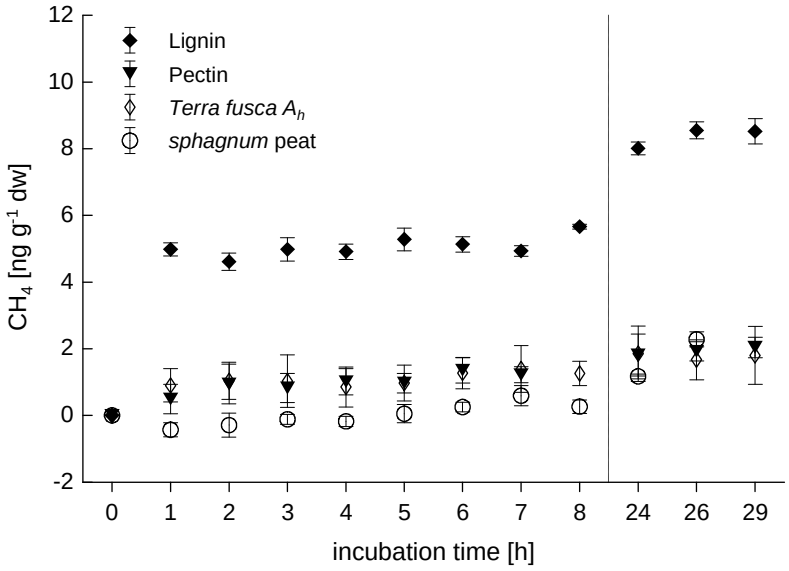

Figure 7.2: Methane release with time from soil samples and soil organic compounds when incubated at 40 °C. Error bars represent the SD (n=3); no measurements were made between 8 and 24 hours, indicated by the dashed line.

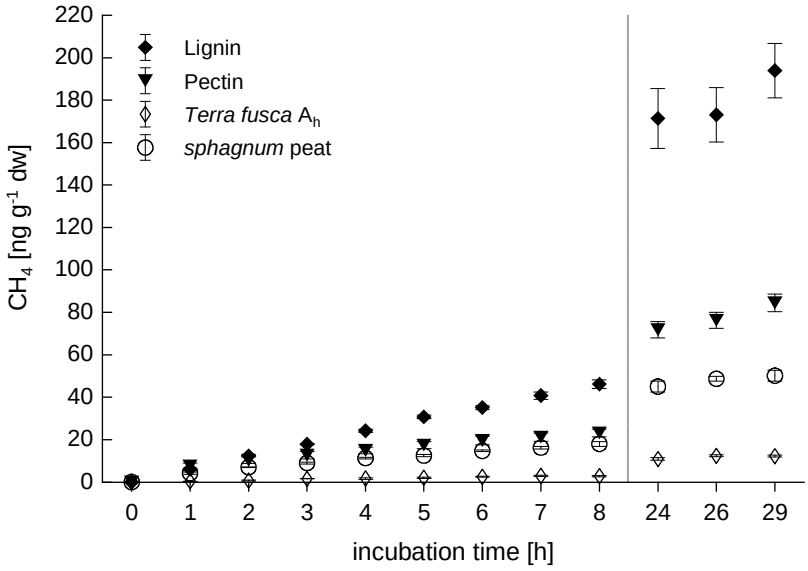

Figure 7.3: Methane release with time from soil samples and soil organic compounds when incubated at 70 °C. Error bars represent the SD (n=3); no measurements were made between 8 and 24 hours, indicated by the dashed line.

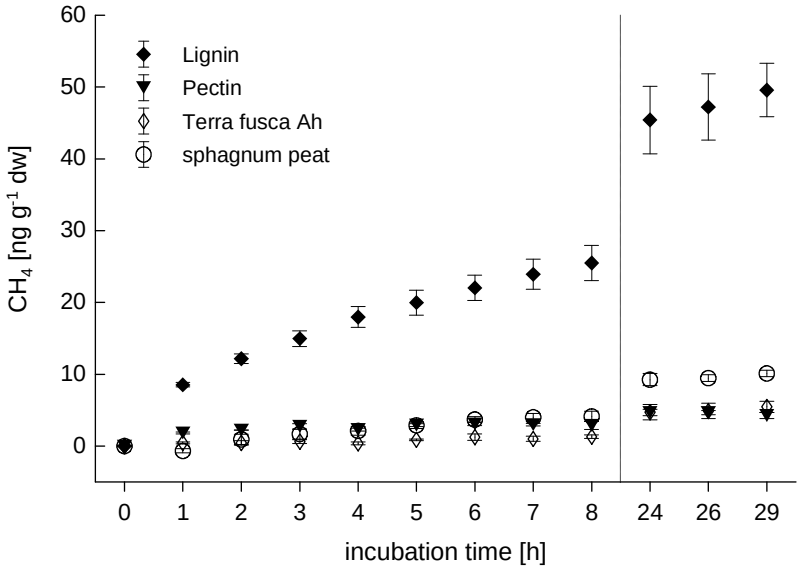

Figure 7.4: Methane release with time from soil samples and soil organic compounds when incubated at 40 °C following the addition of H_2O. Error bars represent the SD (n=3); no measurements were made between 8 and 24 hours, indicated by the dashed line.

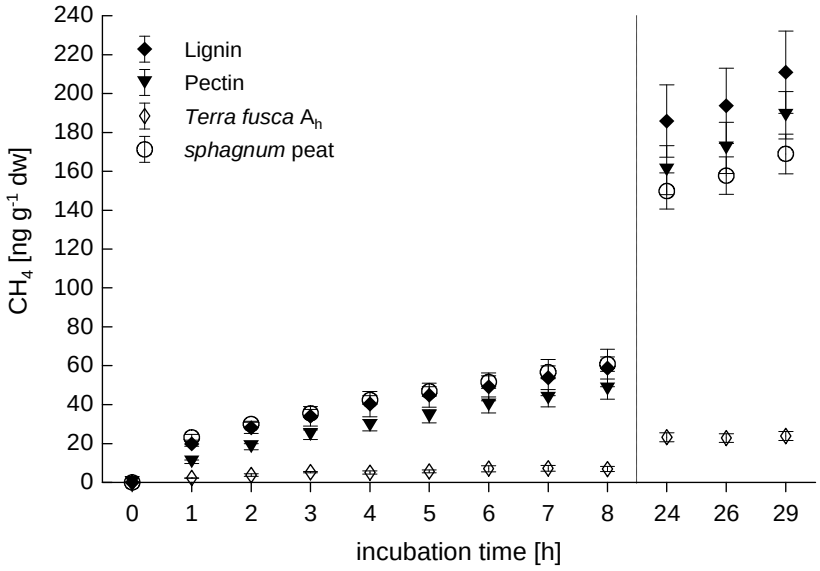

Figure 7.5: Methane release with time from soil samples and soil organic compounds when incubated at 70 °C following the addition of H_2O. Error bars represent the SD (n=3); no measurements were made between 8 and 24 hours, indicated by the dashed line.

7.3.4 Release rates of methane under dry and wet conditions

Methane release rates of all investigated samples were in the range of 0 to 7.74 ng g^{-1} dw h^{-1} under the incubation conditions employed for this study. With the exception of lepidocrocite, vermiculite, and sea sand, all other samples acted as emitters of CH_4. Incubation of lignin at 70 °C under wet conditions was found to give the highest release rate (Table 7.1).

7.4 Conclusion and outlook

This study indicates that CH_4 release may occur in aerobic soils by a hitherto unrecognized chemical process. The three soil sample types released CH_4 in the range of 0.03 to 6.24 ng g^{-1} dw h^{-1} under the experimental conditions employed for this study. All experiments were conducted under aerobic conditions with sterile equipment and lyophilized sample material. We cannot fully exclude some microbial activity at this time, the observed kinetics of CH_4 release and also response to temperature under aerobic conditions do not lend support for formation via a microbiological pathway. Additional experiments using both inorganic (minerals) and organic soil components provided further information regarding CH_4 release. Whereas for all minerals no CH_4 emissions were found under dry conditions, organic compounds such as lignin and pectin showed substantial release of CH_4. However, another important soil component, cellulose, did not release measurable amounts of CH_4 indicating that the type and chemical structure of the organic matter plays an important role in aerobic CH_4 release from soil. Another noteworthy observation made during this study was that addition of H_2O significantly enhanced release rates of CH_4 from soil samples and the organic compounds lignin and pectin.

This work should be regarded as the first attempt to investigate the possible formation of CH_4 in soil by non-microbial processes. Therefore further research is required not only to verify CH_4 release from aerobic soils but also to investigate this phenomenon in greater detail. In that respect we would suggest that future studies include a larger number of different soil types in order to confirm that the chemical process is widespread in nature. Exclusion of active microbial metabolism during our investigations was performed by lyophilisation of the samples. However, we would recommend that in addition to lyophilisation, sample sterilisation, by either gamma radiation or a high temperature steam process (autoclaving), be performed. We would also encourage the employment of

molecular biological methods on the sterilized samples to demonstrate the absence of microbial activity. The employment of stable isotope analysis would not only verify in-situ formation of CH_4, but also exclude contamination issues and further assist with identification of the organic precursor compounds in the soil.

As was previously demonstrated (Keppler et al., 2008; McLeod et al., 2008; Vigano et al., 2008), leaf foliage showed enhanced CH_4 formation after exposure to UV light. Similar experiments could be conducted with soils to demonstrate how they respond to UV irradiation. McLeod et al. (2008) and Messenger et al. (2009) reported that reactive oxygen species (ROS), such as hydroxyl radicals, play an important role in the release of CH_4 from pectin and might be the driving force in CH_4 release during UV radiation of plant foliage. The ROS H_2O_2 is an important reactant in many degradation processes in soil, being widely abundant with its frequent release by roots, soil bacteria and white rot fungi (Kersten and Kirk, 1987; Frahry and Schopfer, 1998). Hence it would be interesting to investigate the influence of H_2O_2 on CH_4 release from soils.

Finally, the role of water should be investigated in much more detail. For example, how does the water content of soil affect CH_4 emissions? Thus additional experiments would be beneficial to determine the optimum amount of H_2O necessary for maximum CH_4 production and also investigate the effect of drying and rewetting of soils on CH_4 release.

Acknowledgements

We thank Carl Brenninkmeijer and Dieter Scharffe for analytical support. This work was funded by the ESF (EURYI Award to F.K.) and DFG (KE 884/2-1).

Chapter 8

My contribution to the work presented in this chapter was to help planning, running and measuring several experiments, supporting with laboratory assistance and developing procedures and tools, such as the UV-Cell. Furthermore, results were interpreted and intensely discussed among us.

Non-microbial methane formation in oxic soils

Submitted to *Nature Geoscience*, 2012.

Alke Jugold[1], Frederik Althoff[1], Miriam Hurkuck[2], Markus Greule[1], Jos Lelieveld[1] and Frank Keppler[1]

Abstract

Methane plays an important role as a radiatively and chemically active gas in our atmosphere. Until recently, sources of atmospheric methane in the biosphere have been attributed to strictly anaerobic microbial processes during degradation of organic matter. However, a large fraction of methane produced in the anoxic soil layers does not reach the atmosphere due to methanotrophic consumption in the overlaying oxic soil. Although methane fluxes from aerobic soils have been observed an alternative source other than methanogenesis has not been identified thus far.

Here we provide evidence for non-microbial methane formation in soils under oxic conditions. We found that soils release methane upon heating and other environmental factors like ultraviolet irradiation, and drying-rewetting cycles. We suggest that chemical formation of methane during degradation of soil organic matter may represent the missing soil source that is needed to fully understand the complete methane cycle within the pedosphere. Although the emission fluxes are relatively low when compared to those from wetlands, they may be important in warm and wet regions subjected to ultraviolet radiation. We suggest that this methane source is highly sensitive to global change.

Keywords: greenhouse gas; organic matter; UV irradiation; photo degradation; peat

[1] Max-Planck-Institute for Chemistry, Hahn-Meitner-Weg 1, 55128 Mainz, Germany.
[2] Johann Heinrich von Thünen-Institute, Institute of Agricultural Climate Research, Federal Research Institute for Rural Areas, Forestry and Fisheries, Bundesallee 50, 38116 Braunschweig, Germany.

8.1 Introduction

Traditionally, biogenic methane (CH_4) was thought to be formed only by methanogens under strictly anaerobic conditions in wetland soils and rice paddies, intestinal tracts of termites and ruminants, human and agricultural waste. However, Keppler et al. (2006) demonstrated that plants produce CH_4 under aerobic conditions. Subsequently, this possibility has been critically debated (Dueck et al., 2007; Ferretti et al., 2007; Keppler and Röckmann, 2007; Kirschbaum et al., 2007; Beerling et al., 2008; Vigano et al., 2008; Wang et al., 2008; Keppler et al., 2009; Nisbet et al., 2009) and some researchers have suggested alternative explanations for the observed release of CH_4 from plants. Nevertheless, (Terazawa et al., 2007; Kirschbaum and Walcroft, 2008; Nisbet et al., 2009) recent observations have provided unambiguous evidence for several pathways by which CH_4 is generated under aerobic conditions, independent of microbial activity (Cao et al., 2008; Keppler et al., 2008; McLeod et al., 2008; Wang et al., 2008; Brüggemann et al., 2009; Bruhn et al., 2009; Messenger et al., 2009; Qaderi and Reid, 2009; Althoff et al., 2010). Although details of the mechanism(s) are still unknown, methoxy groups of plant pectin have been identified in several studies as a precursor compound of aerobic CH_4 emission from detached plant (Keppler et al., 2008; McLeod et al., 2008; Vigano et al., 2008; Bruhn et al., 2009). Furthermore, temperature and UV light have been confirmed as environmental factors that control CH_4 emission from dried plant matter (Keppler et al., 2008; Vigano et al., 2008).

8.1.1 Previous observations of methane formation in aerobic soils

Whilst aerobic soils are considered to be net CH_4 sinks due to methanotrophic oxidation of CH_4 it has been shown that oxic upland forest soils produce CH_4. Although observations of CH_4 production in oxic soil are numerous (Hao et al., 1988; Andersen et al., 1998; von Fischer and Hedin, 2007; Megonigal and Guenther, 2008), all have been attributed to methanogenesis. Methane production by oxic eubacteria (Rimbault et al., 1988) and anaerobic microsites, a refuge for methanogens (Peters and Conrad, 1995), were offered as possible explanations even though CH_4 production from eubacteria could only be detected in trace quantities. In experiments by Kammann et al. (2009) soil cores emitted up to 6 µg CH_4 per core even after homogenization, which may be expected to lead to the destruction of anoxic microsites. Von Fisher and Hedin (2007) using stable carbon isotope studies showed that our understanding of CH_4 formation in oxic soils is incomplete and discussed that methanogens as the sole source for CH_4 in oxic soils should be critically reviewed.

8.1.2 Possibility of non-microbial methane formation in soil

In this study we tested the previously postulated hypothesis that non-microbial CH_4 formation occurs in soils (Jugold and Keppler, 2009; Hurkuck et al., 2012). Following preliminary observations, we undertook a series of experiments measuring CH_4 formation from soils (Table 8.1 and Methods section 8.3) as a function of temperature, water content and UV-B irradiation. We used five different soils, including one highly organic soil (referred to as peat, Table 8.1), which had been lyophilised and homogenized prior to the experiments. Humic acid and lignin were used as alternatives for soil organic matter. Additionally, sub-samples of peat and lignin, sterilised using gamma radiation or autoclaving, were also used in our investigations.

8.1.3 Temperature dependency

The first experiment was designed to determine the temperature dependency and the required activation energy of CH_4 formation in a deciduous forest soil (SL), a coniferous forest soil (SG) and a sphagnum peat sample (PH). Samples were incubated at temperatures ranging from 30 to 90 °C. Methane emissions reached 7.11 ± 0.59 ng g^{-1} dw h^{-1}, 1.19 ± 0.15 ng g^{-1} dw h^{-1} and 1.12 ± 0.16 ng g^{-1} dw h^{-1} at 90 °C for PH, SL and SG, respectively (Figure 8.1). Whereas CH_4 release could be observed for PH and SL at 30 °C and 40 °C respectively (Table 8.1), CH_4 release from SG was only measureable above 50 °C. Soil Hainich (SHA) which had a similar organic carbon content to soils SL and SG (Table 8.1) was also investigated and CH_4 emissions of 0.45 ± 0.02 ng g^{-1} dw h^{-1} at 70 °C were observed. For all samples the temperature curves showed an exponential increase of CH_4 emissions with temperature. Interestingly, the results found for the soil and peat samples (Figure 8.1) showed a similar pattern to those reported by Keppler et al. (2006) and Vigano et al. (2008) for heated plant matter. Whereas biotically mediated reactions usually have their optimum temperatures between 25 and 40 °C (Dunfield et al., 1993) the observed strong increase in CH_4 emissions over the whole temperature range from 30 to 90 °C supports a chemically driven process. Furthermore, sterile peat samples (exposed to γ-radiation) showed similar or slightly higher emissions of CH_4 when compared to untreated peat samples. The fact that the emissions were not reduced in the sterile sample is further evidence for a non-microbial pathway. The slightly higher emissions observed for some of the sterile samples may possibly be ascribed to CH_4 production during the sterilisation process.

Since humic substances are usually the main constituents of organic-rich soils, commercially available lignin and humic acid were investigated for CH_4 release. These substances, with an organic carbon content of 49.5 % and 43.5 % respectively, when similarly heated up to 90 °C,

showed even higher CH_4 emissions (at 30 °C 0.1 ± 0.01 ng g^{-1} dw h^{-1} for lignin and at 90 °C 18.3 ± 0.4 and 6.6 ± 0.9 ng g^{-1} dw h^{-1} for lignin and humic acid, respectively) than the organic rich soil PH. The similar dependency of CH_4 formation in soils and organic soil components on temperature strongly suggests that the organic soil fraction is the source of CH_4 thermally produced in soils.

The experimental data obtained from samples SL, SG and PH were used to draw Arrhenius plots for CH_4 formation (Supplementary Figure 8.6). The activation energies (E_a) for CH_4 formation, calculated from these plots, yielded values of 50.1 kJ mol^{-1} for SL, 101.3 kJ mol^{-1} for SG and 79.2 kJ mol^{-1} for PH. These activation energies, being higher than 50 kJ mol^{-1}, provide supportive evidence of an abiotic process (Schönknecht et al., 2008). Since adsorption/desorption processes of CH_4 can occur with organic materials, it was considered that in this instance desorption might explain the observed emissions upon heating of the soil samples. Therefore, a series of experiments were performed to test such a possibility. From these it was found that a desorption process did not give rise to significant CH_4 fluxes from any of the soil samples employed in this study except when exceptionally high levels of CH_4 were added (12,500 ppm, see Supplementary Information). These results are in accordance with the findings of Kirschbaum and Walcroft (2008) who reported no significant desorption of CH_4 from plant matter and concluded that desorption is not a quantitatively important artefact contributing to observed aerobic CH_4 fluxes in dry plant leaves.

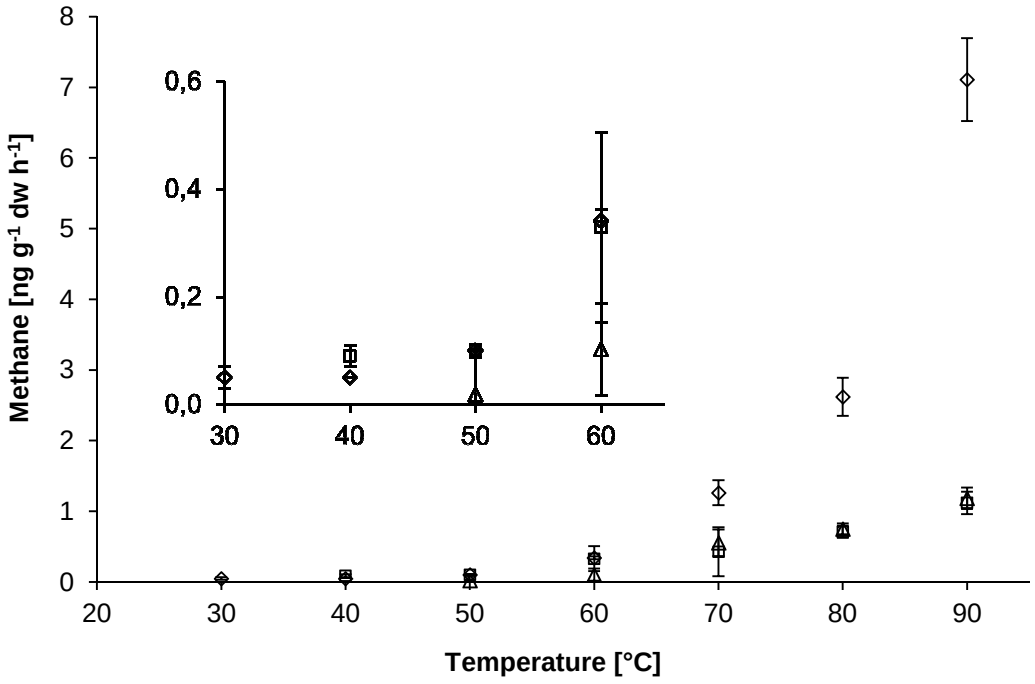

Figure 8.1: Formation of CH_4 from soil with increasing temperature. Temperature dependency of CH_4 emissions from peat PH (diamonds), soil SL (squares) and soil SG (triangles). Inset shows magnified area between 30 and 60 °C. Data show mean value ± SD (n=5).

Table 8.1: Organic carbon content, pH value and CH_4 emissions from dry and wetted samples heated at 30 and 40 °C and under UV irradiation of different soils and soil components.

Sample	pH	C_{org} [% dw]	Methane emission [ng g^{-1} dw h^{-1}]				[µg m^{-2} h^{-1}]
			dry (30 °C)	dry (40 °C)	wet (30 °C)	wet (40 °C)	UV-B radiation (2 W m^{-2})
Sphagnum peat (PH)	3.7	49.2	0.05 ± 0.02	0.05 ± 0.00	0.19 ± 0.01	0.41 ± 0.01	0.76 ± 0.24
Sphagnum peat, sterile (PHS)	3.7	49.2	0.11 ± 0.15	0.03 ± 0.02	0.32 ± 0.09	0.52 ± 0.03	n.m.
Deciduous forest soil O_h (SW)	7.4	23.4	n.d.	n.d.	0.23 ± 0.02	0.24 ± 0.06	0.25 ± 0.13
Coniferous forest soil A_h (SG)	7.2	5.0	n.d.	n.d.	n.d.	0.04 ± 0.01	1.73 ± 0.41
Deciduous forest soil A_h (SL)	4.4	4.0	n.d.	0.09 ± 0.02	0.06 ± 0.01	0.10 ± 0.04	4.92 ± 1.46
Deciduous forest soil A_h (SHA)	6.7	5.8	n.d.	0.08 ± 0.03	n.d.	0.20 ± 0.05	0.50 ± 0.13
Humic acid (HA)	5.5	43.5	0.06 ± 0.02	0.82 ± 0.06	0.18 ± 0.03	3.10 ± 0.34	0.80 ± 0.17
Lignin (LN)	9.6	49.5	0.1 ± 0.01	0.33 ± 0.01	0.65 ± 0.02	1.89 ± 0.20	0.40 ± 0.11
Lignin sterile (LNS)	9.6	49.5	n.d.	0.39 ± 0.03	1.45 ± 0.48	2.70 ± 0.57	n.m.

Subscript h indicates soil horizon, C_{org} is organic carbon content, PH is peat Hille, Germany; SW is soil Häverstädt, Wiehen Mountains, Germany; SG is soil Gonsenheim, Germany; SL is soil Lerchenberg, Germany; SHA is soil Hainich, Germany; n.d. is not detectable (rate cannot be provided as increase in headspace CH_4 was less than 0.02 ppm); n.m. is not measured. Data show mean value ± SD (n=3-5).

8.1.4 Effect of wetting and drying

Many surface soils and sediments are frequently subjected to changing precipitation and evaporation conditions and as a consequence undergo changes in water content. In extreme cases these conditions range from droughts to flooding events, including anthropogenic influences on the water budget like damming rivers or drainages for land reclamation. It is therefore important to study the effect of sample water content on the release of CH_4. This was investigated in an experiment where soil samples were exposed to repeated cycles of wetting and drying. The sample PH emitted up to five times more CH_4 after addition of water, compared to the dried sample when incubated at the same temperature (Figure 8.2). Interestingly, this increase appeared to be independent of the amount of water added, when the water content of the sample was in the range of 17 to 67 %. In a succession of five wetting-drying cycles no decline in CH_4 release rate was observed. A highly significant rise in

emissions was noted with increasing temperature ($p<0.001$). Emissions from dry samples doubled when the temperature was increased from 30 to 50 °C and a similarly strong effect was also observed for the wetted samples at these temperatures.

To rule out the influence of CH_4 consuming bacteria on our findings, a selection of measurements was repeated after addition of difluoromethane (DFM) (Miller et al., 1998) as described in the supplementary section. No differences were observed between samples with and without added DFM. Considerable CH_4 emissions could also be detected after wetting samples of lignin and humic acid, where, respectively, 1.9 ± 0.2 and 3.1 ± 0.3 ng g^{-1} dw h^{-1} were released (Table 8.1).

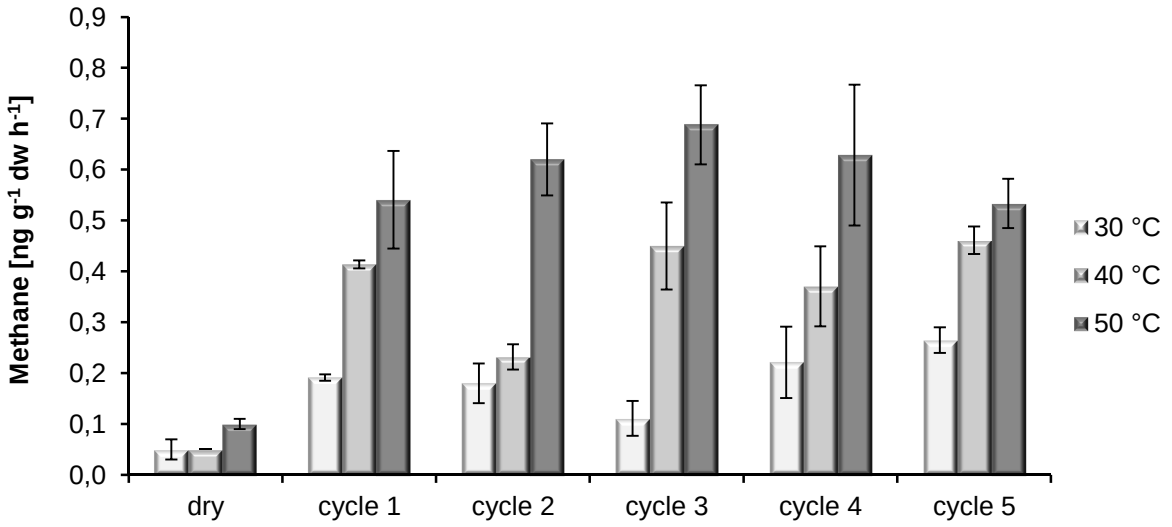

Figure 8.2: Methane formation from wetted and dry peat samples. Effect of repeated wetting and drying cycles on CH_4 release from peat PH at 30, 40 and 50 °C. Data show mean value ± SD (n=5).

8.1.5 Effect of hydrogen peroxide

Reactive oxygen species (ROS) such as hydroxyl radicals (HO·) have been suggested to play an important role in the release of CH_4 from pectin and might be the driving force in the CH_4 release during UV radiation of plant foliage (McLeod et al., 2008; Messenger et al., 2009). Hydrogen peroxide (H_2O_2) as a precursor of HO· is an important reactant in many degradation processes in soils, being abundant due to its release by roots, soil bacteria and white rot fungi (Kersten and Kirk, 1987; Frahry and Schopfer, 1998). We therefore investigated the influence of H_2O_2 on CH_4 emissions from peat PH and soil SHA.

Interestingly, it was found that peat and soil responded rather differently following addition of H_2O_2. A strong increase in CH_4 emissions and a linear relationship (R^2=0.99) with

increasing amounts of added H_2O_2 to sample PH (Figure 8.3) was observed whereas for soil sample SHA no additional emissions were observed. It is not clear why the soil and peat samples behaved so differently to the addition of H_2O_2. One possible explanation might be related to the differences in the composition of soil SHA and peat PH. Peat consists mostly of organic matter and low mineral content which might make it more prone to be attacked by ROS. Soil, on the other hand, contains other major components such as clay minerals and metal oxides that might more efficiently interact with H_2O_2.

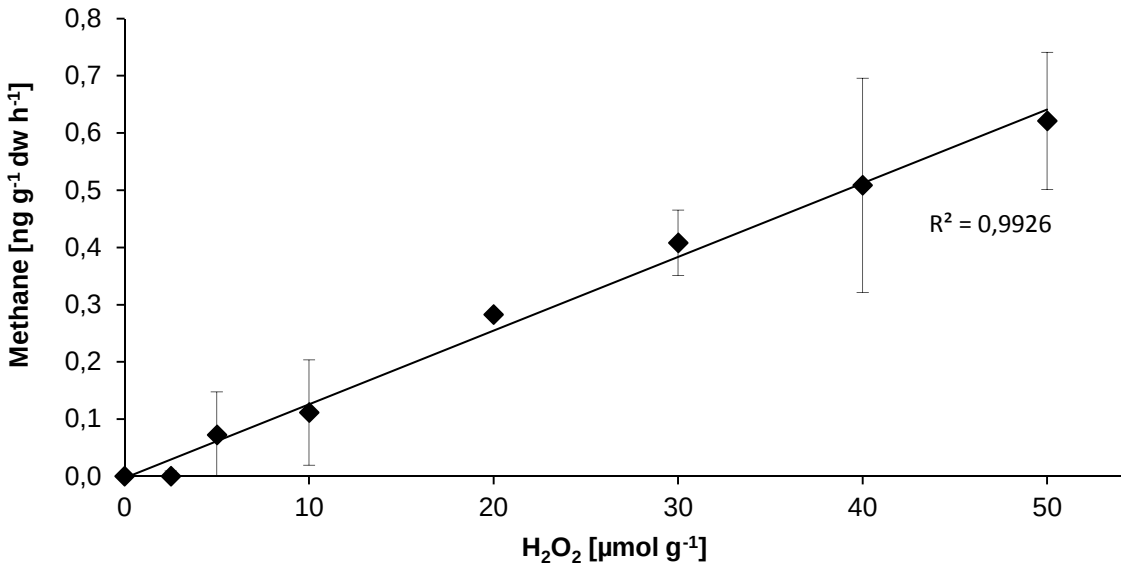

Figure 8.3: Relationship between CH_4 emission from peat PH and added amount of H_2O_2. Data show mean value ± SD (n=3, except 20 µmol (n=1)). Incubation: 24 h at 30 °C.

Samples of lignin and humic acid were also treated with H_2O_2. Whereas increased CH_4 emissions were observed for humic acid, no elevated emissions were found for lignin. Thus it is evident that the structural composition of the organic matter in soil has a major impact on the CH_4 emissions.

8.1.6 Effect of ultraviolet radiation

Ultraviolet (UV) radiation has been shown to be an important factor for aerobic production of CH_4 from plant tissues and pectin. It was demonstrated that both UV-A (320-400 nm) and UV-B (280-320 nm) induce CH_4 emissions from plant tissue (McLeod et al., 2008; Vigano et al., 2008), with UV-B radiation showing a much stronger effect. Nevertheless, because average UV-A intensities are around 30-fold higher than UV-B values, UV-A is also an important component on a global level for UV induced CH_4 emissions (Bruhn et al., 2009).

Thus, the effect of UV radiation on the formation of CH_4 from soil was evaluated. For most experiments we used a total UV-B irradiance of 2 W m^{-2}, typical for mid-latitudes at the surface. In the tropics, where the UV-filtering ozone layer is thinner, ambient UV-B irradiances are about 3.7 W m^{-2} (Bernhard et al., 1997).

Measurements at 2 W m^{-2} UV-B and temperatures of 28 to 32 °C showed emissions of 0.25 to 4.92 µg m^{-2} h^{-1} (Table 8.1), which were linear over two a day period. Methane emission rates were also found to be a function of UV-B intensity. With increasing intensities from 1 to 4 W m^{-2} CH_4 emissions from soil SL increased linearly from 1.33 ± 0.22 to 7.28 ± 2.75 µg m^{-2} h^{-1}. Emissions from soil SG increased from 0.56 ± 0.12 to 2.75 ± 0.69 µg m^{-2} h^{-1} over the same intensity range (Figure 8.4).

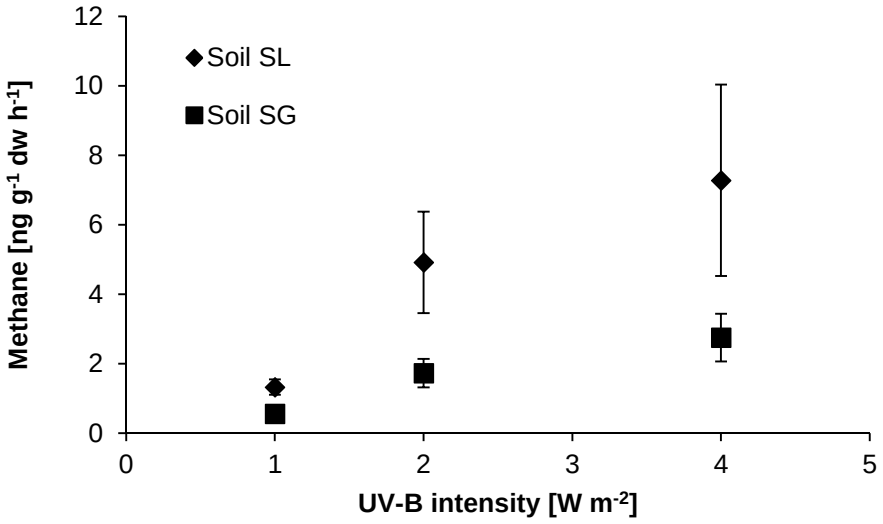

Figure 8.4: Relationship between CH_4 emissions from soils SL and SG and UV-B intensity. Data show mean value ± SD (n=3).

The combined emission rates under the influence of UV and temperature are similar to those reported for plant foliage (Keppler et al., 2008; Vigano et al., 2008). Interestingly, variations in CH_4 emissions under UV are not correlated to soil organic content (see Table 8.1). However, the emission rates might be influenced by organic photo sensitizers, which have been shown to have a positive effect on CH_4 emissions from pectin (Messenger et al., 2009), or by clay minerals, often described as photo-catalysts (Katagi, 1990; Wu et al., 2008; Kibanova et al., 2011).

8.1.7 Stable carbon isotope composition of methane emitted from soil

In addition to CH_4 emission rates, the stable isotope composition ($\delta^{13}C$ values) of the released CH_4 from soil SHA, peat PH, humic acid and lignin were also measured. Heating

experiments showed $\delta^{13}C$ values of –56 to –65 ‰ for lignin, –51 to –56 ‰ for PH and –42 to –52 ‰ for humic acid. Methane emitted from wet samples of lignin, humic acid and peat PH showed $\delta^{13}C$ values ranging from –53 to –69 ‰ with humic acid again being the substrate with the highest (less negative) CH_4 values (–53.2 ‰ ± 0.3 ‰). The $\delta^{13}C$ values measured for CH_4 emitted from humic acid and peat PH over a 24 h period following the addition of H_2O_2 were –54.9 ± 1.2 ‰ and –60.2 ± 4.5 ‰, respectively.

The $\delta^{13}C$ values measured for CH_4 emitted during 48 h under UV irradiation were –56.0 ± 6.0 ‰ for lignin, –63 ± 3.3 ‰ for SHA, –44.2 ± 1.4 ‰ for PH and –35.3 ± 9.4 ‰ for humic acid. In summary, the $\delta^{13}C$ values of CH_4 emitted from soil differed between substrates and experimental conditions and ranged from –35.5 to 69 ‰ whereas the $\delta^{13}C$ values for the organic matter of the bulk soil samples were in the range of –22 to –29 ‰. Thus, it appears that all treatments caused substantial fractionation between the precursor carbon and emitted CH_4. Similar $\delta^{13}C$ values and isotope fractionations have been reported for CH_4 emitted from plant foliage due to UV radiation or upon heating (Vigano et al., 2009). Both the isotopic values reported for the chemical formation of CH_4 from soil and vegetation are commonly also found for terrestrial biogenic sources (Vigano et al., 2009).

8.2 Conclusions and Outlook

Our study shows that there exist several hitherto unknown processes that produce CH_4 in soil and peat which is clearly not related to methanogenic activity. Figure 8.5 summarizes our results regarding non-microbial CH_4 formation in the aerobic layers of soils and the environmental factors that might control emissions. From our findings we suggest that the abiotic formation of CH_4 through degradation of organic soil matter represents a thus far undiscovered pathway for CH_4 formation in oxic soils. Our results imply that there are at least two different mechanisms for non-microbial CH_4 formation in soils. This can be best distinguished by comparing thermal and UV-B induced CH_4 release. Samples that released only minor amounts of CH_4 when heated or wetted emitted significant amounts when irradiated with UV-B, and vice versa.

The amounts of CH_4 produced at ambient temperatures of 30 °C are small but increase considerably with increasing temperature. Wetted samples during the drying and rewetting cycle experiments showed much higher emissions than the dry sample itself at low temperatures. Assuming that the first five centimetres of the soil horizon account for most

of the CH_4 production, the emission rates from dry and wet soil at 30 to 40 °C (Table 8.1) would correspond to emission rates of 0 to 18 µg m^{-2} h^{-1}, assuming a dry bulk density of 1.5 g cm^{-3} for soil and 0.1 g cm^{-3} for peat (Minkinnen and Laine, 1998). These emissions increase up to an order of magnitude when the soil surface temperature reaches 50 to 70 °C. Although these temperatures are often only observed at soil surfaces in tropical and savannah regions, when compared to field measurements from wetlands with observed CH_4 emissions up to 11.9 mg m^{-2} h^{-1} (286.5 mg m^{-2} d^{-1}) and calculated average emission rates of 2.1 mg m^{-2} h^{-1} (51 mg m^{-2} d^{-1}) (Morrissey and Livingston, 1992; Roulet et al., 1992; Cao et al., 1998), these are relative minor emissions. However, given the large global soil areas and the frequency at which dried and rewetted soils release CH_4, this source can nevertheless be an important factor in aerobic soil organic matter degradation.

The CH_4 emissions under UV light are consistent with findings by Vigano et al. (2008) and McLeod et al. (2008), who showed that UV irradiation drives CH_4 production from dried plant matter. Thus soil organic matter is most likely the precursor of CH_4 emissions observed in our studies. This is supported by CH_4 emissions that were observed when lignin and humic acid were exposed to UV irradiation under the same conditions as that for the soil samples. However, it is interesting that under UV irradiation there was no apparent correlation between CH_4 production and the soil organic matter content. This indicates that other soil components also play a role in CH_4 formation. Organic photo-sensitisers such as tryptophan (Messenger et al., 2009) or the mineral soil fraction, e.g., clay minerals and metal oxides (Katagi, 1990; Wu et al., 2008; Kibanova et al., 2011) may catalyze surface reactions of organic matter leading to CH_4 formation. This would also be in agreement with the recent observation that meteoritic matter such as carbonaceous chondrites, containing only a few per cent organic matter, releases large amounts of CH_4 when exposed to UV irradiation (Keppler et al., 2012).

Methane emissions under UV radiation were found to be in the range of 0.25 to 7.28 µg m^{-2} h^{-1} for various soils in the UV-B intensity range of 1 to 4 W m^{-2}. Again, these emission rates are considerably lower than emissions observed from natural wetlands (Morrissey and Livingston, 1992; Roulet et al., 1992; Cao et al., 1998). However, a large fraction of the terrestrial surface is directly exposed to UV radiation, and this might even increase due to anthropogenic activities leading to deforestation and desertification. Interesting regions for on-site studies of UV induced CH_4 release could be steppes regions, newly deforested land,

and freshly ploughed fields, whereas for water mediated CH_4 release flooding plains and irrigation areas in dry climates would be relevant. However, it has to be considered that more than 90 % of CH_4 formed within soils is oxidised by methanotrophic bacteria before it reaches the atmosphere (King, 1990). Methane uptake into aerated temperate forest soils ranges from 10 to 204 µg m^{-2} h^{-1}, depending on soil type, temperature and water saturation (Born et al., 1990; Castro et al., 1995; King, 1997). Field measurements regarding the temperature and water mediated CH_4 emissions may thus be impaired by methanotrophic consumption. In contrast, direct photolysis of soil organic matter will occur at the upper soil surface at maximum depths of 0.2 to 0.4 mm and indirect photolysis processes might affect the soil down to 2 mm depth (Hebert and Miller, 1990). Thus CH_4 formation induced by UV irradiation at the soil surface might lead to direct CH_4 emissions to the atmosphere. It will be a challenge to differentiate between microbial and non-microbial sources in the field.

Hydrogen peroxide was found to have a positive effect on CH_4 production from peat. Levels of H_2O_2 in soils are influenced by the activity of plant roots, fungi and bacteria (Miller et al., 1998; Schönknecht et al., 2008). As the release of H_2O_2 from living organisms is often a defence mechanism, the amount released might be affected by organism density in the soil and the level of stress applied by (changing) environmental factors. All effects shown to increase CH_4 production might gain importance in the course of climate change considering predicted changes in temperatures, precipitation levels and evaporation rates. Flood plains and other environments with strong fluctuations in the water budget might be of particular interest. Further investigations will be essential to fully understand the biogeochemical cycle of CH_4 in soils and its relevance for the atmosphere.

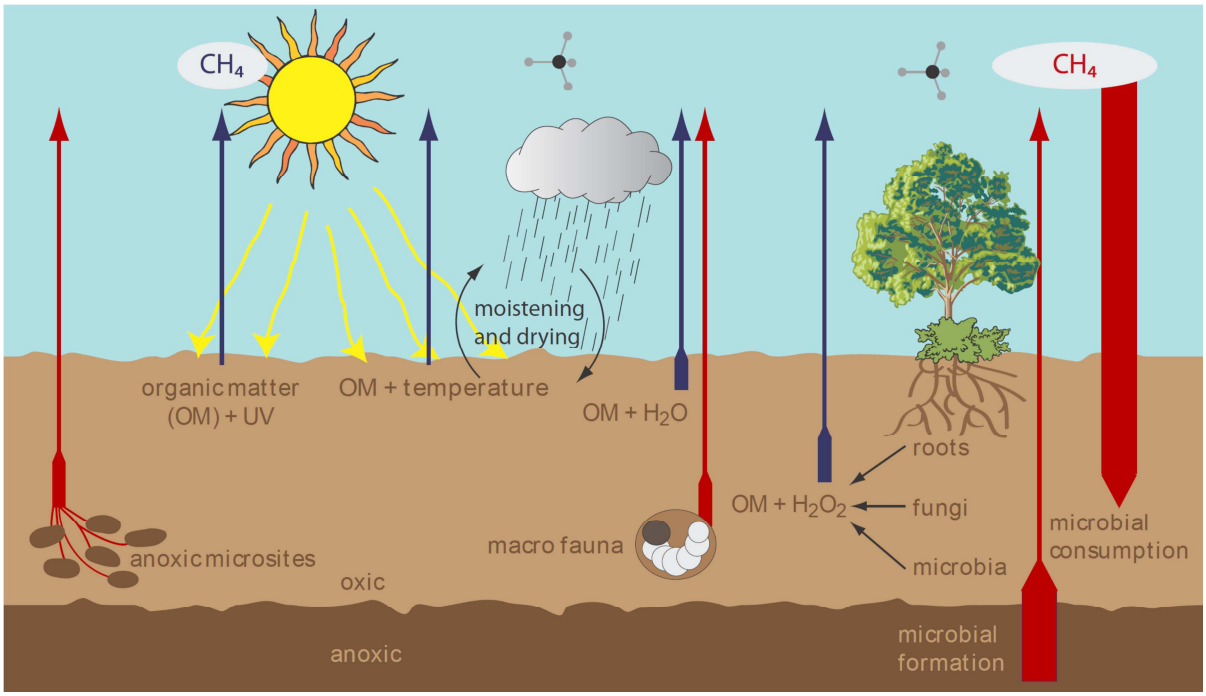

Figure 8.5: Scheme of CH_4 cycling in soil including non-microbial (blue) and the previously known microbial sources (red). Environmental factors such as temperature, UV irradiation, drought/wet cycles and formation of hydrogen peroxide produced by biota might control chemical formation of CH_4 in soil.

8.3 Materials and Methods

8.3.1 Origin of samples and preparation

Four soils and one peat type were used. If present, stones and larger wood particles were removed from the samples before they were lyophilised and then milled using an electronic coffee grinder (Elta UM105).

Soil SL was sampled at the Lerchenberg forest south of Mainz, Germany (N 49° 57’ 47’’, E 8° 11’ 01’’). The sampling site is a deciduous forest dominated by beech trees (*Fagus sylvatica*), featuring few oaks and nearly no undergrowth. The sample was collected from the surface after brushing away the layer of leaf litter.

For soil SG the upper 10 cm of a pine forest soil was sampled at Mainz-Gonsenheim, Germany (N 50° 0' 24.4", E 8° 11' 50.3"). The soil in this area is rich in medium to coarse sand and powdery clay particles. It also contains rotting wood debris, pine twigs and is densely rooted.

Soil SHA was topsoil of a *terra fusca* sampled at the ‘Nationalpark Hainich’, Germany (N 51° 04' 46'', E 10° 27' 08 ''). The sampling site is a deciduous forest dominated by beech trees.

Soil SW was collected from the organic rich O-horizon of a deciduous forest soil. The vegetation is dominated by beech trees. The sampling site is situated south of Minden, Germany (N 52° 15' 17.4", E 8° 52' 29.5")

Peat PH was sampled at the peat bog "Großes Torfmoor" near Hille, Germany (N 52° 19' 23.7" E 8° 42' 34.7"). The top 10 cm of *sphagnum* peat was collected as a bulk sample. A subsample was sterilised using gamma irradiation.

8.3.2 Reaction Vials

Samples were incubated in glass vials (360 mL); made in-house by modification of a 300 mL Erlenmeyer-flask (Duran group) fitted with the neck of a 40 mL screw top vial (Supelco) sealed with a hole type screw cap (Supelco) containing a PTFE/silicone septum (Supelco). The UV reaction chambers were also custom built; 200 mL glass chambers with a quartz glass lid and a septa sealed side port for headspace sampling. The irradiated surface was 19.63 cm^2.

8.3.3 Determination of organic carbon

Organic carbon content of the samples was determined with a SC Analyser (SC-144 DR, LECO) by combustion of 0.1-0.5 g of sample material at 1300 °C. The carbon content was calculated by comparison to a calcium carbonate standard. For soil SW the organic carbon content was determined by loss on ignition. Therefore the weight loss after two hours at 600 °C was determined. Half of the loss was assigned to carbon combustion.

8.3.4 Methane measurements

Headspace above samples in the sealed vials were sampled (5 mL) with a Hamilton gas syringe and analysed using a gas chromatograph (Shimadzu GC-14B) with flame ionization detector (GC-FID). Two reference CH_4 standards (containing 8.905 ppm and 1.736 ppm) were used.

8.3.5 Isotopic data

$\delta^{13}C$ sample analysis was carried out using gas chromatography combustion isotope ratio mass spectrometry (GC-C-IRMS) which consisted of a cryogenic pre-concentration unit directly coupled to an HP 6890N gas chromatograph (Agilent, Santa Clara, USA), which was connected to a Delta^{PLUS}XL isotope ratio mass spectrometer (ThermoQuest Finnigan, Bremen, Germany) via an oxidation reactor [ceramic tube (Al_2O_3), length 320 mm, 0.5 mm i.d., with oxygen activated Cu/Ni/Pt wires inside, reactor temperature 960 °C] and a GC

Combustion III Interface (ThermoQuest Finnigan, Bremen, Germany). The gas chromatograph (GC) was fitted with a GS-Carbonplot capillary column (30 m x 0.32 mm i.d., d_f 1.5 µm; Agilent, Santa Clara, USA) and a PoraPlot capillary column (25 m x 0.25 mm i.d., d_f 8 µm; Varian, Lake Forest, USA). Both columns were coupled using a press fit connector.

A tank of high purity carbon dioxide (carbon dioxide 4.5, Messer Griesheim, Frankfurt, Germany) with a known $\delta^{13}C$ value of –23.6 ‰ (VPDB) was used as the working reference gas. All $\delta^{13}C$ values obtained from analysis of methane were corrected using three CH_4 working standards (isometric instruments, Victoria, Canada) calibrated against IAEA and NIST reference substances. The calibrated $\delta^{13}C$ values of the three working standards in ‰ vs. VPDB were –23.9 ± 0.2 ‰, –38.3 ± 0.2 ‰ and –54.5 ± 0.2 ‰.

All $^{13}C/^{12}C$ -isotope ratios are expressed in the conventional δ notation in per mil versus VPDB, defined as (Eq. 8.1):

$$\delta\,^{13}C = (({}^{13}C/{}^{12}C)_{sample} / ({}^{13}C/{}^{12}C)_{standard}) - 1 \qquad \text{(Eq. 8.1)}$$

8.3.6 Temperature dependency

Sets of non-sterile and sterile peat samples (PH, 5 g per 360 mL screw cap vial, n=5) as well as non-sterile sets of each soil sample were incubated for 24 h at temperatures ranging from 30 to 90 °C at 10 °C intervals. At the end of the incubation period a sample of the vial headspace was analysed for CH_4 content.

8.3.7 Drying-rewetting cycles

Peat PH (5 g in 360 mL screw cap vials, n=5) was incubated for 24 h at either 30, 40 or 50 °C. Another set of samples was incubated under the same conditions but supplemented with 5 mL doubly distilled water. After incubation a sample of the headspace was analysed for CH_4 content. The samples were frozen and lyophilised again directly after measurements. After being rewetted and incubated again, headspace samples were analysed again for CH_4. This cycle was repeated five times.

In a further experiment dependency of CH_4 release on the water-sample-ratio was investigated. For this samples of peat PH (5 g in 360 mL screw cap vials, n=5) were supplemented with 1, 5 and 10 mL doubly distilled water.

8.3.8 Experiments with H_2O_2

Samples PH or SHA (5 g in 360 mL vials, n=3) and 10 mL aqueous solution with varying concentrations of H_2O_2 (0-25 mM) were added and vials immediately sealed. The samples were incubated for 24 h at 30 °C, after which a sample of the vial headspace was analysed for CH_4 content. The experiment was also repeated for lignin and humic acid with 25 mM H_2O_2.

8.3.9 UV irradiation experiments

An Osram Ultra-Vitalux lamp (300 W) served as UV source. The radiation of this lamp shows an UV-A/UV-B content comparable to solar radiation when the source is located at the appropriate distance. The total unweighted UV-B radiation was determined with a UV radiometer (UVlog, sglux, Berlin, Germany) precalibrated for the used lamp type. For more details of the lamp characteristics we refer to Vigano et al. (2008). The UV lamp was placed above the leak tight UV reaction chambers. The height was adjusted so as to set the UV-B intensities to the desired value between 1 and 4 W m^{-2}. To exclude undesired UV-C radiation the quartz glass lids were covered with a 95 nm film of cellulose diacetate. Two fans were employed in order to keep the temperatures in the chambers at 30 °C (± 2 °C). Temperature was monitored with a thermocouple. All experiments were conducted with 2-5 g of sample material but the data is presented based on irradiated area rather than sample weight. Methane concentrations in the headspace were measured after 0, 24 and 48 h. The difference between 0 and 24 h was used to calculate emission rates.

The emissions induced solely by UV-B were calculated by subtracting the CH_4 concentration measured for the control samples from that measured for the UV irradiated samples so as to eliminate the temperature effect. The temperature monitored in the vials during UV experiments ranged from 28 to 32 °C. The control samples, which were also placed under the UV lamp, but covered with UV-opaque glass, showed emissions (transferred to ng g^{-1} dw h^{-1}) comparable to those observed for the temperature experiments which were incubated in the dark at similar temperatures.

8.3.10 Statistical methods

The statistical comparison of different samples was examined with the open-source software

'The R Project for Statistical Computing', version 2.11.1 (The R Foundation for Statistical Computing).

8.4 Acknowledgements

The authors thank Michael Kersten for comments on the methods and John T. G. Hamilton for comments on the draft, Colin McRoberts, for sterilising the peat sample and Jennifer Rinne and Ilka Hermes for laboratory assistance. Thanks to Carl Brenninkmeijer and Dieter Scharffe for provision and maintenance of the GC-FID system. We acknowledge the Environmental Agency of Minden and Mr. Lübbert for permission and help with sampling in Hille.

This work was funded by the ESF (EURYI Award to F.K.) and DFG (KE 884/2-1) and by the DFG research unit 763 'Natural Halogenation Processes in the Environment - Atmosphere and Soil' (KE 884/6-1; KE 884/7-1).

8.5 Supplemental

8.5.1 Possibility of desorption

It has been suggested, that CH_4 release from plant materials might be a result of CH_4 desorption under low CH_4 environments, e.g. after flushing with CH_4 free air (Kirschbaum et al., 2007).

It has previously been shown by Kirschbaum and Walcroft (2008) that desorption does not play a significant role under ambient conditions regarding moisture, temperature and CH_4 concentrations (Kirschbaum and Walcroft, 2008). However, whereas Kirschbaum and Walcroft used ambient CH_4 levels for adsorption and investigated the desorption at ambient temperatures under low CH_4 conditions, we investigated adsorption to peat at much higher CH_4 concentrations of 12,500 ppm, 100 ppm and 10 ppm and its desorption at 50 °C. For each concentration level 6 vials were prepared and left to rest at room temperature for 3 days to allow the CH_4 to adsorb to the peat surfaces. The samples were then divided into two groups, one being lyophilised over night, then flushed with CH_4 free air, the other one was just flushed with CH_4 free air. A third group, which consisted of three peat samples

without added CH_4 and was lyophilised and flushed with CH_4 free air, served as control. Finally all three groups were supplemented with water and incubated at 50 °C for 17 h.

The objective of this experiment was to determine whether the observed CH_4 emissions were indeed formed during the incubations or were due to an artefact caused by desorption of CH_4, possibly arising from microbial origin, from the material under higher than ambient CH_4 levels in the soil or peat. Moreover, this experiment would also enable us to determine if any of the adsorbed CH_4 following the lyophilisation process could account for some of the CH_4 observed in our measurements.

The peat samples treated with the highest CH_4 levels (12,500 ppm) showed an increased CH_4 release in both CH_4 supplemented groups (2.2 ± 0.9 ng g^{-1} dw h^{-1} and 3.3 ± 0.3 ng g^{-1} dw h^{-1} for samples with and without lyophilisation, respectively) compared to the untreated control group (0.4 ± 0.1 ng g^{-1} dw h^{-1}). However, the samples treated with 100 and 10 ppm CH_4 showed no significant increase neither with nor without lyophilisation. Furthermore samples of kaolinite and sea sand were tested for their adsorption potential of CH_4 using 10 ppm CH_4 but again no adsorption/desorption processes could be observed.

8.5.2 Exclusion of methane oxidation by methane consuming bacteria

Several experiments from the water dependency study were repeated in order to investigate the possible influence of methanotrophic bacteria on CH_4 emissions. For the dry samples and those with a sample to water ratio of 2:1, 1:1 and 1:2 the experiment was repeated at 40 °C with the addition of 20 µL diflouromethane (DFM) per vial. Addition of DFM was done in order to inhibit CH_4 oxidation by any methanotrophic bacteria (Miller et al., 1998) possibly present in the non-sterile samples. No significant effect was observed on the emission rates after adding DFM which allowed us to conclude that there were no methanotrophic bacteria active in the lyophilised samples. Measured CH_4 emissions were 0.8 ± 0.2 ng g^{-1} dw h^{-1} without DFM and 0.4 ± 0.02 ng g^{-1} dw h^{-1} with DFM for the dry samples. The wetted samples showed emissions ranging from 1.6 ± 0.1 to 1.9 ± 0.1 ng g^{-1} dw h^{-1} with and without added DFM.

8.5.3 Arrhenius plots

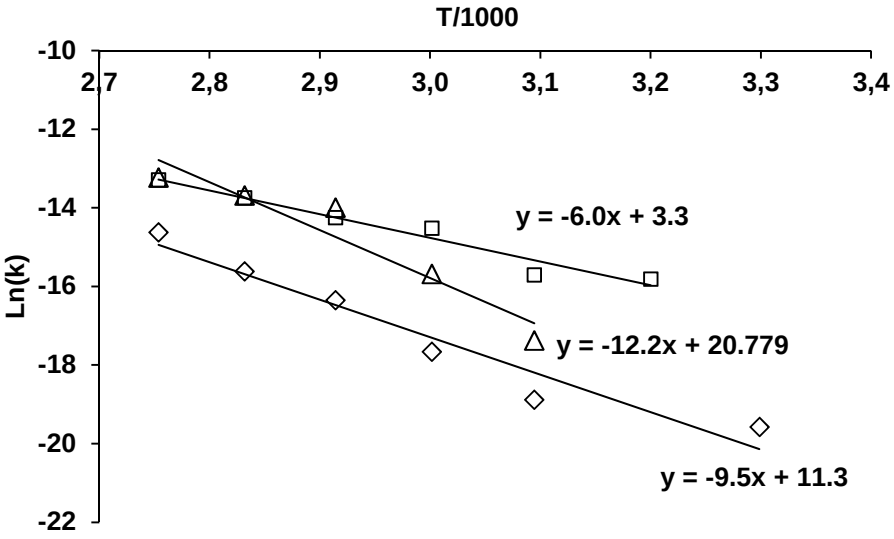

Figure 8.6: Arrhenius plot for formation of CH_4 in peat PH (diamonds) and soils SL (squares) and SG (triangles).

We used the experimental data from samples SL, SG and PH to draw Arrhenius plots for CH_4 formation (Figure 8.6). For all samples the Arrhenius plots were found to follow a straight line at temperatures ranging from 30 to 90 °C. The activation energies (E_a) for CH_4 formation for each sample, calculated from the slope of the line, yielded values of 50.1 kJ mol^{-1}, 101.3 kJ mol^{-1} and 79.2 kJ mol^{-1} for SL, SG and PH, respectively. Again, this is strong supportive evidence of an abiotic underlying process as reactions with activation energies above 50 kJ mol^{-1} are considered to be abiotic (Schönknecht et al., 2008).

Chapter 9

Main findings, conclusions and outlook

9.1 Main findings

The goal of the work presented in this dissertation was the investigation of the non-microbial aerobic methane formation. The central aims included the development of a chemical system that produces CH_4 under highly oxidative conditions and the transfer of these findings to living plants and soil systems.

In Chapter 4 the development of this chemical system is described. This reaction system consists of three chemical compounds including ascorbic acid, ferrihydrite and H_2O_2 in aquatic solution. The special structure of ascorbic acid containing two vicinal hydroxyl groups was found to be essential for the formation of CH_4 in the system. Equally important are the substance ratio of 2:1 between H_2O_2 and ascorbic acid, catalytic amounts of ferrihydrite and a pH of 3. All enhanced formation of CH_4 under aerobic conditions. However, it was observed that increasing oxygen concentrations above ambient levels severely inhibited the formation of CH_4 in the reaction system.

For the first time a detailed reaction mechanism of non-biotical aerobic CH_4 formation was described (Chapter 5). The scheme is based on the reaction of ascorbic acid, ferrihydrite and H_2O_2 with the amino acid methionine. Together with methionine sulfoxide methionine showed the highest amount of formed CH_4 of the investigated methyl donation compounds (MDCs). Compared to the reaction of ascorbic acid, ferrihydrite and H_2O_2 (Chapter 4) compound ratio of maximal CH_4 production showed similar results. For methionine the amount of formed CH_4 rose linear with the amount of the amino acid. Main difference of the reaction using methionine is the formation of CH_4 in an atmosphere of pure oxygen (56 % of ambient air). Isotopic labelling of the sulphur bond methyl group C-atom identified this carbon and probably the whole methyl group as precursor of the formed CH_4.

Using the information gathered in Chapter 4 and 5 a direct transfer to living plants was possible (Chapter 6). An increased CH_4 formation was only observed in cases when methionine was applied to tobacco cells (*Nicotiana tabacum*) treated with a complex IV

inhibitor, i.e. N_3^-, CN^- or CO. This further indicates that mitochondria could be responsible for CH_4 production in living organisms. Applying ^{13}C-isotope labelled methionine to intact tobacco plants unambiguously showed the suggested methyl group to act as precursors of plant produced CH_4.

The precursor studies concerning CH_4 emission from soil and its components, presented in Chapter 7, already showed that so far unknown processes lead to CH_4 formation from organic contents. All three investigated soil samples and the components lignin and pectin emitted CH_4 under aerobic conditions when temperature was increased. Interestingly, wet samples emitted higher amounts of CH_4 than dry samples. No CH_4 formation was found from heated mineral soil components or cellulose, whereas a small formation was measured when the cellulose was wetted previously. Furthermore, the results indicate a higher CH_4 emission with increased organic soil content.

More detailed investigations on the CH_4 formation from soils (Chapter 8) confirmed the findings described in Chapter 7. Furthermore, with the results a novel scheme for CH_4 formation in oxic soils was developed. This scheme includes the influence of temperature, water and H_2O_2 which increased the CH_4 formation from organic rich soils. Interestingly, an increase of the amount of added H_2O seemed to have no effect on the amount of emitted CH_4 in the experiments. Experiments of drying and rewetting showed similar values after each cycle.

In addition, the scheme contains the implication of UV irradiation on soils. Considerable amounts of CH_4 have been measured after the radiation of dry samples using UV-B light. By far the highest emission rates were found for irradiated deciduous forest soil.

The effect of changes in chemical and physical parameters to the formation of CH_4 from soils supports the idea of abiotic processes leading to the CH_4 production. Besides, results of experiments with sterilised sample material, the observed kinetic of the CH_4 formation and the handling of the samples in an ambient atmosphere exclude the presence of methanogens.

In summary, the findings presented in this work support a non-biotical aerobic CH_4 formation in both chemical and living systems. The methyl groups of MDCs were found to serve as CH_4 precursors. The identification of a precursor component for CH_4 generation in

chemical systems enabled to formulate for the first time a detailed reaction scheme of the aerobic CH_4 formation. Moreover, the precursor component allowed to follow the CH_4 carbon from a plant applied substance to the released CH_4. The results of CH_4 formation by the usage of complex IV inhibitors suggest that the CH_4 generation is located in the mitochondria of the plants.

For soils a novel scheme was established including both biotical and chemical sinks and sources of CH_4 formation. Regarding the abiotic formation of CH_4 in soil important environmental parameter such as temperature, UV irradiation and water content were identified to control CH_4 formation. The organic content of the sample as well as water and hydrogen peroxide might also play a major role in the formation of CH_4 from soils.

9.2 Outlook

The here presented results suggest the mitochondria as source of CH_4 formation in living plant tissue. Further experiments with separated plant mitochondria could be used to confirm this hypothesis. These experiments could also include methionine and azide applications. Stable isotope labelling could be used to confirm methionine or to identify other substances as precursors of formed CH_4.

Still unclear is the biochemical mechanism of the plant produced CH_4. An investigation of these pathways could deliver new and important findings for our understanding of biochemical processes. Furthermore, regarding the results of Ghyczy et al. (2008), who found animal mitochondria to generate CH_4 under hypoxic conditions, the findings made by plant mitochondrial CH_4 formation could give information about CH_4 formation by animals but also by humans.

Additionally, biochemical investigations of CH_4 formation in plants, produced by mitochondria, might offer explanations to the reason why CH_4 is formed. For plants this could answer the question if CH_4 plays a metabolic role or if it is a by-product appearing during a metabolic process. A similar research could explain if human CH_4 formation is connected to the state of health.

The contribution of the chemical system described in Chapter 4 and 5 to CH_4 formation from soils is still unclear. The proposed chemical pathways might also take place in soils. In combination with local generated reactive oxygen species (ROS) the methyl groups of the

organic components could serve as precursors of produced CH_4. Further investigations with soils offering a more complex composition are of great interest. The investigation of single soil components, such as clay, humic acid and lignin could deliver more information about their role in CH_4 formation in soils. Finally, the role of water and hydrogen peroxide in CH_4 production in soil needs to be clarified.

Chapter 10

Developments

10.1 Vial-In-Vial

This Vial-In-Vial system is the result of the required combination of a small reaction volume and a large headspace that makes a dilution of CH_4 in the gas phase for measurements unnecessary. The small vial containing the reaction solution is placed in a larger vial fixed with a double-sided adhesive pad (Figure 10.1). The pad is removable without stains.

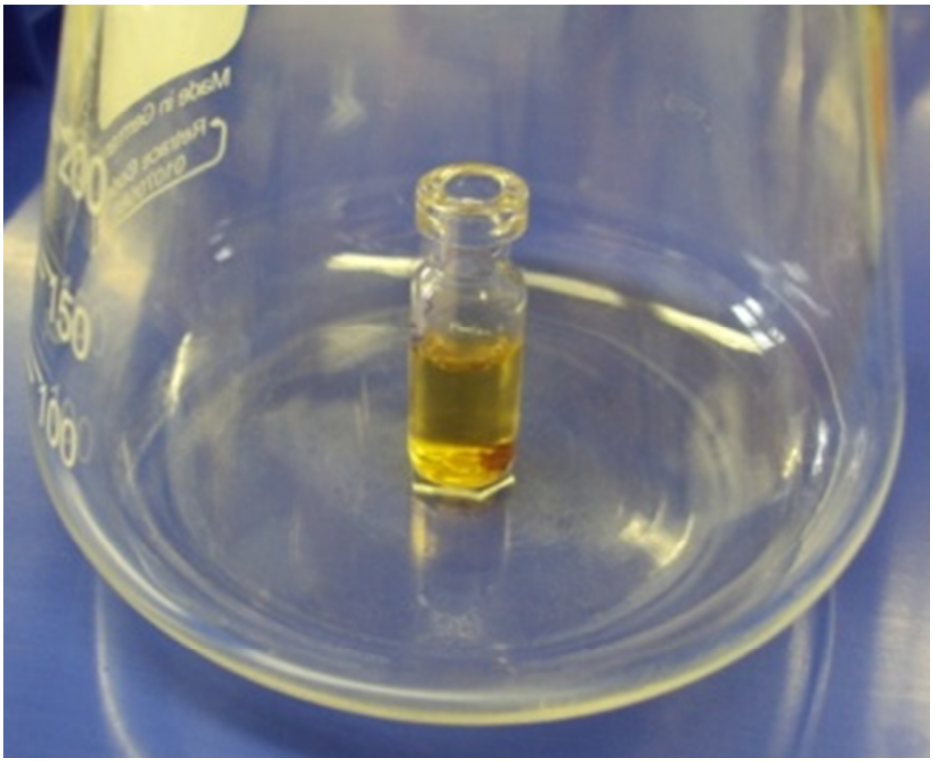

Figure 10.1: Image of the "Vial-In-Vial" system.

10.2 Electrolysis Chamber

Investigations of electron transfer reactions which result in CH_4 formation were carried out using a cyclic voltammetry (CV) and chronoamperometry (CA) device. For measurements of the amount of formed CH_4 a gas tight cell offering a possibility for gas sample extraction was required. Furthermore, different electrodes must be adapted gas tight. The consequence of these requirements is the developed electrolysis lid (Figure 10.2) that is used with a standard glass vial for the CV and CA measurements.

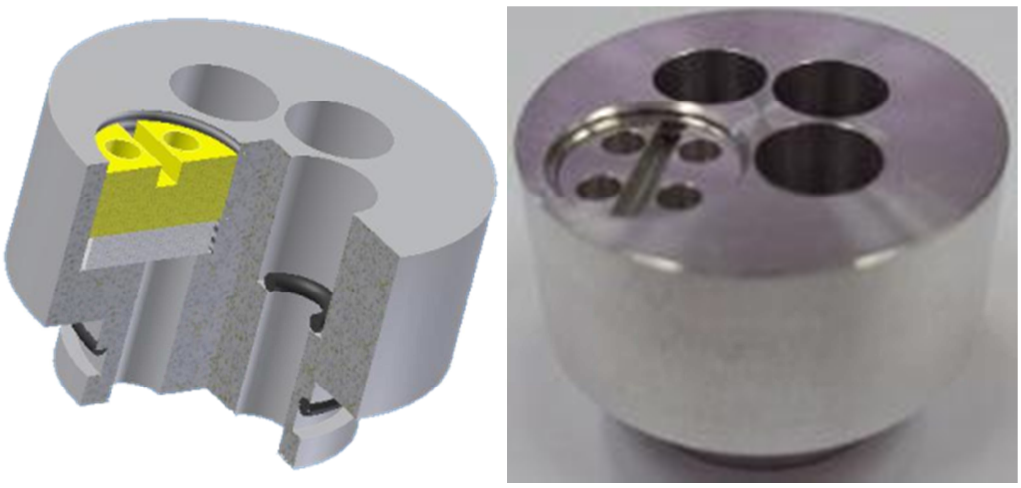

Figure 10.2: Sketch (left) and picture (right) of the electrolysis chamber lid.

10.3 UV-Cell

The UV-Cell is a sample chamber for radiation experiments. Its cylindrical shape allows an undisturbed pass through the chamber to irradiate the sample. Due to the flat bottom the radiated sample surface can be calculated easily and also experiments to determine to penetration depth can be carried out. The standardised flange enables to change non-optical glass pane by a quartz glass pane. Additional several wavelength filters can be adapted. For gas sampling it is equipped with a septa sealed side port (Figure 10.3).

Beside the usage described in Chapter 8 this UV-Cell was also used for further investigations not described in this dissertation. I assisted the authors in laboratory work but have not co-written the publication (Keppler et al., 2012).

Figure 10.3: Sketch (left) and picture (right) of the "UV-Cell".

10.4 Plant-Cell

The Plant-Cell is laid on the UV-Cell since an irradiation of a sample, i.e. a grown plant, is the main function of this cell. The lower part of the cell accommodates leaves of the plant. Using a standardised flange in the same size of the UV-Cell enables to use the same panes used for the UV-Cells. With the diameter of 5 cm the top opening is large enough to place sample plants in the cell. It is also equipped with a side port, sealed with a septa, for gas sampling (Figure 10.4).

Figure 10.4: Sketch (left) and picture (right) of the "Plant-Cell".

Danksagung

Bibliography

Allan, W., Lowe, D.C., Gomez, A.J., Struthers, H., Brailsford, G.W., **2005**. Interannual variation of C-13 in tropospheric methane: Implications for a possible atomic chlorine sink in the marine boundary layer. Journal of Geophysical Research 110 (D11).

Althoff, F., Benzing, K., Comba, P., McRoberts, C., Keppler, F., **2012 (submitted)**. Abiotic methanogenesis from biomolecules under ambient conditions. Nature Chemistry.

Althoff, F., Greiner, S., Greule, M., Keppler, F., **2012 (under review)**. Methionine as a precursor of methane in living plants. Plant Cell Environ.

Althoff, F., Jugold, A., Keppler, F., **2010**. Methane formation by oxidation of ascorbic acid using iron minerals and hydrogen peroxide. Chemosphere 80 (3), 286–292.

Althoff, F., Keppler, F., **2011**. Abiotic synthesis of methane from biomolecules under ambient conditions. Mineralogical Magazine 75 (3), 429.

Andersen, B.L., Bidoglio, G., Leip, A., Rembges, D., **1998**. A new method to study simultaneous methane oxidation and methane production in soils. Global Biogeochem. Cycles 12 (4), 587.

Bautz, J., Bukowski, M.R., Kerscher, M., Stubna, A., Comba, P., Lienke, A., Münck, E., Que, L., **2006**. Formation of an aqueous oxoiron(IV) complex at pH 2–6 from a nonheme iron(II) complex and H_2O_2. Angew. Chem. Int. Ed. 45 (34), 5681–5684.

Bautz, J., Comba, P., Lopez de Laorden, C., Menzel, M., Rajaraman, G., **2007**. Biomimetic High-Valent Non-Heme Iron Oxidants for the cis-Dihydroxylation and Epoxidation of Olefins. Angew. Chem. Int. Ed. 46 (42), 8067–8070.

Beerling, D.J., Gardiner, T., Leggett, G., McLeod, A.R., Quick, W.P., **2008**. Missing methane emissions from leaves of terrestrial plants. Global Change Biology 14, 1821–1826.

Bernhard, G., Mayer, B., Seckmeyer, G., Moise, A., **1997**. Measurements of spectral solar UV irradiance in tropical‐Australia. J. Geophys Res. (Journal of Geophysical Research D - Atmosphere) 102 (D7), 8719–8730.

Blake, D.R., Rowland, F.S., **1988**. Continuing Worldwide Increase in Tropospheric Methane, 1978 to 1987. Science 239 (4844), 1129–1131.

Bloom, A.A., Lee-Taylor, J., Madronich, S., Messenger, D.J., Palmer, P.I., Reay, D.S., McLeod, A.R., **2010**. Global methane emission estimates from ultraviolet irradiation of terrestrial plant foliage. New Phytol 187 (2), 417–425.

Born, M., Dörr, H., Levin, I., **1990**. Methane consumption in aerated soils of the temperate zone. Tellus 42, 2–8.

Boros, M., Ghyczy, M., Erces, D., Varga, G., Tőkés, T., Kupai, K., Torday, C., Kaszaki, J., **2012**. The anti-inflammatory effects of methane. Crit. Care Med. 40 (4), 1269–1278.

Boros, M., Wolfárd, A., Ghyczy, M., **1999**. In vivo evidence of reductive stress-induced methane production. Shock 56, 199.

Bousquet, P., Ciais, P., Miller, J.B., Dlugokencky, E.J., Hauglustaine, D.A., Prigent, C., van der Werf, G.R., Peylin, P., Brunke, E.-G., Carouge, C., Langenfelds, R.L., Lathiere, J., Papa, F., Ramonet, M., Schmidt, M., Steele, L.P., Tyler, S.C., White, J., **2006**. Contribution of anthropogenic and natural sources to atmospheric methane variability. Nature 443 (7110), 439–443.

Brüggemann, N., Meier, R., Steigner, D., Zimmer, I., Louis, S., Schnitzler, J., **2009**. Nonmicrobial aerobic methane emission from poplar shoot cultures under low-light conditions. New Phytol 182 (4), 912–918.

Bruhn, D., Mikkelsen, T.N., Willats, W.G.T., Ambus, P., **2009**. Effects of temperature, ultraviolet radiation and pectin methyl esterase on aerobic methane release from plant material. Plant biology, 1–6.

Bruhn, D., Møller, I.M., Mikkelsen, T.N., Ambus, P., **2012**. Terrestrial plant methane production and emission. Physiol Plant 144 (3), 201–209.

Buckley, T.N., Sack, L., Gilbert, M.E., **2011**. The role of bundle sheath extensions and life form in stomatal responses to leaf water status. Plant Physiol 156 (2), 962–973.

Cao, G.M., Xu, X.L., Long, R.J., Wang, Q.L., Wang, C.T., Du, Y.G., Zhao, X.Q., **2008**. Methane emissions by alpine plant communities in the Qinghai-Tibet Plateau. Biol. Lett 4, 681–684.

Cao, M., Gregson, K., Marshall, S., **1998**. Global methane emissions from wetlands and its sensitivity to climate change. Atmospheric Environment 32 (19), 3293–3299.

Castro, M.S., Steudler, P.A., Melillo, J.M., **1995**. Factors controlling atmospheric methane consumption by temperate forest soils. Global Biogeochem. Cycles 9 (1), 1–10.

Chen, Y.-H., Prinn, R.G., **2005**. Atmospheric modeling of high- and low-frequency methane observations: Importance of interannually varying transport. J. Geophys. Res. 110 (D10).

Chernobaev, I.I., Yakubovich, M.N., Tripol'skif, A.I., Pavlenko, N.V., Strnzhko, V.L., **1997**. Investigation of the mechanism of methane formation in the Fischer-Tropsch synthesis on a Co/SiO2-Zr(IV) catalyst. Theoretical and Experimental Chemistry 33 (1), 38–40.

Cicerone, R.J., Oremland, R.S., **1988**. Biogeochemical aspects of atmospheric methane. Global Biogeochem. Cycles 2 (4), 299–327.

Comba, P., Fukuzumi, S., Kotani, H., Wunderlich, S., **2010**. Electron-Transfer Properties of an Efficient Nonheme Iron Oxidation Catalyst with a Tetradentate Bispidine Ligand. Angew. Chem. Int. Ed. 49 (14), 2622–2625.

Comba, P., Kanellakopulos, B., Katsichtis, C., Lienke, A., Pritzkow, H., Rominger, F., **1998**. Synthesis and characterisation of manganese(II) compounds with tetradentate ligands based on the bispidine backbone. J. Chem. Soc., Dalton Trans. (23), 3997–4002.

Comba, P., Kerscher, M., Schiek, W., **2008**. Bispidine Coordination Chemistry, in: Karlin, K.D. (Ed.), Progress in Inorganic Chemistry, vol. 55. John Wiley & Sons, Inc, Hoboken, NJ, USA, pp. 613-704.

Comba, P., Kuwata, S., Linti, G., Pritzkow, H., Tarnai, M., Wadepohl, H., **2006**. Oxidative N-dealkylation in cobalt-bispidine-H_2O_2 systems. Chem. Commun. (19), 2074.

Comba, P., Maurer, M., Vadivelu, P., **2009**. Oxidation of Cyclohexane by High-Valent Iron Bispidine Complexes: Tetradentate versus Pentadentate Ligands. Inorg. Chem. 48 (21), 10389–10396.

Conrad, R., **2007**. Microbial Ecology of Methanogens and Methanotrophs, in: Donald L. Sparks (Ed.), Advances in Agronomy, vol. 96. Academic Press, pp. 1–63.

Conrad, R., **2009**. The global methane cycle: recent advances in understanding the microbial processes involved. Environmental Microbiology Reports 1 (5), 285–292.

Conrad, R., Bak, F., Seitz, H.J., Thebrath, B., Mayer, H.P., Schütz, H., **1989**. Hydrogen turnover by psychrotrophic homoacetogenic and mesophilic methanogenic bacteria in anoxic paddy soil and lake sediment. FEMS Microbiology Letters 62 (5), 285–293.

Crutzen, P.J., Andreae, M.O., **1990**. Biomass Burning in the Tropics: Impact on Atmospheric Chemistry and Biogeochemical Cycles. American Association for the Advancement of Science 250 (4988), 1669-1678.

Crutzen, P.J., Sanhueza, E., Brenninkmeijer, C.A.M., **2006**. Methane production from mixed tropical savanna and forest vegetation. Atmos. Chem. Phys. Discuss 6, 3093–3097.

Das, K., Baruah, K.K., **2008**. Methane emission associated with anatomical and morphophysiological characteristics of rice (Oryza sativa) plant. Physiol Plant 134 (2), 303–312.

Denman, K.L., Brasseur, G., Chidthaisong, A., Ciais, P., Cox, P.M., Dickinson, R.E., Hauglustaine, D., Heinze, C., Holland, E., Jacob, D., Lohmann, U., Ramachandran, S., Da Silva Dias, P.L., Wofsy, S.C., Zhang, X., **2007**. Couplings between changes in the climate system and biogeochemistry, in: Solomon, S., Qin, D., Manning, M., Chen, Z., Marquis, M., Averyt, K.B., Tignor, M., Miller, H. (Eds.), Climate Change 2007. The Physical Science Basis. Contribution of Working Group I to the Forth Assessment Report of the Intergovernmental Panel on Climate Change. Cambridge University Press, Cambridge, United Kingdom and New York, NY, USA.

DiMarco, A.A., Bobik, T.A., Wolfe, R.S., **1990**. Unusual Coenzymes Of Methanogenesis. Annual Review of Biochemistry 59 (1), 355–394.

Dueck, T.A., Visser, R. de, Poorter, H., Persijn, S., Gorissen, A., Visser, W. de, Schapendonk, A., Verhagen, J., Snel, J., Harren, F.J.M., Ngai, A.K.Y., Verstappen, F., Bouwmeester, H.,

Voesenek, L.A.C.J., van der Werf, A., **2007**. No evidence for substantial aerobic methane emission by terrestrial plants: a 13 C-labelling approach. New Phytol 175, 29–35.

Dunfield, P., Knowles, R., Dumont, R., Moore, T.R., **1993**. Methane production and consumption in temperate and subarctic peat soils: Response to temperature and pH. Soil Biology and Biochemistry 25 (3), 321–326.

Dunfield, P.F., **2007**. The soil methane sink, in: Reay, D.S. (Ed.), Greenhouse gas sinks. CABI, Wallingford, Oxfordshire, UK ;, Cambridge, MA, pp. 152–170.

Ehhalt, D., Prather, M., **2001**. Atmospheric chemistry and greenhouse gases, in: Houghton, J.T., Ding, Y., Griggs, D.J., Noguer, M., van der Linden, P.J., Dai, X., Maskell, K., Johnson, C.A. (Eds.), Climate Change 2001: The Scientific Basis. Cambridge University Press, New York, NY, USA, pp. 239–287.

Ehhalt, D., Prather, M., Dentener, F.J., Derwent, E., Dlugokencky, E.J., Holland, E., Isaksen, I., Katima, J., Kirchhoff, V., Matson, P., Midgley, P., Wang, M., **2001**. Atmospheric chemistry and greenhouse gases, in: , Climate Change 2001: The Physical Science Basis. Contribution of Working Group I to the Third Assessment Report of the Intergovernmental Panel on Climate Change.

Ellefson, W.L., **1982**. Nickel-Containing Factor F430: Chromophore of the Methylreductase of Methanobacterium. Proceedings of the National Academy of Sciences 79 (12), 3707–3710.

Farquhar, G.D., Sharkey, T.D., **1982**. Stomatal Conductance and Photosynthesis. Annu. Rev. Plant. Physiol. 33 (1), 317–345.

Ferretti, D.F., Miller, J.B., White, J.W.C., Lassey, K.R., Lowe, D.C., Etheridge, D.M., **2007**. Stable isotopes provide revised global limits of aerobic methane emissions from plants. Atmospheric Chemistry and Physics 7, 237–241.

Fischer, H., Behrens, M., Bock, M., Richter, U., Schmitt, J., Loulergue, L., Chappellaz, J., Spahni, R., Blunier, T., Leuenberger, M., Stocker, T.F., **2008**. Changing boreal methane sources and constant biomass burning during the last termination. Nature 452, 864-867.

Fischer, J.C. von, Hedin, L.O., **2007**. Controls on soil methane fluxes: Tests of biophysical mechanisms using stable isotope tracers. Global Biogeochem. Cycles 21 (2).

Forster, P., Ramaswamy, V., Artaxo, P., Berntsen, T., Betts, R., Fahey, D., Haywood, J., Lean, J., Lowe, D., Myhre, G., Nganga, J., Prinn, R., Raga, G., Schulz, M., Dorland, R., **2007**. Changes in atmospheric constituents and in radiative forcing, in: Solomon, S., Qin, D., Manning, M., Chen, Z., Marquis, M., Averyt, K.B., Tignor, M., Miller, H. (Eds.), Climate Change 2007. The Physical Science Basis. Contribution of Working Group I to the Forth Assessment Report of the Intergovernmental Panel on Climate Change. Cambridge University Press, Cambridge, United Kingdom and New York, NY, USA.

Frahry, G., Schopfer, P., **1998**. Hydrogen peroxide production by roots and its stimulation by exogenous NADH. Physiol Plant 103 (3), 395–404.

Frankenberg, C., Bergamaschi, P., Butz, A., Houweling, S., Meirink, J.F., Notholt, J., Petersen, A.K., Schrijver, H., Warneke, T., Aben, I., **2008**. Tropical methane emissions: A revised view from SCIAMACHY onboard ENVISAT. Geophys. Res. Lett. 35 (15).

Fry, S.C., **1998**. Oxidative scission of plant cell wall polysaccharides by ascorbate-induced hydroxyl radicals. Biochem. J. 332, 507-515.

Fry, S.C., Miller, J.G., Dumville, J.C., **2002**. A proposed role for copper ions in cell wall loosening. Plant Soil 247, 57-67.

Garcia-Alfonso, C., Lopez-Barea, J., Sanz, P., Repetto, G., Repetto, M., **1996**. Changes in Antioxidative Activities Induced by Fe (II) and Fe (III) in Cultured Veto Cells. Arch. Environ. Contam. Toxicol 30, 431-436.

Ghyczy, M., Torday, C., Boros, M., **2003**. Simultaneous generation of methane, carbon dioxide, and carbon monoxide from choline and ascorbic acid – a defensive mechanism against reductive stress? FASEB 17 (9), 1124–1126.

Ghyczy, M., Torday, C., Kaszaki, J., Szabo, A., Czobel, M., Boros, M., **2008**. Hypoxia-Induced Generation of Methane in Mitochondria and Eukaryotic Cells - An Alternative Approach to Methanogenesis. Cell Physiol Biochem 21, 251–258.

Greule, M., Huber, S.G., Keppler, F., **2012**. Stable hydrogen-isotope analysis of methyl chloride emitted from heated halophytic plants. Atmospheric Environment under review.

Hansen, J., Johnson, D., Lacis, A., Lebedeff, S., Lee, P., Rind, D., Russell, G., **1981**. Climate impact of increasing atmospheric carbon dioxide. Science 213 (4511), 957–966.

Hanson, R.S., Hanson, T.E., **1996**. Methanotrophic bacteria. Microbiological Reviews 60 (2), 439+.

Hao, W.M., Scharffe, D., Crutzen, P.J., Sanhueza, E., **1988**. Production of N2O, CH4, and CO2 from soils in the tropical savanna during the dry season. J Atmos Chem 7 (1), 93–105.

Hart, J.W., Filner, P., **1969**. Regulation of sulfate uptake by amino acids in cultured tobacco cells. Plant Physiol 44 (9), 1253–1259.

Hebert, V.R., Miller, G.C., **1990**. Depth dependence of direct and indirect photolysis on soil surfaces. J. Agric. Food Chem. 38 (3), 913–918.

Hinderberger, D., Ebner, S., Mayr, S., Jaun, B., Reiher, M., Goenrich, M., Thauer, R.K., Harmer, J., **2008**. Coordination and binding geometry of methyl-coenzyme M in the red1m state of methyl-coenzyme M reductase. J Biol Inorg Chem 13 (8), 1275–1289.

Holm, N.G., Charlou, J.L., **2001**. Initial indications of abiotic formation of hydrocarbons in the Rainbow ultramafic hydrothermal system, Mid-Atlantic Ridge. Earth and Planetary Science Letters 191 (1-2), 1–8.

Houweling, S., Röckmann, T., Aben, I., Keppler, F., Krol, M., Meirink, J.F., Dlugokencky, E.J., Frankenberg, C., **2006**. Atmospheric constraints on global emissions of methane from plants. Geophys. Res. Lett. 33, 1–5.

Hurkuck, M., Althoff, F., Jungkunst, H.F., Jugold, A., Keppler, F., **2012**. Release of methane from aerobic soil: An indication of a novel chemical natural process? Chemosphere 86 (6), 684–689.

Inaba, K., Fujiwara, T., Hayashi, H., Chino, M., Komeda, Y., Naito, S., **1994**. Isolation of an arabidopsis thaliana mutant, mto1, that overaccumulates soluble methionine: Temporal

and Spatial Patterns of Soluble Methionine Accumulation. Plant Physiol 104 (3), 881–887.

Jaccob, M., Comba, P., Maurer, M., Vadivelu, P., Venuvanalingam, P., **2011**. A combined experimental and computational study on the sulfoxidation by high-valent iron bispidine complexes. Dalton Trans. 40 (42), 11276.

Jansson, P.J., Hawkins, C.L., Lovejoy, D.B., Richardson, D.R., **2010**. The iron complex of Dp44mT is redox-active and induces hydroxyl radical formation: An EPR study. Journal of Inorganic Biochemistry 104 (11), 1224–1228.

Janzen, E.G., Zhang, Y.-K., **1995**. Identification of reactive free radicals with a new ^{31}P-labeled DMPO spin trap. J. Org. Chem. 60 (17), 5441–5445.

Jarvis, P.G., Mansfield, T.A. (Eds.), **1981**. Stomatal physiology. Cambridge University Press, Cambridge [Eng.] ;, New York, 295 pp.

Jugold, A., Althoff, F., Hurkuck, M., Greule, M., Lelieveld, J., Keppler, F., **2012 (submitted)**. Non-microbial methane formation in oxic soils. Nature Geoscience.

Jugold, A., Keppler, F., **2009**. Possibility of non-methanogenic methane formation in soils. Geochimica et Cosmochimica Acta 73 (13, Suppl. S), A608.

Kammann, C., Hepp, S., Lenhart, K., Müller, C., **2009**. Stimulation of methane consumption by endogenous CH4 production in aerobic grassland soil. Soil Biology and Biochemistry 41 (3), 622–629.

Katagi, T., **1990**. Photoinduced oxidation of the organophosphorus fungicide tolclofos-methyl on clay minerals. J. Agric. Food Chem. 38 (7), 1595–1600.

Keppler, F., Boros, M., Frankenberg, C., Lelieveld, J., McLeod, A.R., Pirttilä, A.M., Röckmann, T., Schnitzler, J., **2009**. Methane formation in aerobic environments. Environ. Chem 6 (6), 459–465.

Keppler, F., Eiden, R., Niedan, V., Pracht, J., Schöler, H.F., **2000**. Halocarbons produced by natural oxidation processes during degradation of organic matter. Nature 403 (6767), 298–301.

Keppler, F., Hamilton, J.T.G., Braß, M., Röckmann, T., **2006**. Methane emissions from terrestrial plants under aerobic conditions. Nature 439, 187–191.

Keppler, F., Hamilton, J.T.G., McRoberts, C.W., Vigano, I., Braß, M., Röckmann, T., **2008**. Methoxyl groups of plant pectin as a precursor of atmospheric methane: evidence from deuterium labelling studies. New Phytol 178, 808–814.

Keppler, F., Röckmann, T., **2007**. Methane, Plants and Climate Change. Scientific American 296 (2), 52–57.

Keppler, F., Vigano, I., McLeod, A., Ott, U., Früchtl, M., Röckmann, T., **2012**. Ultraviolet-radiation-induced methane emissions from meteorites and the Martian atmosphere. Nature.

Kersten, P.J., Kirk, T.K., **1987**. Involvement of a new enzyme, glyoxal oxidase, in extracellular H2O2 production by phanerochaete-chrysosporium. J Bacteriol 169 (5), 2195–2201.

Kibanova, D., Trejo, M., Destaillats, H., Cervini-Silva, J., **2011**. Photocatalytic activity of kaolinite. Catalysis Communications 12 (8), 698–702.

King, G.M., **1990**. Regulation by light of methane emissions from a wetland. Nature 345, 513–515.

King, G.M., **1997**. Responses of atmospheric methane consumption by soils to global climate change. Global Change Biology 3, 351–362.

Kirschbaum, M.U.F., Bruhn, D., Etheridge, D.M., Evans, J.R., Farquhar, G.D., Gifford, R.M., Paul, K.I., Winters, A.J., **2006**. A comment on the quantitative significance of aerobic methane release by plants. Functional Plant Biol. 33 (6), 521.

Kirschbaum, M.U.F., Niinements, Ü., Bruhn, D., Winters, A.J., **2007**. How Important is Aerobic Methane Release by Plants? Functional Plant Biol. 1 (1), 138–145.

Kirschbaum, M.U.F., Walcroft, A., **2008**. No detectable aerobic methane ef ux from plant material, nor from adsorption/desorption processes. Biogeosciences 5, 1551–1558.

Kremer, M.L., **2003**. The Fenton Reaction. Dependence of the Rate on pH. The Journal of Physical Chemistry A 107 (11), 1734-1741.

Kvenvolden, K.A., **2005**. Gaia's breath-global methane exhalations. Marine and petroleum geology 22 (4), 579–590.

Lacis, A., Hansen, J., Lee, P., Mitchell, T., Lebedeff, S., **1981**. Greenhouse effect of trace gases, 1970-1980. Geophys. Res. Lett. 8 (10), 1035.

Lange, O.L., Lösch, R., Schulze, E.-D., Kappen, L., **1971**. Responses of stomata to changes in humidity. Planta 100 (1), 76–86.

Lazar, C., Manning, C.E., **2010**. Methane-bearing fluids in subduction zones: an experimental study of abiotic methanogenesis during serpentinization at 12 kbar and 300 °C.

Lelieveld, J., Crutzen, P.J., Dentener, F., **1998**. Changing concentration, lifetime and climate forcing of atmospheric methane. Tellus 50B, 128–150.

Levy, H., **1971**. Normal Atmosphere: Large Radical and Formaldehyde Concentrations Predicted. Science 173 (3992), 141–143.

Lewin, A., Moore, G.R., Le Brun, N.E., **2005**. Formation of protein-coated iron minerals. Dalton transactions (22), 3597-3610.

Liou, M.-j., Lu, M.-c., **2008**. Catalytic degradation of explosives with goethite and hydrogen peroxide. Journal of Hazardous Materials 151, 540-546.

Loulergue, L., Schilt, A., Spahni, R., Masson-Delmotte, V., Blunier, T., Lemieux, B., Barnola, J.-M., Raynaud, D., Stocker, T.F., Chappellaz, J., **2008**. Orbital and millennial-scale features of atmospheric CH4 over the past 800,000 years. Nature 453 (7193), 383–386.

McLeod, A.R., Fry, S.C., Loake, G.J., Messenger, D.J., Reay, D.S., Smith, K.A., Yun, B., **2008**. Ultraviolet radiation drives methane emissions from terrestrial plant pectins. New Phytol 180, 124–132.

Megonigal, J.P., Guenther, A.B., **2008**. Methane emissions from upland forest soils and vegetation. Tree Physiol 28, 491–498.

Messenger, D.J., McLeod, A.R., Fry, S.C., **2009**. The role of ultraviolet radiation, photosensitizers, reactive oxygen species and ester groups in mechanisms of methane formation from pectin. Plant Cell Environ 32, 1–9.

Michal, G., **1999**. Biochemical pathways: An atlas of biochemistry and molecular biology. Wiley; Spektrum, New York, Heidelberg, xi, 277.

Miller, L.G., Sasson, C., Oremland, R.S., **1998**. Difluoromethane, a new and improved inhibitor of methanotrophy. Appl. Environ. Microbiol 64 (11), 4357–4362.

Minkinnen, K., Laine, J., **1998**. Effect of forest drainage on the peat bulk density of peat mires in Finland. Can. J. Forest Res. (Canadian Journal of Forest Research) 28 (2), 178–186.

Møller, I.M., **2007**. Mitochondrial Electron Transport and Oxidative Stress, in: , Annual Plant Reviews Volume 31: Plant Mitochondria. John Wiley & Sons, Inc, pp. 185-211.

Morrissey, L.A., Livingston, G.P., **1992**. Methane Emissions From Alaska Arctic Tundra: An Assessment of Local Spatial Variability. J. Geophys. Res. 97 (D15), 16661–16670.

Mott, K.A., Parkhurst, D.F., **1991**. Stomatal responses to humidity in air and helox. Plant Cell Environ 14 (5), 509–515.

Neubeck, A., Duc, N., Bastviken, D., Crill, P.M., Holm, N.G., **2011**. Formation of H2 and CH4 by weathering of olivine at temperatures between 30 and 70 °C. Geochem Trans 12 (1), 6.

Nisbet, R.E.R., Fisher, R., Nimmo, R.H., Bendall, D.S., Crill, P.M., Gallego-Sala, A.V., Hornibrook, E.R.C., López-Juez, E., Lowry, D., Nisbet, P.B.R., Shuckburgh, E.F., Sriskantharajah, S., Howe, C.J., Nisbet, E.G., **2009**. Emission of methane from plants. Proc. R. Soc. B 276, 1347–1354.

Ortega, J., Helmig, D., **2008**. Approaches for quantifying reactive and low-volatility biogenic organic compound emissions by vegetation enclosure techniques. Chemosphere 72 (3), 343–380.

Parsons, A.J., Newton, P.C.D., Clark, H., Kelliher, F.M., **2006**. Scaling methane emissions from vegetation. Trends EcolEvol 21 (8), 423–424.

Peters, V., Conrad, R., **1995**. Methanogenic and other strictly anaerobic bacteria in desert soil and other oxic soils. Applied and Environmental Microbiology 61 (4), 1673–1676.

Platt, U., Allan, W., Lowe, D., **2004**. Hemispheric average Cl atom concentration from C-13/C-12 ratios in atmospheric methane. Atmospheric Chemistry and Physics 4, 2393–2399.

Pracht, J., Boenigk, J., Isenbeck-Schröter, M., Keppler, F., Schöler, H.F., **2001**. Abiotic Fe(III) induced mineralization of phenolic substances. Chemosphere 44 (4), 613-619.

Qaderi, M.M., Reid, D.M., **2009**. Methane emissions from six crop species exposed to three components of global climate change: temperature, ultraviolet-B radiation and water stress. Physiol Plant 137 (2), 139–147.

Qaderi, M.M., Reid, D.M., **2011**. Stressed crops emit more methane despite the mitigating effects of elevated carbon dioxide. Functional Plant Biol. 38 (2), 97–105.

Rasmussen, R.A., Khalil, M.A.K., **1984**. Atmospheric methane in the recent and ancient atmospheres: Concentrations, trends, and interhemispheric gradient. J. Geophys. Res. 89 (D7), 11599–11605.

Reeburgh, W.S., **2003**. Global Methane Biogeochemistry, in: Holland, H.D., Turekian, K.K. (Eds.), Treatise on Geochemistry. Pergamon, Oxford, pp. 1–32.

Repine, J.E., Eaton, J.W., Anders, M.W., Hoidal, J.R., Fox, R.B., **1979**. Generation of hydroxyl radical by enzymes, chemicals, and human phagocytes in vitro. J. Clin. Invest 64 (December), 1642–1651.

Rimbault, A., Niel, P., Virelizier, H., Darbord, J.C., Leluan, G., **1988**. L-Methionine, a Precursor of Trace Methane in Some Proteolytic Clostridia. Appl. Environ. Microbiol 54 (6), 1581–1586.

Roulet, N.T., Ash, R., Moore, T.R., **1992**. Low Boreal Wetlands as a Source of Atmospheric Methane. J. Geophys Res. (Journal of Geophysical Research D - Atmosphere) 97 (D4), 3739–3749.

Sanhueza, E., Donoso, L., **2006**. Methane emission from tropical savanna Trachypogon sp. grasses. Atmospheric Chemistry and Physics 6, 5315–5319.

Schönknecht, G., Brown, J.E., Verchot-Lubicz, J., **2008**. Plasmodesmata transport of GFP alone or fused to potato virus X TGBp1 is diffusion driven. Protoplasma 232 (3-4), 143–152.

Schwertmann, U., Carlson, L., Murad, E., **1987**. Properties of iron oxides in two finnish lakes in relation to the environment of their formation. Clay and Clay Minerals 35 (4), 297-304.

Schwertmann, U., Cornell, R.M., **2000**. Iron Oxides in the: Laboratory Preparation and Characterization, 2nd ed. Wiley-VCH, Weinheim, 188 pp.

Seinfeld, J.H., Pandis, S.N., **2006**. Atmospheric chemistry and physics: From air pollution to climate change, 2nd ed. John Wiley & Sons, Inc, Hoboken, N.J, 1203 pp.

Sharpatyi, V.A., **2007**. On The Mechanism Of Methane Emission By Terrestrial Plants. Oxidation Communications 30 (1), 48–50.

Sherwood Lollar, B., Frape, S., Weise, S., Fritz, P., Macko, S., Welhan, J., **1993**. Abiogenic methanogenesis in crystalline rocks. Geochimica et Cosmochimica Acta 57 (23-24), 5087–5097.

Sherwood Lollar, B., Westgate, T.D., Ward, J.A., Slater, G.F., Lacrampe-Couloume, G., **2002**. Abiogenic formation of alkanes in the Earth's crust as a minor source for global hydrocarbon reservoirs. Nature 416 (6880), 522–524.

Simpson, I.J., Blake, D.R., Rowland, F.S., Chen, **2002**. Implications of the recent fluctuations in the growth rate of tropospheric methane. Geophys. Res. Lett. 29 (10).

Sleep, N.H., Meibom, A., Fridriksson, T., Coleman, R.G., Bird, D.K., **2004**. H2-rich fluids from serpentinization: geochemical and biotic implications. PNAS 101 (35), 12818-12823.

Solomon, S., Qin, D., Manning, M., Chen, Z., Marquis, M., Averyt, K.B., Tignor, M., Miller, H. (Eds.), **2007**. Climate Change 2007. The Physical Science Basis. Contribution of Working Group I to the Forth Assessment Report of the Intergovernmental Panel on Climate Change. Cambridge University Press, Cambridge, United Kingdom and New York, NY, USA.

Spahni, R., Chappellaz, J., Stocker, T., Loulergue, L., Hausammann, G., Kawamura, K., Flckiger, J., Schwander, J., Raynaud, D., Masson-Delmotte, V., Jouzel, J., **2005**. Atmospheric methane and nitrous oxide of the Late Pleistocene from Antarctic ice cores. Science 310 (5752), 1317–1321.

Takai, K., Komatsu, T., Inagaki, F., Horikoshi, K., **2001**. Distribution of Archaea in a Black Smoker Chimney Structure. Applied and Environmental Microbiology 67 (8), 3618–3629.

Terazawa, K., Ishizuka, S., Sakata, T., Yamada, K., Takahashi, M., **2007**. Methane emissions from stems of Fraxinus mandshurica var. japonica trees in a floodplain forest. Soil Biology and Biochemistry 39, 2689–2692.

Thauer, R.K., **1998**. Biochemistry of methanogenesis: A tribute to Marjory Stephenson. Microbiology 144, 2377-2406.

Treut, H., Somerville, R., Cubasch, U., Ding, Y., Mauritzen, C., Mokssit, A., Peterson, T., Prather, M., Qin, D., Manning, M., Chen, Z., Marquis, M., Averyt, K.B., Tignor, M., Kingdom, U., **2007**. Historical overview of climate change science, in: Solomon, S., Qin, D., Manning, M., Chen, Z., Marquis, M., Averyt, K.B., Tignor, M., Miller, H. (Eds.), Climate Change 2007. The Physical Science Basis. Contribution of Working Group I to the Forth Assessment Report of the Intergovernmental Panel on Climate Change. Cambridge University Press, Cambridge, United Kingdom and New York, NY, USA.

Trotsenko, Y.A., Murrell, J.C., **2008**. Metabolic Aspects of Aerobic Obligate Methanotrophy, in: Laskin, A.I., Sariaslani, S., Gadd, G.M. (Eds.), vol. 63. Academic Press, pp. 183–229.

Vigano, I., **2010**. Aerobic methane production from organic matter. Dissertation, Utrecht.

Vigano, I., Röckmann, T., Holzinger, R., van Dijk, A., Keppler, F., Greule, M., Brand, W.A., Geilmann, H., van Weelden, H., **2009**. The stable isotope signature of methane emitted from plant material under UV irradiation. Atmospheric Environment 43 (35), 5637–5646.

Vigano, I., van Weelden, H., Holzinger, R., Keppler, F., McLeod, A.R., Röckmann, T., **2008**. Effect of UV radiation and temperature on the emission of methane from plant biomass and structural components. Biogeosciences 5, 937–947.

Vikesland, P.J., Valentine, R.L., **2002**. Iron Oxide Surface-Catalyzed Oxidation of Ferrous Iron by Monochloramine: Implications of Oxide Type and Carbonate on Reactivity. Environ. Sci. Technol. 36 (3), 512-519.

Voinnet, O., Rivas, S., Mestre, P., Baulcombe, D., **2003**. An enhanced transient expression system in plants based on suppression of gene silencing by the p19 protein of tomato bushy stunt virus. The Plant Journal 33 (5), 949–956.

Wang, Z.-P., Gulledge, J., Liu, W., **2009**. Physical injury stimulates aerobic methane emissions from terrestrial plants. Biogeosciences 6 (4), 615–621.

Wang, Z.-P., Han, X.G., Wang, G.G., Song, Y., Gulledge, J., **2008**. Aerobic methane emission from plants in the Inner Mongolia steppe. Environ. Sci. Technol. 42 (1), 62–68.

Wang, Z.-P., Keppler, F., Greule, M., Hamilton, J.T.G., **2011**. Non-microbial methane emissions from fresh leaves: Effects of physical wounding and anoxia. Atmospheric Environment 45 (28), 4915–4921.

Wishkerman, A., Greiner, S., Ghyczy, M., Boros, M., Rausch, T., Lenhart, K., Keppler, F., **2011**. Enhanced formation of methane in plant cell cultures by inhibition of cytochrome c oxidase. Plant Cell Environ 34 (3), 457–464.

Wu, F., Li, J., Peng, Z., Deng, N., **2008**. Photochemical formation of hydroxyl radicals catalyzed by montmorillonite. Chemosphere 72 (3), 407–413.

Yoshimura, Y., Inomata, T., Nakazawa, H., Kubo, H., Yamaguchi, F., Ariga, T., **1999**. Evaluation of Free Radical Scavenging Activities of Antioxidants with an H_2O_2/NaOH/DMSO System by Electron Spin Resonance. J. Agric. Food Chem. 47 (11), 4653–4656.

List of figures

Figure 1.1: Global tropospheric CH_4 (left) and CO_2 (right) in the year 2005 and 2009, respectively 25
Figure 1.2: Temporal development of atmospheric greenhouse gas concentrations 26
Figure 1.3: Summary of the principal components of the radiative forcing of climate change between 1750 and 2005 27
Figure 1.4: An idealised scheme of the natural greenhouse effect 28
Figure 1.5: Reactions in the atmosphere that leads to the formation hydroxyl radicals (·OH) and to the decomposition of methane (CH_4) 29
Figure 1.6: Methane consumption by methanotrophs 30
Figure 1.7: Pathways of microbial CH_4 production by reduction of CO_2 31
Figure 2.1: Scheme of the composition of an animal cell and a plant cell 35
Figure 2.2: Schematic drawing of a mitochondrion cut longitudinally 36
Figure 2.3: Scheme of mitochondrial electron transport chain. Wiggly lines indicate the target of the attributed inhibitors 38
Figure 2.4: Scanning electron resonance (SEM) images of stomata 39
Figure 3.1: Scheme of an flame ionisation detector 41
Figure 3.2: Scheme of the cryogenic pre-concentration unit 43
Figure 3.3: A scheme of a typical GC-C-IRMS system 44
Figure 3.4: Components of the LC-TOFMS 45
Figure 4.1: Formation of methane using different iron mineral species 54
Figure 4.2: Chemical structure of organic compounds tested for methane formation. 55
Figure 4.3: Time course formation of methane 56
Figure 4.4: Effect on ferrihydrite and hydrogen peroxide on methane production 57
Figure 4.5: Effect of pH and reaction volume on methane formation 58
Figure 4.6: Methane formation under different gas atmospheres 59
Figure 5.1: Methane formation from different organic compounds in the reaction with ASC, FH, and H_2O_2 65
Figure 5.2: The effect of different iron species on CH_4 formation from MET 66
Figure 5.3: Dependency on substance ratio 67

Figure 5.4: Linear dependency of CH_4 formation on amount of methionine 68
Figure 5.5: Route of CH_4 formation using MET, ASC, FH, and H_2O_2 71
Figure 5.6: Dependency on ferrihydrite (FH) 73
Figure 5.7: Dependency on pH 73
Figure 5.8: Dependency on reaction volume 74
Figure 5.9: Dependency on different atmospheres 74
Figure 5.10: Structure of the bispidine ligand and the corresponding ferryl complex 75
Figure 6.1: Formation of methane from plant cell suspensions when treated with varying concentrations of different cytochrome c oxidase inhibitors (NaN_3, NaCN and CO) 85
Figure 6.2: Methane formation by BY2 cell suspensions supplemented with different MDCs and treated with NaN_3 87
Figure 6.3: Methane formation by BY2 cell suspensions supplemented with different concentrations of methionine 88
Figure 6.4: Change of $\delta^{13}C$ values of CH_4 produced by intact living plants supplemented with ^{13}C-labelled MET 90
Figure 6.5: Hypothetical scheme of CH_4 formation from methionine during disturbance of complex IV at the ETC in mitochondrial intermembrane space 91
Figure 7.1: Methane release from lignin and pectin 100
Figure 7.2: Methane release with time from soil samples and soil organic compounds when incubated at 40 °C 104
Figure 7.3: Methane release with time from soil samples and soil organic compounds when incubated at 70 °C 104
Figure 7.4: Methane release with time from soil samples and soil organic compounds when incubated at 40 °C following the addition of H_2O 105
Figure 7.5: Methane release with time from soil samples and soil organic compounds when incubated at 70 °C following the addition of H_2O 105
Figure 8.1: Formation of CH_4 from soil with increasing temperature. 113
Figure 8.2: Methane formation from wetted and dry peat samples. 115
Figure 8.3: Relationship between CH_4 emission from peat PH and added amount of H_2O_2 116

Figure 8.4: Relationship between CH_4 emissions from soils SL and SG and UV-B intensity 117
Figure 8.5: Scheme of CH_4 cycling in soil including non-microbial (blue) and the previously known microbial sources (red)..... 121
Figure 8.6: Arrhenius plot for formation of CH_4 in peat PH (diamonds) and soils SL (squares) and SG (triangles)..... 127
Figure 10.1: Image of the “Vial-In-Vial” system. 133
Figure 10.2: Sketch (left) and picture (right) of the electrolysis chamber lid. 134
Figure 10.3: Sketch (left) and picture (right) of the “UV-Cell”. 135
Figure 10.4: Sketch (left) and picture (right) of the “Plant-Cell”. 136

List of tables

Table 7.1: Methane release rates from dry and wet samples. 101
Table 8.1: Organic carbon content, pH value and CH_4 emissions from dry and wetted samples heated at 30 and 40 °C and under UV irradiation of different soils and soil components..... 114

Publications

Journal articles (Peer-reviewed)

Althoff, F., Jugold, A., Keppler, F., **2010**. Methane formation by oxidation of ascorbic acid using iron minerals and hydrogen peroxide. Chemosphere 80 (3), 286–292.

Althoff, F., Benzing, K., Keppler, F., **2012** (under review). Methionine as a precursor of methane in living plants. Plant Cell Environ.

Althoff, F., Benzing, K., Comba, P., McRoberts, C., Keppler, F., **2012** (submitted). Abiotic methanogenesis from biomolecules under ambient conditions. Nature Chemistry.

Hurkuck, M., Althoff, F., Jungkunst, H.F., Jugold, A., Keppler, F., **2012**. Release of methane from aerobic soil: An indication of a novel chemical natural process? Chemosphere 86 (6), 684–689.

Jugold, A., Althoff, F., Hurkuck, M., Greule, M., Lelieveld, J., Keppler, F., **2012** (submitted). Non-microbial methane formation in oxic soils. Nature Geoscience.

Oral presentation

Goldschmidt Conference 2011. Prague, Czech Republic. August 14 – 19.

Theme 17: From microbes to macro and cycles; **Session c**: Methane Cycling in Marine and Terrestrial Environments.

Conference abstract

Goldschmidt Conference, 2011.

Abiotic synthesis of methane from biomolecules under ambient conditions

FREDERIK ALTHOFF[1] AND FRANK KEPPLER[2]

[1] Max-Planck-Institute for Chemistry, Joh.-Joachim-Becher-Weg 27, 55128 Mainz; frederik.althoff@mpic.de
[2] Max-Planck-Institute for Chemistry, Joh.-Joachim-Becher-Weg 27, 55128 Mainz; frank.keppler@mpic.de

The formation of methane can be classified in biotic and abiotic reactions. While biotic methanogenesis is related to anaerobic microorganisms, abiotic methane formation requires high pressure and/or temperature. Such conditions can be found for instance during biomass burning or serpentinisation of olivine, under hydrothermal conditions in the deep ocean or below tectonic plates [1].

The bio available substances ascorbic acid, iron and hydrogen peroxide were used in aqueous solution to perform an abiotic methane formation under ambient conditions [2]. In a further step to this reaction other important biomolecules were added which are known from methylation reaction in biosystems, e.g. methionine, or expose a possible methane precursor methyl groups, such as choline or leucine.

Furthermore, the reaction was carried out using different iron species, such as Fe^{2+}, Fe^{3+}, ferrihydrite and other iron hydroxides.

Methionine was found to produce the highest amount of methane. Stable isotope analysis in combination with ^{13}C-labelling of methionine confirmed the assumption of sulphur bond methyl group as methane precursor. Moreover, a linear increase of the generated methane with the amount of added methionine could be found.

The investigation of the iron species basically showed a conversion to methane, however, methane formation is significantly higher using iron minerals in comparison to free Fe ions. By analysing the remaining products within the solution a reaction scheme was created.

The results of these experiments show the possibility of an abiotic aerobe methane formation using biomolecules under ambient conditions.

[1] Sherwood Lollar et al. (2002), Nature 416, 522-524.
[2] Althoff et al. (2010), Chemosphere 80, 286-292.